

DUPLICATE



TEMEX RESOURCES CORP.

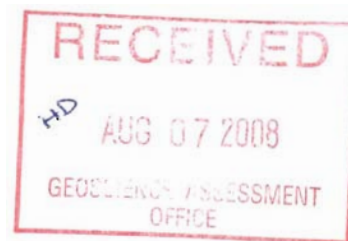
141 Adelaide Street West, Suite 1660
Toronto, Ontario M5H 3L5
416-862-2246 phone 416-862 2244 fax
website: www.temexcorp.com

2.38792

**Report on the
2008 Diamond Drilling Program**

Latchford Diamond Project

**Larder Lake Mining Division, Ontario
NTS 31M/05**



Eric Potter, M.Sc., Ph.D. Candidate
Consulting Geologist

Karen Rees, B.Sc., P.Geo.
General Manager, Temex Resources Corp.

July 14, 2008

TABLE OF CONTENTS

1.0	Introduction.....	1
2.0	Property Description, Location and Access.....	1
3.0	Climate, Local Resources, Infrastructure and Physiography	1
4.0	Regional Geology.....	4
5.0	Diamond Drilling Program.....	6
5.1	Procedures.....	6
5.2	Work Performed.....	8
5.3	Drill Program Discussion	8
6.0	Conclusions and Recommendations	16
7.0	References.....	17
	Statement of Qualifications	18

FIGURES

Figure 1:	General Property Location.....	2
Figure 2:	General Location of Drill Holes.....	3
Figure 3:	General Location of Drill Holes on Ground Magnetic Survey Data.....	7

TABLES

Table 1:	2008 Drilling Statistics.....	6
Table 2:	Samples Taken for Petrographic Examination	9

APPENDICES

Appendix 1:	Drill Hole Location Plan on Claim
Appendix 2:	Drill Sections
Appendix 3:	Drill Hole Lithological Logs and Magnetic Susceptibility Readings

1.0 Introduction

From May 20 to June 15, 2008, Temex Resources Corp. (“Temex”) conducted a diamond drill program in the Latchford region of northeastern Ontario (Figure 1). The program was planned and supervised by Temex field personnel from Temex’s field office located in the community of Temagami North, Ontario.

Four diamond drill holes were drilled to attempt to define the shape and size of the diamondiferous KRVY body discovered by Temex in 2006 in drill hole TD-06-03. A total of 1,646 metres were drilled during this program. This report documents the location and lithology of the four drill holes TD-08-07 to TD-08-10.

2.0 Property Description, Location and Access

Temex land-holdings in the Latchford to Temagami area cover 63,480 acres. The 2008 drill program occurred on NTS map 31M/05 and more specifically on claim 3007432 (see Figure 2). The claim is in the Larder Lake Mining Division, recorded in the name of Temex Resources Corp. (Client #303055).

The Municipality of Temagami is centred approximately 100 km north of the city of North Bay, which is in turn located 350 km north of Toronto. New Liskeard is located a further 60 km north of Temagami on the northwestern shore of Lake Timiskaming. The community of Latchford is located 4 km northwest of the subject claim.

The region encompassing the Latchford Diamond Project is accessed via Trans Canada Highway 11, the major paved highway running north from North Bay through Temagami, Latchford, New Liskeard and on to the Kirkland Lake area. The Temex claim blocks are accessed via well-established secondary gravel roads traversing east or west from Highway 11 and various logging roads and trails with walking distances to drill sites ranging from 0.5 to 4 km.

3.0 Climate, Local Resources, Infrastructure and Physiography

The climate of the property is continental in nature, with cold winters (-10°C to -35°C) and warm summers (+10°C to +40°C).

The communities of Sudbury, Timmins, Kirkland Lake and Cobalt are close to the property areas; these communities all have the equipment and trained personnel to support exploration and mining activities. The property has excellent access to all infrastructure required for mining. A major hydro line, gas pipeline and railway traverse or are close to the properties, water is abundant, and the property area spans Highway 11. The mineral rights held by Temex provide the prerogative to mine ore discovered on their properties, subject to a 400' surface rights reservation around all lakes and rivers, and a 300' surface reservation around major roads (this may be waived by the Crown).

The properties have a gently rolling to locally rugged topography with maximum relief on the order of 100-200 m. Much of the region has been logged so present-day forests typically are second growth mixtures of jack pine, spruce, birch and poplar. In the Cobalt-New Liskeard area, large tracts of land have been cleared for dairy and beef cattle farms or the growth of cash crops. Gravel resources are abundant in the area as evidenced by numerous sand and gravel pits developed on glaciofluvial deposits.

Figure 1: General Property Location

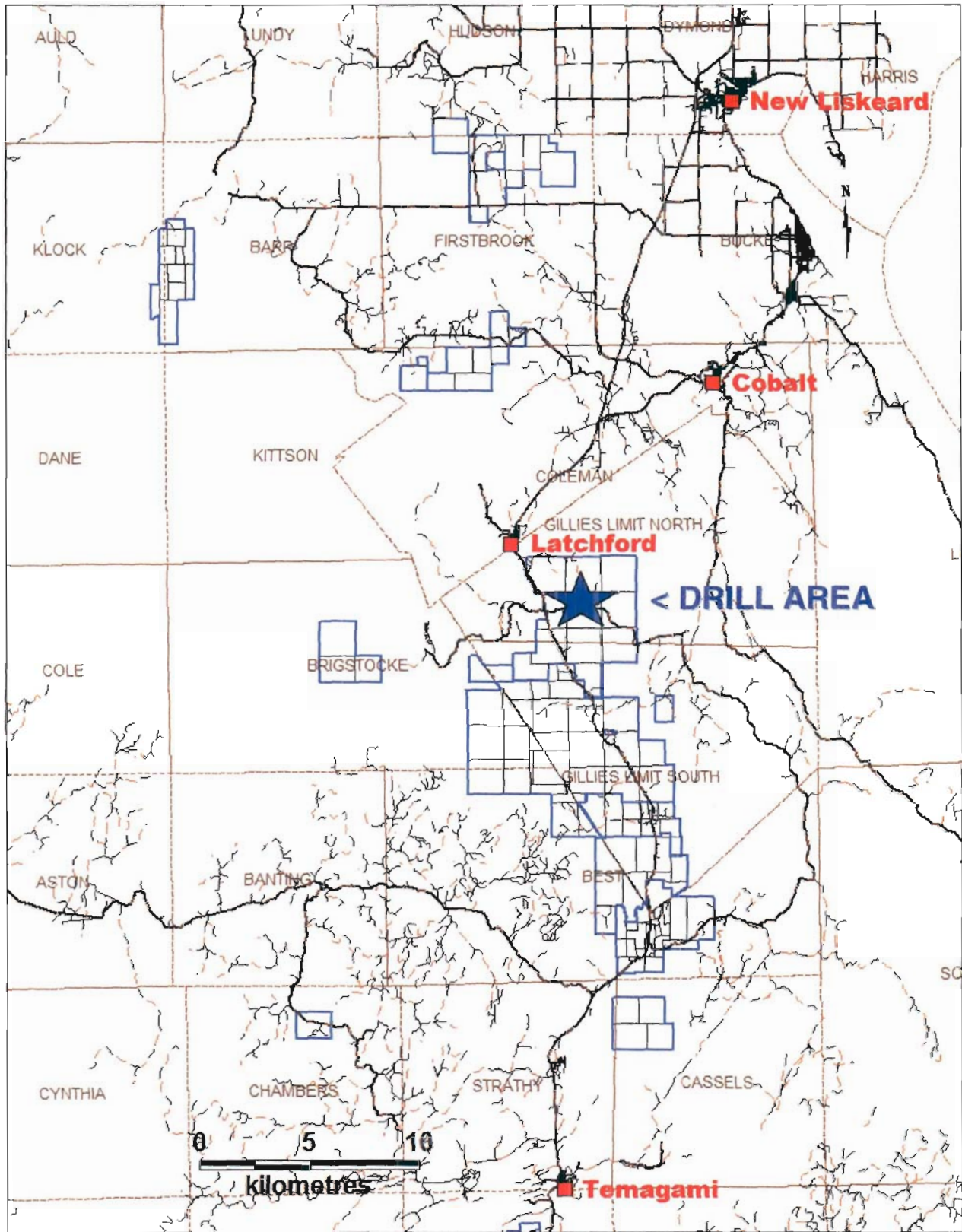
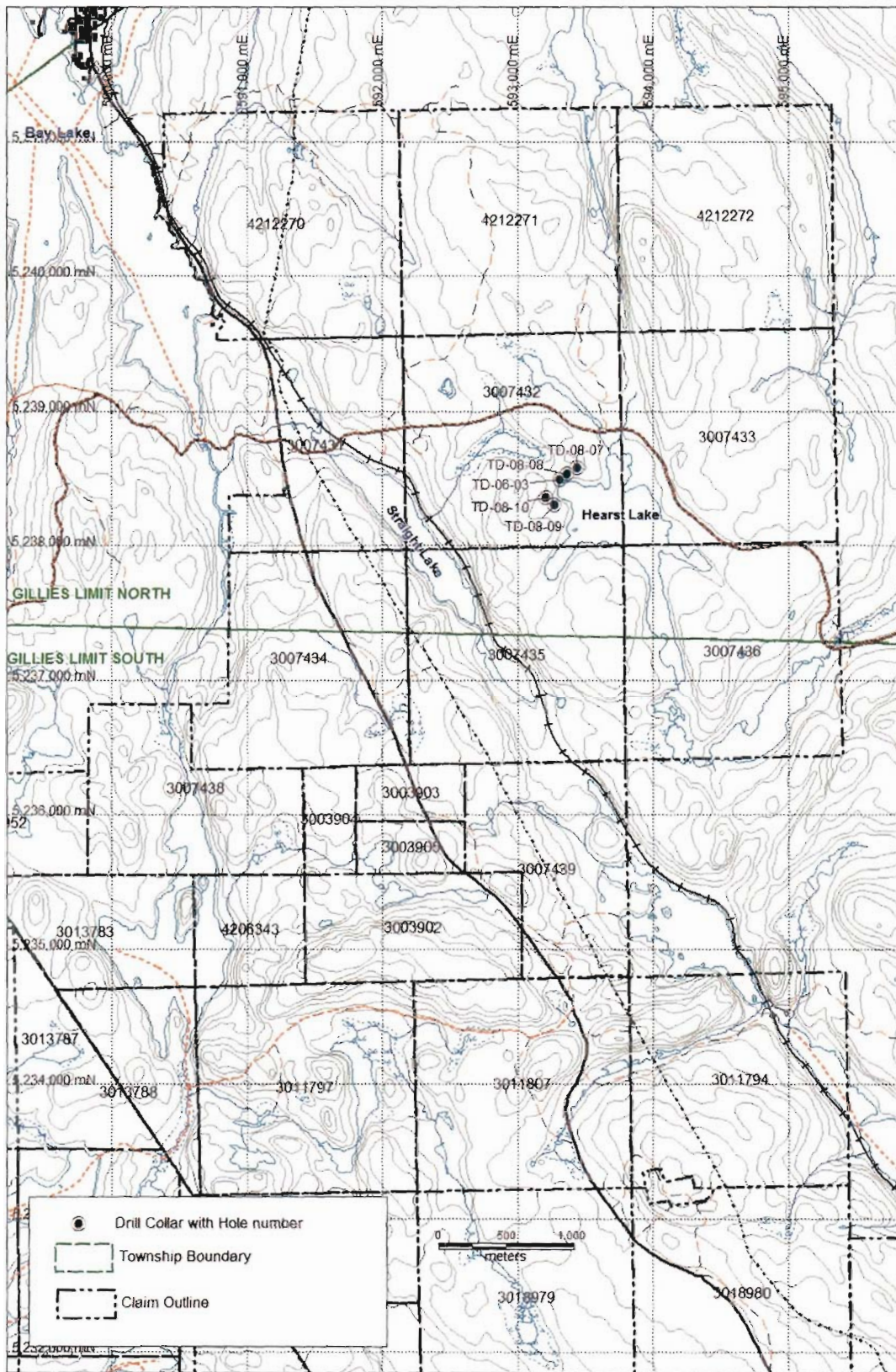


Figure 2: General Location of Drill Holes



4.0 Regional Geology

The Temagami-New Liskeard region occurs within and adjacent to the Cobalt Embayment of the Southern Province, which occurs at the boundary between the Superior Province to the northwest and the Grenville Province to the southeast. The Archean Superior Province, represented in this area by the Abitibi sub province, is dominated by orthogneisses and large intrusions, but also contains ultramafic to felsic volcanic and sedimentary rocks comprising so-called greenstone belts. The Grenville Province contains rocks that were complexly deformed and metamorphosed during a series of orogenic events that culminated at approximately 1.1 Ga, probably as a result of northwest-directed thrusting and imbrication (Easton, 1992). The Grenville Front Tectonic Zone (GFTZ) is accepted as the surface expression of the northwest boundary of the Grenville Province. The Southern Province in this area consists of the 2.5 to 2.2 Ga Huronian Supergroup comprised of the Elliot Lake, Hough Lake, Quirke Lake and Cobalt Groups, all of which are predominantly sedimentary packages intruded by dykes and sills of 2219 Ma Nipissing diabase (Bennett et al., 1991). The Huronian Supergroup unconformably overlies the Superior province, with windows of Superior Province greenstone belts exposed within the Cobalt Embayment and these have been proved to be high potential targets for base and precious metal exploration. Phanerozoic-aged clastic sediments are found to the north and northwest of New Liskeard in fault-bounded basins that also are the sites of thick sequences of Quaternary-aged glacial sediments.

The Elliot Lake, Hough Lake and Quirke Lake Groups are not well represented in the project area; the Cobalt Group is subdivided primarily into the Gowganda Formation, dominated by a distinctive coarse basal conglomerate and the Lorrain Formation consisting predominantly of sandstone and finely laminated highly indurated siltstone. Nipissing diabase is the term given to a voluminous suite of gabbro/diabase sills and dykes, which intrude the Huronian from Cobalt to Sault Ste Marie. Bedrock geology in the area is not critical to the emplacement of kimberlite except for near-surface control by local structures on pipe form and deep seated structures, which may have been active from the Archean to the present and controlled the emplacement of Nipissing Diabase, that form the Lake Timiskaming Graben and Phanerozoic and younger alkaline rocks.

The subject area is underlain by Archean mafic to intermediate volcanics and related volcanoclastic and epiclastic sediments, which have been intruded by late Archean granite and overlain in the eastern, central and northern parts of the area by Huronian sediments of the Gowganda and Lorrain Formations. Five ages of diabase dykes cross-cut Archean and Proterozoic-aged rocks; Proterozoic-aged diabase sills are common throughout the area, particularly in the Cobalt-New Liskeard districts where they are spatially and temporally related to Ag-rich vein mineralization.

The rationale of searching for diamonds in the Temagami region is the diamond-bearing kimberlite pipes and dykes that have been known in the Kirkland Lake area for almost 50 years. Schulze (1996) described two main kimberlite clusters totalling 29 bodies, including 23 bodies in the Kirkland Lake area, and six bodies in the Lake Timiskaming area. Kimberlites of the Kirkland Lake cluster intrude Archean rocks, whereas the Lake Timiskaming cluster is hosted at the present erosional level largely by sedimentary rocks and diabase dykes and sills of the Huronian Supergroup. Pipe dimensions are typically 100-300 m in diameter, with the largest in the New Liskeard area being 220 x 350 m in size and measuring up to 10-12 ha on surface (e.g. Contact Diamond Corporation MR-6, KL-1 and KL-22). The Tres-Or Resources' "Lapointe" kimberlite, located ~36 km southwest of Kirkland Lake may be up to 23 ha, distinguishing it as the largest kimberlite discovered to date in Ontario.

Preserved crater facies material (tuffs) have been found in Contact Diamond's MR-6 pipe and Tres-Or's Lapointe body. Kimberlites in the Lake Temiskaming cluster range in age from 155 to 134 Ma (Sage, 2000). The diamond potential of this region is considered to be related to the kimberlite magmas exploiting deep seated faults related to the present-day Lake Timiskaming Rift Valley (Morris and Kaszycki, 1995; Sage, 1996 and 2000). The Lake Timiskaming Rift Valley is expressed as large-scale normal movement along northwest-trending faults, including the Montreal River and Cross Lake fault systems. Nipissing diabase and gabbro intrusives likely were funnelled through conduits created by this rifting event and kimberlite magmatism is likely to have exploited these same features.

The surficial geology of the southern portion of the project area is dominated by lodgment and ablation till with significantly lesser amounts of glaciofluvial/glaciolacustrine sediments and organic deposits (Veillette, 1986), the latter occurring on the surface in narrow valleys between prominent *roche moutonnée*. In contrast, glaciofluvial/glaciolacustrine deposits dominate the area west, north and northwest of New Liskeard. Ice flow indicators such as striations are biased south-southeast, the last direction of ice movement during deglaciation in the late Wisconsin (23,000 to 10,000 years before present; Veillette and McClenaghan, 1996). However, surficial mapping and dispersal train studies completed over the past decade indicate that glacial ice initially flowed to the southwest, and it is postulated that this phase was the dominant ice flow direction in terms of bedrock molding and mineral dispersal (Veillette, 1989). Averill and McClenaghan (1994) agree with the theory that south-southeast flow is less influential in terms of mineral dispersal, however they suggest that dispersal in this direction is important in regions where a thin blanket of till mantles abundant outcrops and where glaciofluvial sediments such as eskers are oriented south-southeast. These conditions appear to be the case in the area investigated by Temex, so the dominant ice flow direction is likely to have been south-southeast, but the possibility of southwest movement should also be considered.

5.0 Diamond Drilling Program

From May 20 to June 15, 2008, a drill program was conducted on the diamondiferous KRVY kimberlitic breccia body, previously discovered in 2006 with drill hole TD-06-03, with the intent to define its character and shape. Four holes TD-08-07 to TD-08-10, aggregating to 1,646 metres were drilled on the KRVY target. Kimberlitic and volcanic breccia material was intersected in three of four holes. Following detailed petrographic and electron microprobe examination, samples will be selected, split and sent for caustic fusion analysis.

5.1 Procedures

Drill hole locations are shown generally on Figure 2 and in more detail on the claim plan in Appendix 1. Figure 3 presents the drill plan in relation to the anomaly resulting from the ground magnetic survey conducted by Temex in 2007 (RDF Consulting Ltd., 2007); data from that survey was collected at 5 metre station spacings on lines that were 25 metres apart. Drill statistics and UTM coordinates (NAD 27, UTM Zone 17) of drill holes are listed in Table 1. The results of the previous drill hole on the KRVY target is documented in Rees, 2007 though information for drill hole TD-06-03 is included in this report for reference and because that hole was re-logged during this program in order to be consistent with the logging of the new drill holes. All holes were drilled on claim 3007432.

Table 1: 2008 Drilling Statistics

Drill hole	UTM East	UTM North	Azimuth	Dip	Length (m)
TD-06-03	593311	5238492	134	-45	353
TD-08-07	593442	5238577	180	-45	282
TD-08-08	593365	5238528	180	-60	504
TD-08-09	593275	5238300	042	-60	224
TD-08-10	593209	5238353	060	-55	636
Total drilled in 2008					1,646

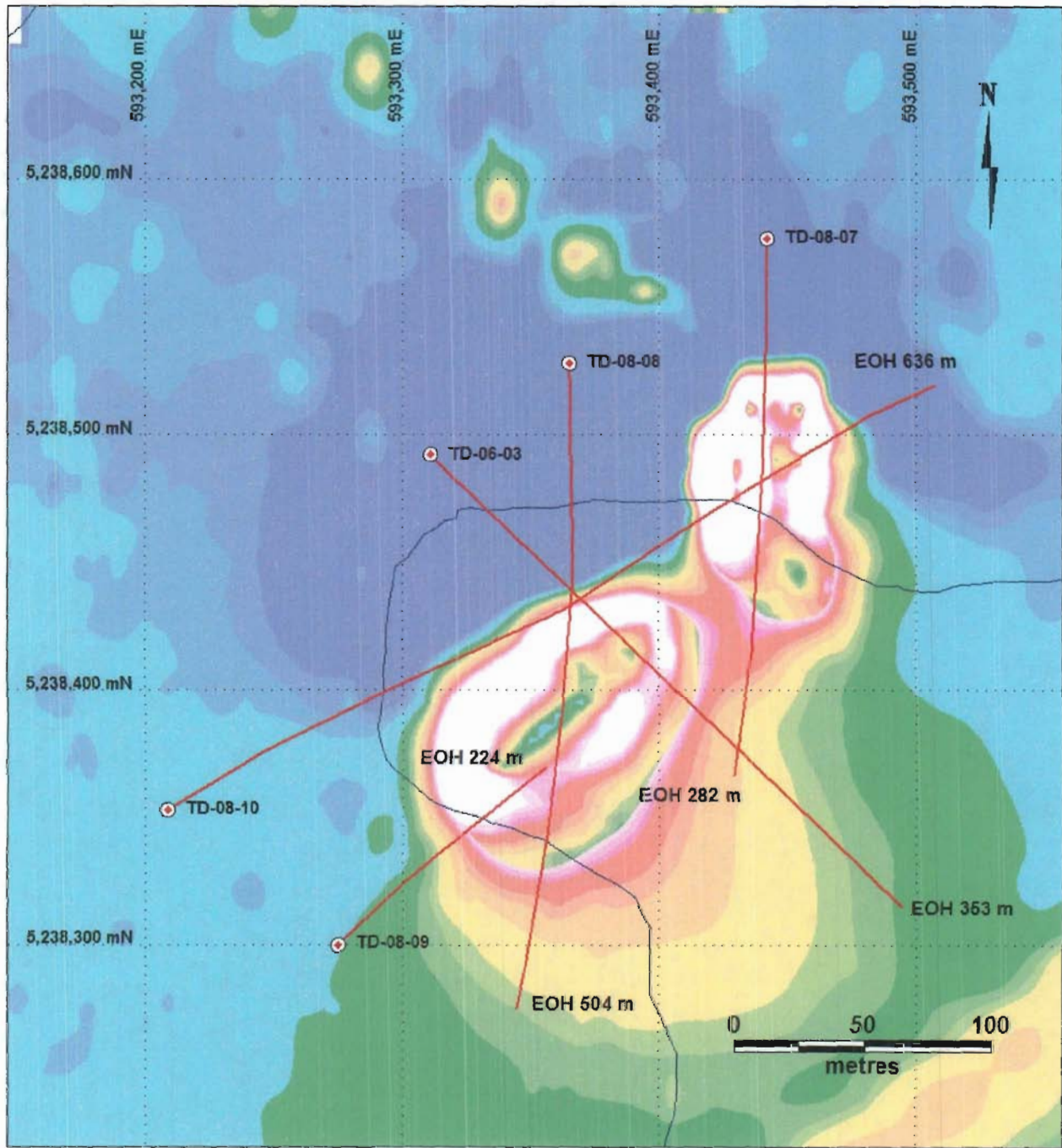
Drill collars were located utilizing the Garmin Handheld GPS units and checking/chaining from known topographic feature locations and from a ground grid established for the 2007 magnetometer survey (RDF Consulting Inc., 2007). Azimuth at the drill collar was established utilizing compass measurements and both back and fore sites. Flex-it tests were taken down the hole to read the dip and azimuth.

Core boxes were individually secured with fiber tape and transported by truck to the Temex field office where core processing was executed in the secure facility. Each box of drill core was photographed for permanent record with a digital camera. During logging, representative samples of each phase were collected for petrologic studies. The core boxes are stored in the locked Temex facility in Temagami North.

Upon removal of the drill from each site, the site was cleaned of debris and the drill collars were marked with a wooden picket placed at the collar location.

The drill hole location plan is presented in Appendix 1, drill sections are presented in Appendix 2, and drill hole lithological logs and magnetic susceptibility logs are included in Appendix 3.

Figure 3: General Location of Drill Holes on Ground Magnetic Survey Data



5.2 Work Performed

Four holes, totalling 1,646 metres were completed, including mobilization and logging of core from May 20 to June 15, 2008. The diamond drilling was performed by Forage M. Lafreniere Inc. of Nedelec, Quebec with the drill mobilized via tractor trailer equipment. The equipment used consisted of a tractor-pulled diamond drill equipped with NQ-size drill rods which recovered 49 mm diameter core. The drill crew consisted of two drillers, two helpers and a foreman.

The drill program was planned by Ian Campbell, P.Geo., President and CEO, and Karen Rees, P.Geo., General Manager. Field logistics and hold spotting was managed by Richard Brett, Senior Technician. Drill core was logged by Eric Potter, consulting geologist. Maps and sections were prepared by Karen Kettles, P.Geo., GIS Specialist.

5.3 Drill hole Discussion

Three of the four holes drilled during this campaign intersected at least one unit of ultramafic, carbonate-bearing, volcanoclastic breccias. Within each intersection, there are intrusive contacts suggestive of multiple intrusions or phases within the KRVY body (previously intersected by TD-06-03). From the initial drill core logging, at least four intrusive phases are noted:

1. A clast-dominated (60-90 modal %) heterolithic, carbonate-bearing volcanoclastic breccia characterized by abundant, rounded clasts set in a calcite or light-green carbonate-rich matrix. At least one potential mantle nodule was noted from this unit.
2. A matrix-supported (30-50 modal %), heterolithic carbonate-bearing volcanoclastic breccia characterized by subangular-to-rounded clasts, that display varying degrees of iron alteration/oxidation. The clasts are set in a light to dark green-grey matrix that is rich in carbonate (reacts well to HCl). These units often display intense iron alteration and corrosion of the matrix material- especially along the unit contacts. At least one potential mantle nodule was noted from this unit.
3. A segregation-textured, intrusive unit immediately distinguished by the presence of ubiquitous lapilli-like spheres (40-70 modal %). The 'lapilli' are surrounded by calcite creating a segregation-like texture in a light green, carbonate-rich matrix. The 'lapilli' segregations are often cored on ilmenite or magnetite, and a bright green mineral, possibly Cr-diopside.
4. Fine-grained to aphanitic, ultramafic porphyritic phases which cross-cut the earlier intrusive phases in small (<2 metre wide) dykes, which exhibit good intrusive contacts. These dykes are strongly magnetic and contain highly iron-altered (typically <1 cm) clasts.

Detailed petrography followed by analysis of heavy-mineral concentrates should be done to confirm these preliminary observations and rule out the possibility that these intrusive phases may represent ultramafic lamprophyre dykes and/or a carbonatitic intrusions rather than a kimberlite body. Table 2 lists the samples taken for petrographic examination which will be reported on at a later date.

Table 2: Samples Taken for Petrographic Examination

Drill hole and Sample Number	Depth (m)	Comment
TD-08-07-112	112.42	clast-supported volcanoclastic breccia
TD-08-07-114	114.22	porphyritic dyke #7-1 (centre)
TD-08-07-121	121.7	porphyritic dyke #7-4 (upper contact)
TD-08-07-197	197.6	porphyritic dyke #7-5 (centre)
TD-08-07-202	202.35	strongly altered volcanoclastic breccia
TD-08-08-149	149.0	alteration of host siltstone at contact with volcanic breccia
TD-08-08-162	162.5	possible mantle nodule with reaction rim
TD-08-08-172	172.59	clast-supported volcanoclastic breccia
TD-08-08-203	203.1	coarse calcite in matrix of volcanic breccia
TD-08-08-234	234.77	fine-grained dyke #8-1
TD-08-08-250	250.7	fine-grained dyke #8-2
TD-08-08-381	381.05	fine-grained dyke #8-4
TD-08-08-382	381.8	lower contact of fine-grained dyke #8-4 with host diamictite
TD-08-08-391	391.25	upper contact of fine-grained dyke #8-6 with host diamictite
TD-08-08-392	391.47	centre of fine-grained dyke #8-6
TD-08-08-399	399.07	upper contact of lapilli-rich volcanoclastic breccia with host diamictite
TD-08-08-421	421.42	lapilli-rich volcanoclastic breccia
TD-08-08-430	430.69	lapilli-rich volcanoclastic breccia
TD-08-08-434	434.18	lapilli-rich volcanoclastic breccia
TD-08-08-444	444.26	lapilli-rich volcanoclastic breccia
TD-08-10-302	302.79	volcanic breccia
TD-08-10-306	306.62	volcanoclastic breccia
TD-08-10-331	331.37	volcanoclastic dyke
TD-08-10-332	332.4	clast-supported volcanoclastic breccia with minor lapilli
TD-08-10-386	385.95	clast-supported volcanoclastic breccia
TD-08-10-410	410.75	volcanoclastic breccia
TD-08-10-421	421.65	volcanoclastic breccia

DDH TD-08-07

Heterolithic, carbonate-bearing volcanoclastic breccias were encountered in drill core from 82 metres to 203 metres downhole depth. Above the volcanoclastic unit, the rocks consist of Huronian-aged sediments such as parallel laminated siltstones, mudstones and arkosic arenites. Approaching the contact with the carbonate-bearing volcanoclastic unit, an increase in calcite stringers and fracturing was noted, culminating in the presence of a light-green, carbonate- and mica-bearing vein just above the contact. Below the volcanoclastic intersection, another thin unit of parallel laminated siltstone was followed by a thin unit of diamictite that was underlain by a relatively thin Nipissing diabase sill or dyke (~29 metres). Contacts with the diabase suggest either a vertical dyke or horizontal sill. Below the diabase, 30 metres of diamictite were drilled before termination of the hole.

Both upper and lower contacts of the volcanoclastic breccia displayed intense iron alteration and decomposition of the core, almost to a gravel-rubble in places. Within the large volcanoclastic intersection, a minimum of three intrusive phases were noted. These phases were distinguished macroscopically by clast content, matrix colour, grain size and carbonate abundance. Below is a brief macroscopic summary of each phase.

The first phase (earliest?) is a clast-supported (≤ 80 modal % clasts), carbonate volcanoclastic breccia consisting of rounded-to-subangular clasts set in a light grey, calcite-rich matrix. The clasts display minor iron alteration/oxidation and at least two possible mantle nodules were noted at 120.10 metres and 106.69 metres depth. A minor modal abundance (<5%) of juvenile lapilli were noted, consisting of a fine-grained rim of biotite-rich matrix material cored on either an ilmenite, pyroxene or biotite crystal. The matrix cementing the clasts together is either: a white-to-rose coloured calcite, or a light grey-green carbonate-bearing matrix. The light grey-green matrix is comprised of 5-10% biotite, trace amounts of ilmenite (including rare macrocrysts), trace pyrite all set in a fine-grained, carbonate-bearing groundmass. This unit was typically non-magnetic.

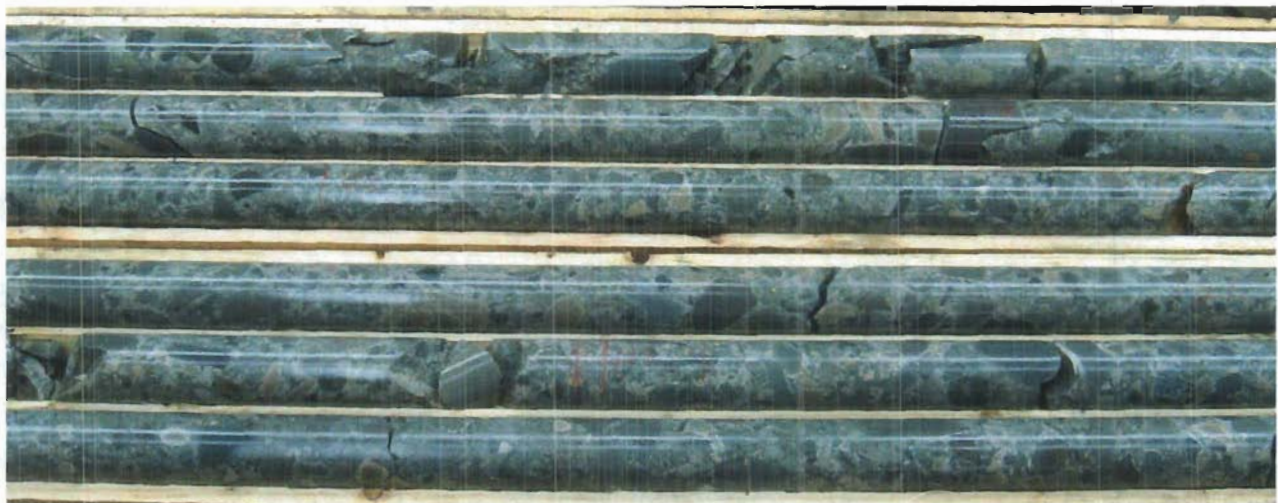


Image 1: Photograph of clast-supported ($\leq 80\%$) volcanoclastic phase one. Note the high modal abundance of rounded clasts and the interstitial calcite cement.

The second phase is matrix-supported (30-50 modal % clasts), heterolithic carbonate-bearing volcanoclastic breccia. Subangular-to-rounded clasts display varying degrees of iron alteration/oxidation, with well-developed patinas. The clasts are set in a light to dark green-grey matrix that is rich in carbonate (reacts well to HCl). The unit contacts display intense iron alteration and corrosion of the matrix material which gradually decreases with depth (see Image 2). Minor (<5%) juvenile lapilli were noted to consist of fine-grained, biotite-rich matrix material cored on either an ilmenite, pyroxene or biotite crystal. The breccia matrix contains 5-10 modal % biotite phenocrysts and macrocrysts, trace ilmenite (with rare macrocrysts), trace magnetite (<0.5 mm) and ultratrace pyrite all hosted within a green, carbonate-rich groundmass. Due to the presence of magnetite, this unit is strongly magnetic.

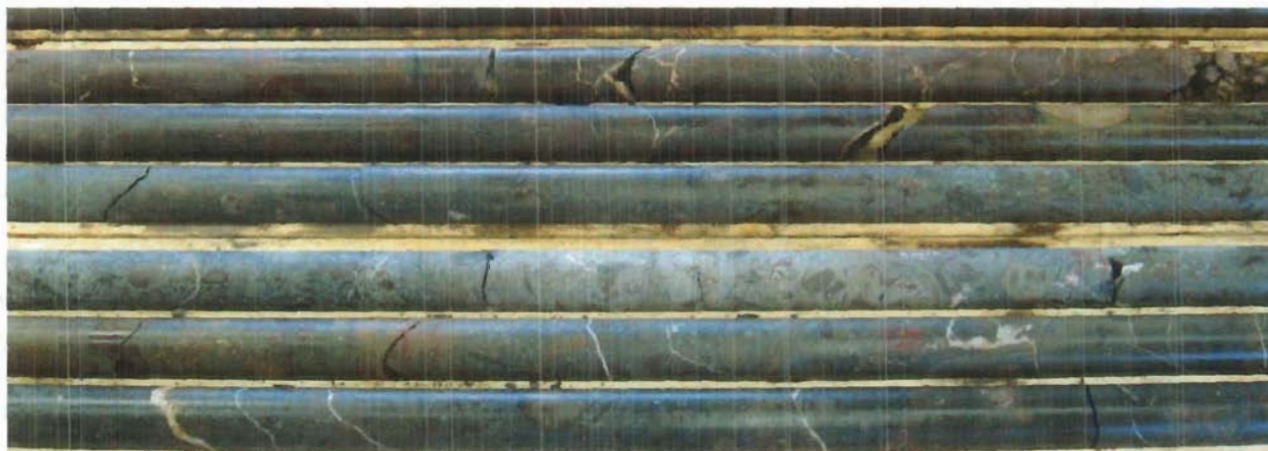


Image 2: Photograph of matrix-supported, volcanoclastic breccia with iron-altered subangular to rounded clasts set in a light to dark green-grey matrix (phase two). Notice the decreasing iron alteration and change in matrix colour. The unit is strongly magnetic and is cross-cut by late calcite stringers.

The third phase consists of matrix-supported (<20 modal % clasts), carbonate volcanoclastic dykes which crosscut both of the early phases. This unit contains rounded clasts typically <1 cm in diameter which have an iron alteration/reaction rim. The groundmass is fine-grained, inequigranular porphyritic in texture with rounded biotite and ilmenite macrocrysts set in a light-grey matrix. Also noted on the matrix were small, serpentinized phenocrysts (possibly olivine or pyroxene) and a euhedral-hexagonal, light-green mineral (likely apatite). These dykes are extremely magnetic and typically less than 1 metre in width. They are also cross-cut by late-stage calcite stringers intersecting the core at approximately 40 degrees to the core axis. This unit is similar to phase four from TD-08-08.



Image 3: Photograph of fine-grained, matrix-supported (<20% clasts), volcanoclastic dyke crosscutting both the early phases of volcanoclastic breccia (similar to phase four in TD-08-08).

DDH TD-08-08

Two carbonate-bearing, volcanoclastic intersections were encountered in the drilling at 150-269 metres and again at 347-472 metres. Above the first volcanoclastic breccia intersection, the country rocks consist of Huronian-aged arkosic arenites, and parallel laminated siltstone and mudstones. Approaching the contact, an increase in light-green carbonate-bearing veinlets was noted, culminating in a 1.3 metre wide zone of intense iron alteration/oxidation and light green carbonate veining. In between the two volcanoclastic intersections a thin (~40m) Nipissing diabase sill is sandwiched by two Gowganda Formation diamictite units. The lower diamictite unit is characterized by abundant matrix-supported kimberlitic dykes and associated iron alteration. Below the lower volcanoclastic unit (347-472 metres) another unit of Gowganda Formation diamictite was intersected; approximately 31 metres into this diamictite unit the drill hole was terminated. As with TD-08-07, several intrusive phases were noted within the two volcanoclastic breccia intersections. These were visually distinguished based on clast content, intrusive contacts, matrix colour, textures and carbonate content. Below is a summary of the major phases.

Phase one is a clast-supported (40-90 modal % clasts), heterolithic, carbonate-bearing volcanoclastic breccia characterized by the occasional presence of interstitial white calcite. The clasts are primarily rounded to subangular in habit and do not display any indication (macroscopic) of the intense iron alteration visible in the other phases. Alteration of the clasts, when present, is a mild discolouration or carbonate-bleaching creating a patina. Minor juvenile lapilli (<5-10%) occur throughout the unit in varying concentrations. The white interstitial calcite occurs primarily near the country rock contacts and decreases in abundance away from the contact. In addition to the white calcite, the breccia matrix is also comprised of a light to dark green

carbonate-bearing groundmass that hosts 5-10% fine-grained, biotite phenocrysts, minor (<5%) magnetite grains, trace potential ilmenite and possible trace apatite. The unit is non-magnetic (calcite-rich) to weakly magnetic (green matrix). This unit is macroscopically similar to phase one in TD-08-07.



Image 4: Photograph of clast-supported (40-90%) heterolithic breccia with white interstitial calcite and rounded to subangular clasts (phase one).

Phase two is characterized by less abundant, more iron-altered clasts set in a dark green to grey matrix. The clast content is slightly variable (30-70 modal %) and displays a higher degree of iron alteration and/or assimilation by the magma. Trace amounts (<5%) of juvenile lapilli were noted. The dark coloured matrix is carbonate-rich and hosts 5-10% rounded biotite grains (<2 mm), trace (<2%) rounded magnetite, trace ilmenite, trace potential apatite and ultratrace pyrite. A few zones displayed increased iron alteration and corrosion of the core, but otherwise the unit is homogenous. The matrix is strongly magnetic and reacts well to dilute HCl. This unit is macroscopically similar to phase two from TD-08-07.



Image 5: Photograph of the matrix-supported volcanoclastic breccia with subangular, iron-altered clasts set in a dark grey-green matrix (phase two).

Phase three is characterized by a dramatic increase in the abundance of juvenile lapilli (40-90%) surrounded by white calcite, creating segregation texture. The unit contains variable clast contents (5-40%), all of which are intensely iron-altered and corroded. The ubiquitous juvenile lapilli are dark green in colour, are biotite-rich, carbonate-bearing and contain trace amounts of serpentinized pseudomorphs. The lapilli are typically not cored, but when present, the core is comprised of possibly an ilmenite, pyroxene or a biotite grain (with a few potential Cr-diopsides). In addition to calcite, a light-green matrix also hosts the lapilli. When present, this breccia matrix contains minor biotite, trace magnetite and trace ilmenite. Late calcite stringers cross-cut the unit at 10-30 degrees to the core axis. The unit is strongly magnetic. This unit is similar to phase three from TD-08-10.



Image 6: Photograph of the lapilli-rich, segregation-textured volcanoclastic breccia with rounded juvenile lapilli surrounded by calcite (phase three).

Phase four is characterized by late-stage, fine-grained porphyritic dykes crosscutting the earlier volcanoclastic units. The dykes are light-to-medium grey in colour and contain late-stage white-to-rose coloured calcite stringers. Also immediately obvious in some of the dykes is the presence of aphanitic banding that runs parallel to the intrusive contacts (see image 7). The dykes are matrix-supported, containing less than 10 modal %, iron-altered and corroded clasts that are typically under 1 cm in diameter. Within the fine-grained groundmass, minor serpentinized phenocrysts were noted. In some of the dykes, abundant, fine-grained biotite grains were present in as much as 10 modal %, with lesser amounts of magnetite and potential ilmenite. A few potential pyrope garnets were noted within these dykes on freshly broken surfaces. The unit is strongly magnetic and is macroscopically similar to phase three from TD-08-07.

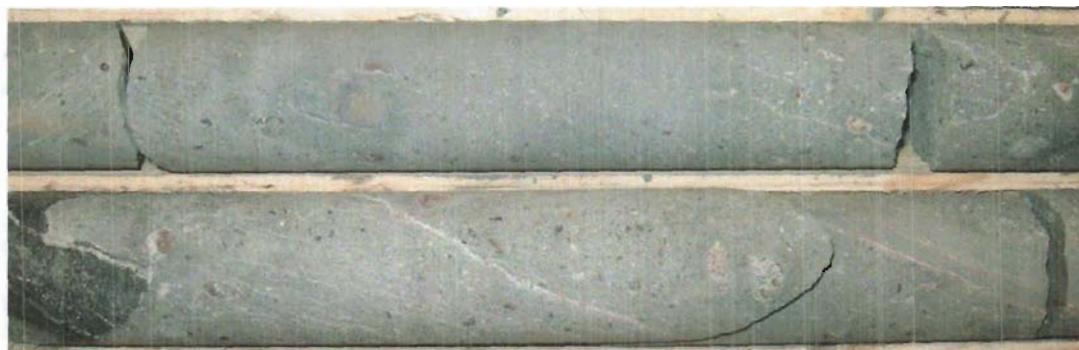


Image 7: Photograph of the fine-grained, matrix-supported, porphyritic volcanoclastic dyke (phase four) with aphanitic banding running parallel to the dyke contacts (also defined by calcite stringers).

DDH TD-08-09

Although no ultramafic or carbonate-bearing volcanoclastic units were intersected by the drilling of hole TD-08-09, a section of drill core (176-180 metres) was not recovered at the contact between the intrusive Nipissing diabase and Gowganda Formation diamictite. The few gravel-sized fragments/rubble that were recovered did show evidence of a light-green carbonate alteration/veining that has been associated with the volcanoclastic dykes in the previous diamond drill holes. Such evidence is suggestive that the volcanoclastic dykes were proximal to the drill hole and/or that the brecciated contact between the two lithological units was a conduit for fluid migration. Furthermore, in drill hole TD-08-08 a second volcanoclastic breccia was encountered beneath the Nipissing diabase sill.

DDH TD-08-10

Phase one is a clast-supported, carbonate-bearing volcanoclastic breccia characterized by abundant, predominantly rounded clasts set in a calcite and light green, carbonate-bearing matrix. The interstitial white calcite matrix increases in abundance approaching contacts or large clasts (such as the quartzite 'clast' at 337-350 metres). Minor (5-10%) juvenile lapilli were noted throughout the unit, often iron-altered/oxidized to a dark red colour. Some lapilli contain cores of ilmenite, pyroxene or biotite and host <1 mm serpentinized grains. The clasts also exhibit moderate iron alteration and are often corroded. When present, the green matrix material hosts minor (~5%) biotite, trace magnetite, and trace potential ilmenite. The unit is non-magnetic except for the occasional magnetite grain. This phase is macroscopically similar to phase one from TD-08-07 and TD-08-08.



Image 8: Photograph of clast-supported volcanoclastic breccia (phase one) illustrating interstitial calcite, dark red (iron-altered) lapilli and rounded clasts.

Phase two has less abundant clasts than phase one (30-60% clasts) and is primarily matrix-supported. The subangular clasts tend to display more iron alteration/oxidation and are heavily corroded in places. The carbonate-rich matrix is a dark green to dark grey colour. Lapilli are abundant along the contacts of the unit and decrease towards the center (20 to 5 modal %). When abundant, the lapilli are surrounded by calcite (faint segregation texture). The lapilli and matrix contain minor biotite (5-10%), trace subeuhedral magnetite and trace potential ilmenite (grains 2-4 mm in length). Smaller intrusive dykes of phase two display faint indications of flow-alignment of clasts and cross-cut the phase one, clast-rich volcanoclastic breccia. This unit is strongly magnetic and is similar to phase two of TD-08-08 and TD-08-07.



Image 9: Photograph of phase two (TD-08-10) illustrating the matrix-supported texture and iron alteration of the subangular clasts.

Phase three is matrix-supported (10-15% clasts) with abundant juvenile lapilli (30-50%) set in a calcite and dark grey, carbonate-rich matrix. When lapilli are abundant, calcite surrounds the lapilli creating segregation texture. The lapilli and very fine-grained, green matrix contains 5-10% biotite grains (<3 mm), trace subeuhedral magnetite, trace potential ilmenite and ultratrace pyrite. Some of the lapilli are cored on ilmenite, biotite or pyroxene grains and contain minor serpentine pseudomorphs. This unit is macroscopically similar to phase three from TD-08-08; albeit with slightly less juvenile lapilli.



Image 10: Photograph of phase three volcaniclastic breccia from TD-08-10 illustrating the lapilli-rich nature of the unit (and segregation textures) and dark red, iron-altered clasts.

6.0 Conclusions and Recommendations

The 2008 drill program consisted of four diamond drill holes aggregating to 1,646 metres. Three out of the four holes intersected at least one unit of ultramafic, carbonate-bearing, volcanoclastic breccias. In each hole there are intrusive contacts suggestive of multiple intrusions or phases with the KRVY body. In addition it is concluded that the KRVY body has a very complex shape and morphology as evidenced by the multiple phases and numerous narrow dykelets.

Due to the presence of multiple phases in the KRVY body, as apparent from the 2008 drill program, several samples were selected for petrographic study. It is recommended that these samples be examined to definitively determine the rock types in each of the four phases. The magnetic susceptibility data collected at one metre intervals down each hole should be modeled and considered with the lithological and petrographic data in an attempt to determine the horizontal and vertical extents, as well as the orientation of the KRVY body.

It is recommended that sample intervals based on the phases, noting particularly the proportion of clasts versus matrix, be selected and split off the core to be sent for caustic fusion analysis. In 2006, six micro-diamonds were recovered by caustic fusion analyses of 285.55 kilograms of fragment-rich breccia material intersected in TD-06-03. The largest of the recovered stones sat on the 0.150 millimetre screen and is a fragment of a transparent white diamond measuring 0.48 millimetres in one dimension; a second large stone, also recovered on the 0.150 millimetre screen, measures 0.35 millimetres in one dimension and is also a fragment of a transparent white diamond. These two diamond fragments indicate the probability that larger stones exist at KRVY. The other three micro-diamonds recovered had octahedroid and cuboid crystal shapes.

The discovery of the KRVY diamondiferous body has expanded the Timiskaming Field 20 kilometres southward and demonstrates the high discovery potential of the area and in particular the Latchford Diamond Project.

7.0 References

- Armstrong, K. A., Nowicki, T. E. and Read, G. H. 2004 Kimberlite AT56: a mantle sample from the north central Superior craton, Canada. Special Issue, Selected Papers from the 8th International Kimberlite Conference, Victoria, BC, 22-27 June 2003, Volume 2: The J. Barry Dawson Volume, 695-704.
- Averill, S. A. and McClenaghan, M. B. 1994 Distribution and character of kimberlite indicator minerals in glacial sediments, C14 and Diamond Lake kimberlite pipes, Kirkland Lake, Ontario. Geological Survey of Canada, Open File 2819, 48 p.
- Bennett, G., Dressler, B.O. and Robertson, J.A. 1991 The Huronian Supergroup and associated intrusive rocks. *In* Geology of Ontario, Ontario Geological Survey, Special Volume 4, Part 1, pp.549-591.
- Easton, R.M. 1992 The Grenville Province and the Proterozoic history of central and southern Ontario. *In* Geology of Ontario, Ontario Geological Survey, Special Volume 4, Part 2, pp.714-904.
- Fugro Airborne Surveys Corp. 2006. Midas High Resolution Magnetic Geophysical Survey for Temex Resources Corp. Cobalt Area, Ontario 31L13, 31M/4,5,12 and 41P/8. May 9, 2006.
- Jago, B.C. 2006. Temex Resources Corp. Wilson Lake Diamond Project 2005 Till Sampling Program Summary, Temagami-New Liskeard Area, Ontario, Sudbury and Larder Lake Mining Division, Ontario. July 31, 2006.
- Grütter, H. S., Gurney, J. G., Menzies, A. and Winter, F. 2004 An updated classification scheme for mantle-derived garnet, for use by diamond explorers. Special Issue, Selected Papers from the 8th International Kimberlite Conference, Victoria, BC, Canada, 22-27 June 2003, Volume 2: The J. Barry Dawson Volume, 819-840.
- McClenaghan, M. B., Kjarsgaard, I. M. and Kjarsgaard, B.A. 2001 Reconnaissance-scale Till Survey in the New Liskeard-Temagami-Region, Ontario: Kimberlite Indicator Mineral and Geochemistry; Geological Survey of Canada, Open File 4086.
- Morris, T. F. and Kaszycki, C. A. 1995 A prospector's guide to drift prospecting for diamonds, northern Ontario. Ontario Geological Survey, Open File Report 5933, 110 p.
- RDF Consulting Ltd. 2007 Logistical Report for Magnetometer Geophysical Surveys Performed on the Hearst Lake Area, New Liskeard, Ontario for Temex Resources Corp.
- Rees, K. 2007 Report on the 2006 Diamond Drilling Program (TD-06-03) Wilson Lake and Latchford Diamond Project, Temagami-New Liskeard Area, Ontario. Larder Lake Mining Division, Ontario NTS 31M/05. Temex Resources Corp.
- Reid, J.L. 2002 Regional Modern Alluvium Sampling Survey of the Mattawa-Cobalt Corridor, Northeastern Ontario; Ontario Geological Survey, Open File Report 6088, 235p.
- Sage, R.P. 1996. Kimberlites of the Lake Timiskaming Structural Zone. Ontario Geological Survey Open File Report 5937, 435 p.
- Sage, R.P. 2000 Kimberlites of the Lake Timiskaming Structural Zone: supplement. Ontario Geological Survey Open File Report 6018, 123 p.
- Schulze, D.J. 1996 Kimberlites in the vicinity of Kirkland Lake and Lake Timiskaming, Ontario and Quebec. *In* Searching for Diamonds in Canada, *edited by* A.N. LeCheminant, D.G. Richardson, R.N.W. DiLabio, and K.A. Richardson. Geological Survey of Canada, Open File 3228, pp.73-78.
- Veillette, J.J. 1986 Surficial geology, Haileybury, Ontario-Quebec. Geological Survey of Canada, Map 1642A, scale 1:100,000.
- Veillette, J.J. 1989 Ice movement, till sheets and glacial transport in Abitibi-Timiskaming Quebec and Ontario. *In* Drift Prospecting, *edited by* R.N.W. DiLabio and W.B. Coker. Geological Survey of Canada, Paper 89-20, pp.139-154.
- Veillette, J.J. and McClenaghan, M.B. 1996 Sequence of glacial flows in Abitibi-Timiskaming; implications for mineral exploration and dispersal of calcareous rocks from the Hudson Bay basin, Quebec and Ontario. Geological Survey of Canada, Open File 3033, map scale 1:500,000.

Statement of Qualifications

I, Karen Joanne Rees, do hereby certify that:

1. I am employed as General Manager for Temex Resources Corp. with offices at 141 Adelaide Street West, Suite 1660, Toronto, Ontario M5H 3L5. 416-862-2246 phone.
2. I attended the University of Saskatchewan and graduated in 1984 with a Bachelor of Science (Honours) degree in Geology.
3. I have worked in the mineral exploration industry since 1987.
4. I participated in the planning of this program, the field supervision and collection of the data in this report.
5. I am a practicing Professional Geoscientist (P. Geo.) in good standing (2002) with the Association of Professional Geologists of Ontario (APGO).
6. I am a core member of the Prospectors and Developers Association of Canada (1997).

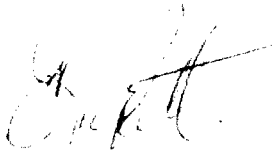


Karen Rees, B.Sc., P. Geo.
General Manager
Temex Resources Corp.

Statement of Qualifications

I, Eric Gordon Potter, do hereby certify that:

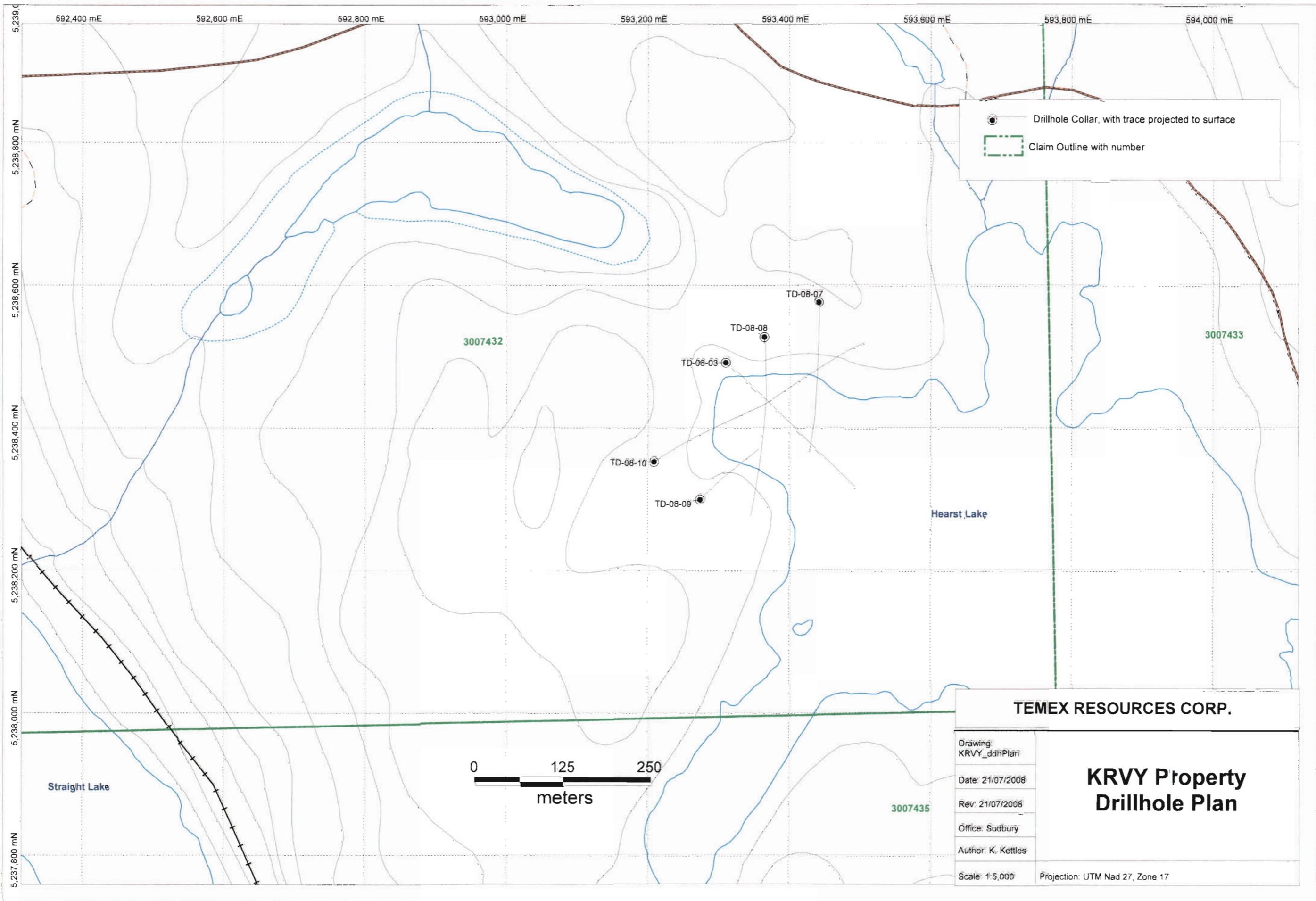
1. I am employed by Temex Resources Corp. as a consulting geologist with offices at 141 Adelaide Street West, Suite 1660, Toronto, Ontario M5H 3L5. Phone: 416-862-2246.
2. I attended Lakehead University and graduated in 2000 with a Bachelor of Science (Honours) degree in Geology and a Master of Science degree in Geology from the same institution in 2002.
3. I have worked as a consulting geologist in the mineral exploration industry since 2002.
4. I participated in the field supervision and collection of the data in this report.



Eric Potter
Ph.D. Candidate & Consulting Geologist
Carleton University
Ottawa, ON

Appendix 1

Drill Hole Location Plan on Claim

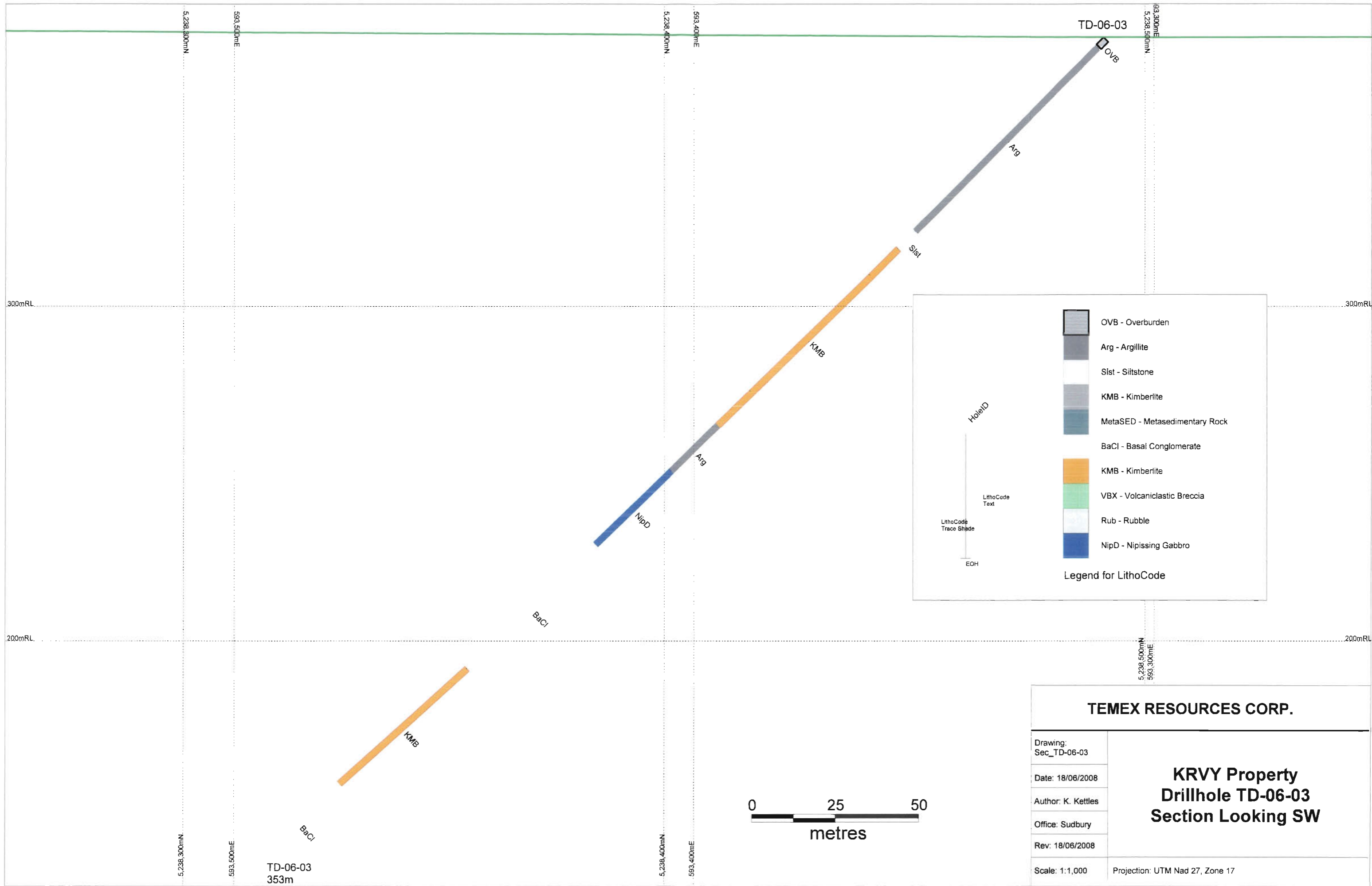


● Drillhole Collar, with trace projected to surface
 [Green dashed line] Claim Outline with number

TEMEX RESOURCES CORP.

Drawing: KRVY_ddhPlan	KRVY Property Drillhole Plan
Date: 21/07/2008	
Rev: 21/07/2008	
Office: Sudbury	
Author: K. Kettles	
Scale: 1:5,000	Projection: UTM Nad 27, Zone 17

Appendix 2
Drill Sections

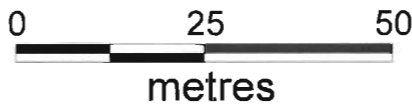


	OVB - Overburden
	Arg - Argillite
	Sist - Siltstone
	KMB - Kimberlite
	MetaSED - Metasedimentary Rock
	BaCl - Basal Conglomerate
	KMB - Kimberlite
	VBX - Volcaniclastic Breccia
	Rub - Rubble
	NipD - Nipissing Gabbro

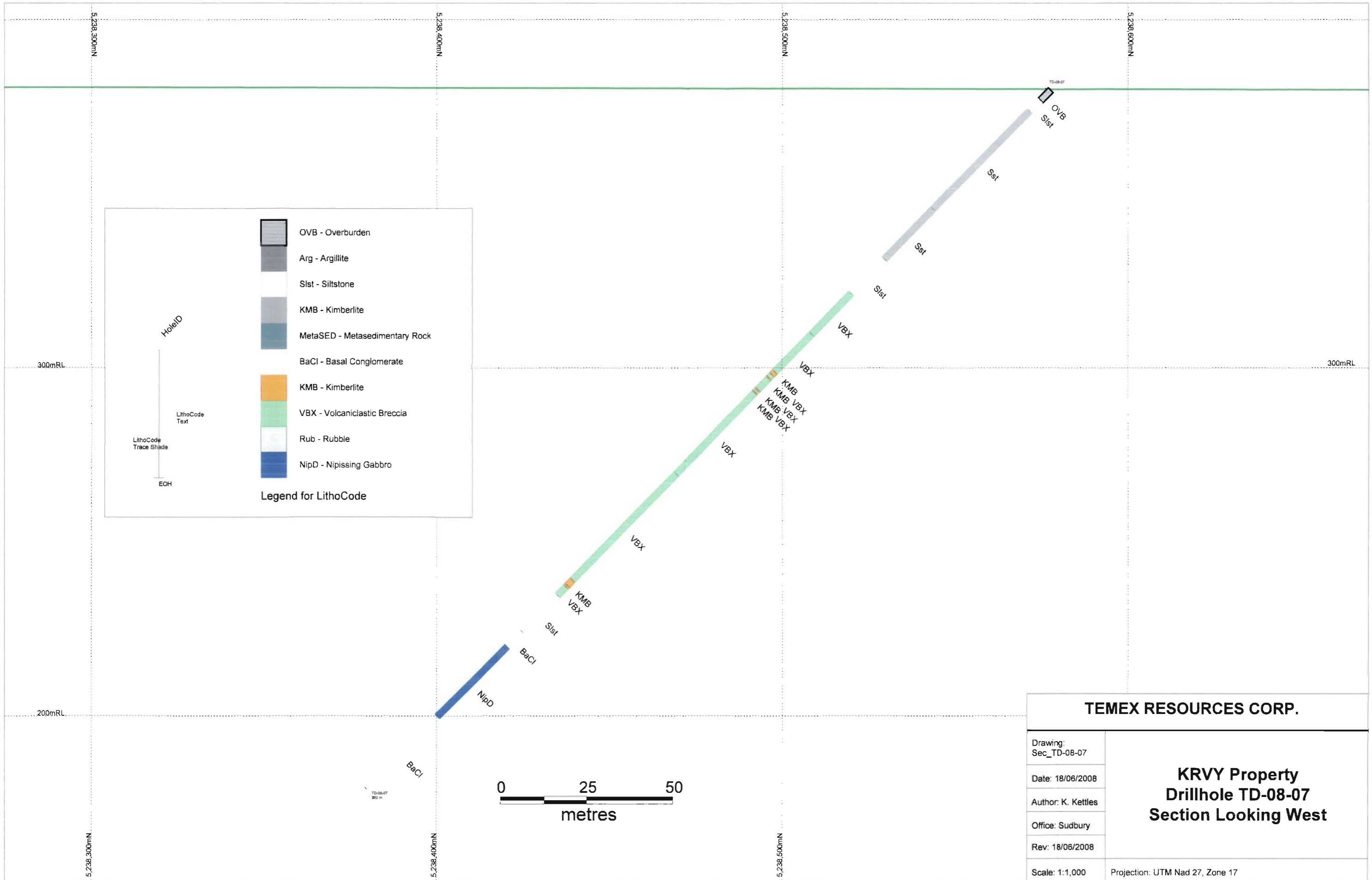
Legend for LithoCode

TEMEX RESOURCES CORP.

Drawing: Sec_TD-06-03	KRVY Property Drillhole TD-06-03 Section Looking SW
Date: 18/06/2008	
Author: K. Kettles	
Office: Sudbury	
Rev: 18/06/2008	
Scale: 1:1,000	Projection: UTM Nad 27, Zone 17



TD-06-03
353m

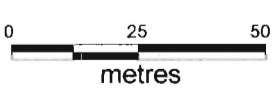
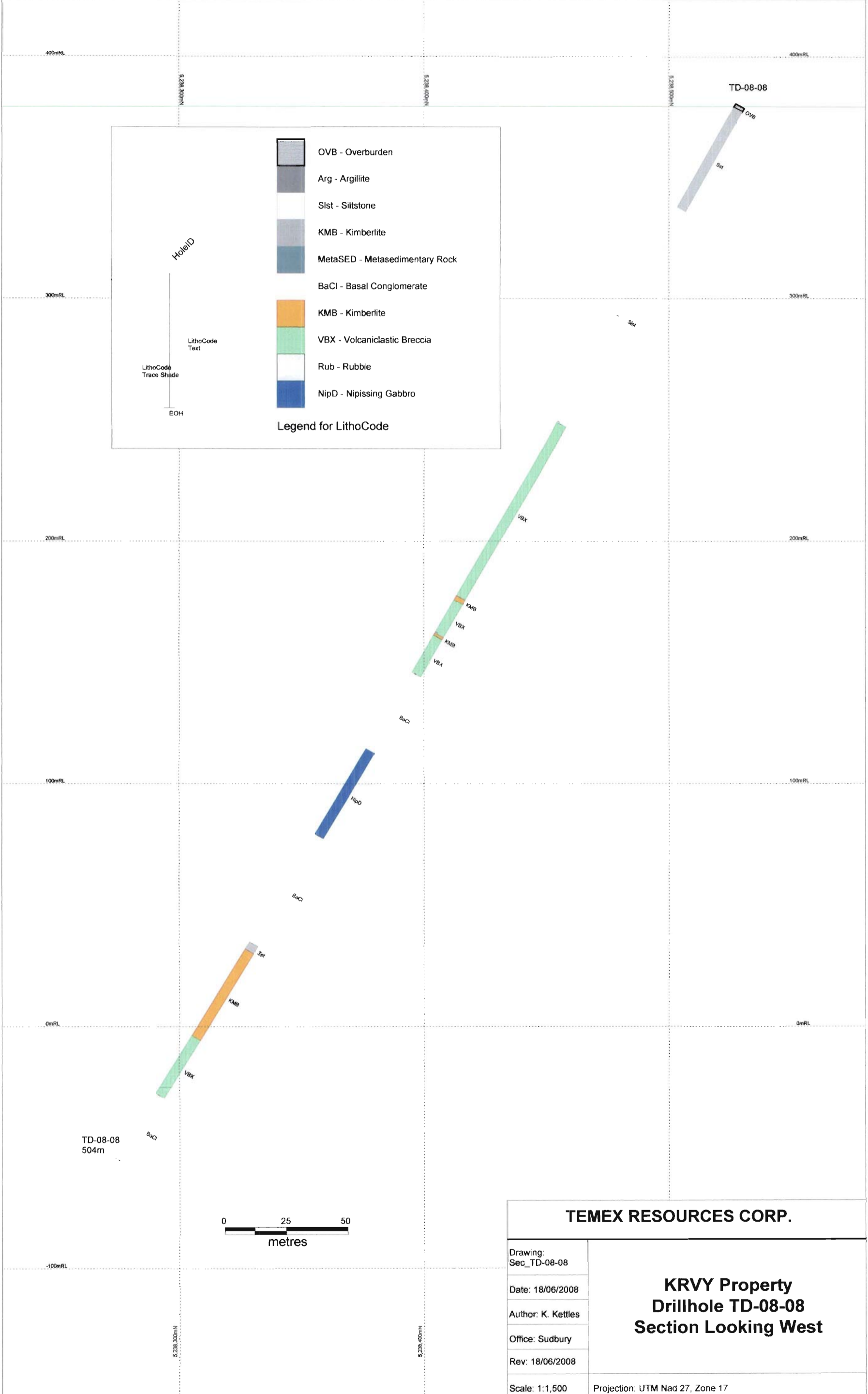
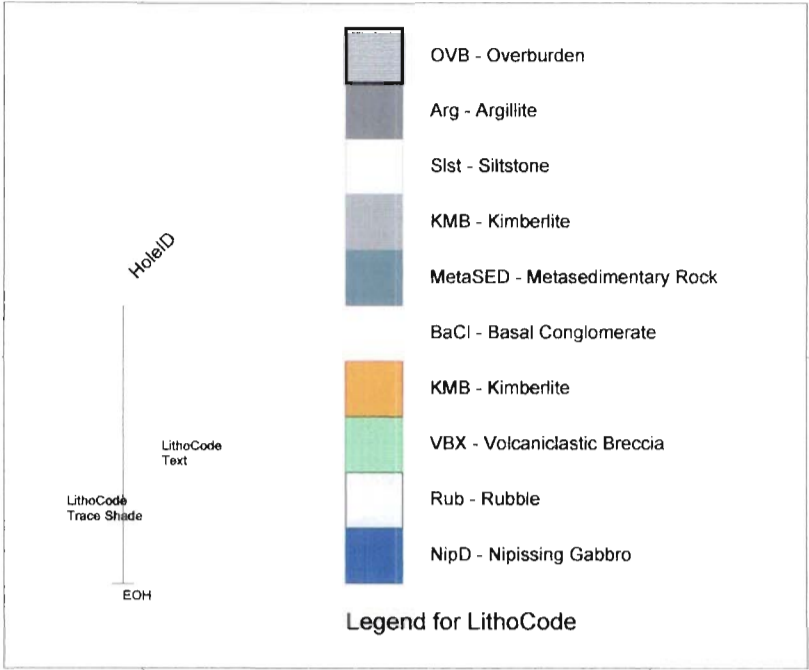


Legend for LithoCode

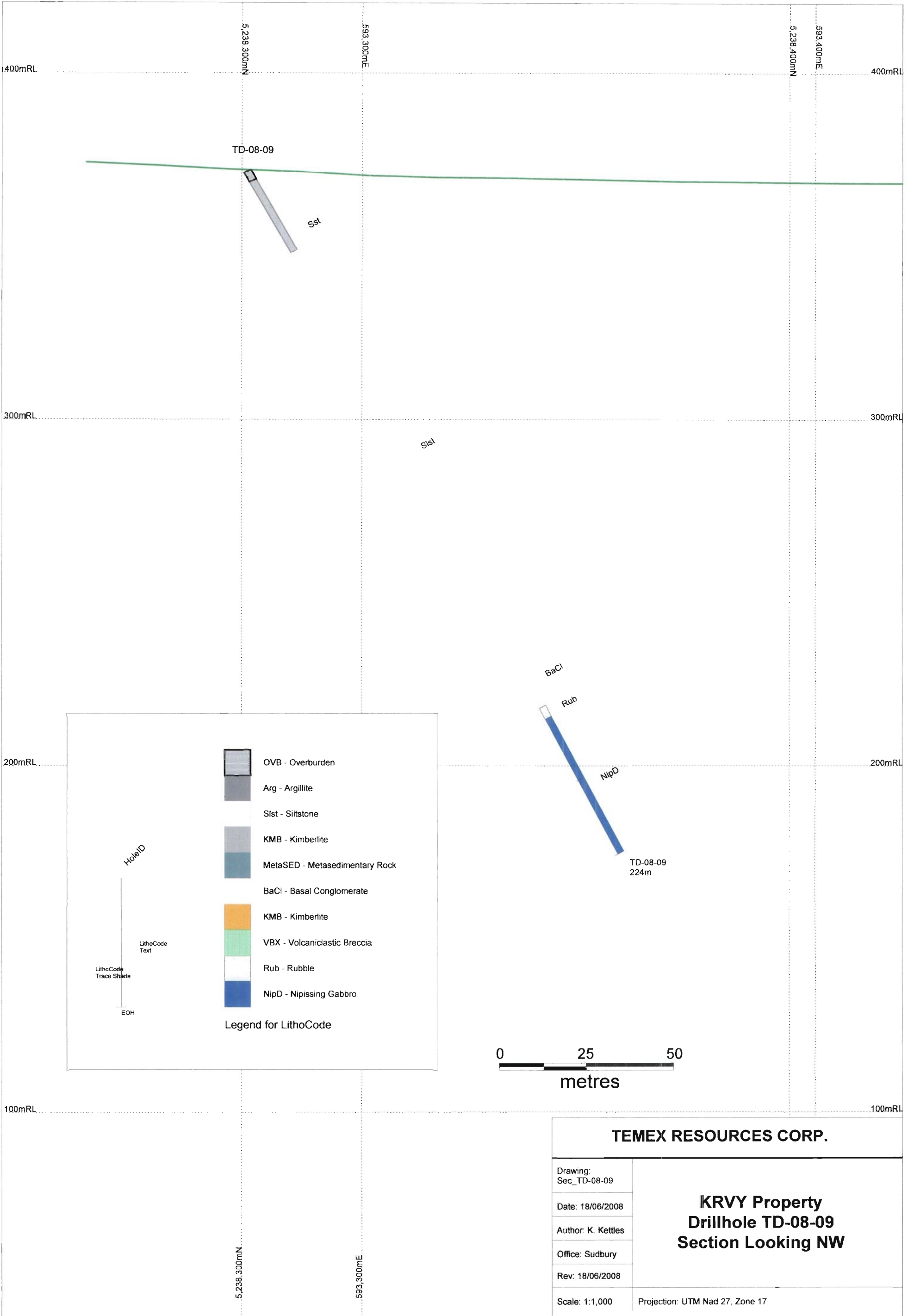
	OVB - Overburden
	Arg - Argillite
	Sst - Siltstone
	KMB - Kimberlite
	MetaSED - Metasedimentary Rock
	BaCl - Basal Conglomerate
	KMB - Kimberlite
	VBX - Volcaniclastic Breccia
	Rub - Rubble
	NipD - Nipissing Gabbro

HoleID
 LithoCode Text
 LithoCode Trace Shade
 EOH

TEMEX RESOURCES CORP.	
Drawing: Sec_TD-08-07	KRVY Property Drillhole TD-08-07 Section Looking West
Date: 18/06/2008	
Author: K. Kettles	
Office: Sudbury	
Rev: 18/06/2008	
Scale: 1:1,000	Projection: UTM Nad 27, Zone 17



TEMEX RESOURCES CORP.	
Drawing: Sec_TD-08-08	KRVY Property Drillhole TD-08-08 Section Looking West
Date: 18/06/2008	
Author: K. Kettles	
Office: Sudbury	
Rev: 18/06/2008	
Scale: 1:1,500	Projection: UTM Nad 27, Zone 17



	OVB - Overburden
	Arg - Argillite
	Sst - Siltstone
	KMB - Kimberlite
	MetaSED - Metasedimentary Rock
	BaCl - Basal Conglomerate
	KMB - Kimberlite
	VBX - Volcaniclastic Breccia
	Rub - Rubble
	NipD - Nipissing Gabbro

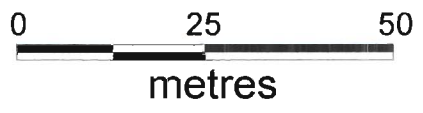
Legend for LithoCode

HoleID

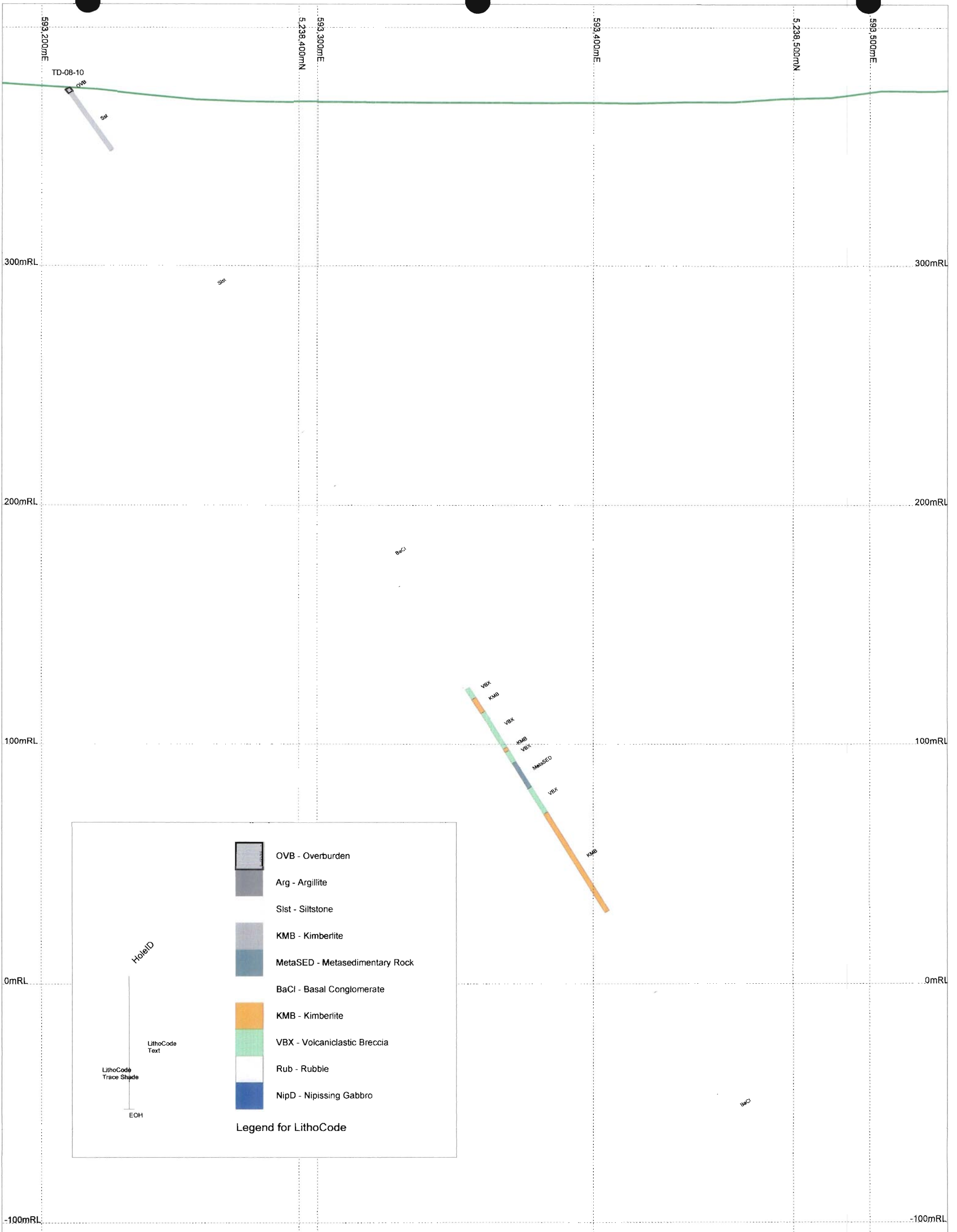
LithoCode Text

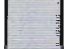








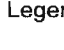
LithoCode Trace Shade

EOH



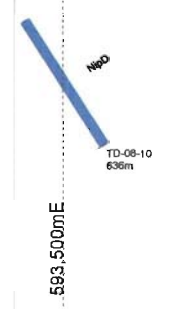
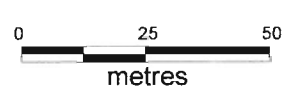
TEMEX RESOURCES CORP.	
Drawing: Sec_TD-08-09	KRVY Property Drillhole TD-08-09 Section Looking NW
Date: 18/06/2008	
Author: K. Kettles	
Office: Sudbury	
Rev: 18/06/2008	
Scale: 1:1,000	Projection: UTM Nad 27, Zone 17



HoleID		OVB - Overburden
		Arg - Argillite
		Slst - Siltstone
		KMB - Kimberlite
		MetaSED - Metasedimentary Rock
		BaCl - Basal Conglomerate
		KMB - Kimberlite
		VBX - Volcaniclastic Breccia
		Rub - Rubble
		NipD - Nipissing Gabbro

Legend for LithoCode

TEMEX RESOURCES CORP.	
Drawing: Sec_TD-08-10	KRVY Property Drillhole TD-08-10 Section Looking NW
Date: 18/06/2008	
Author: K. Kettles	
Office: Sudbury	
Rev: 18/06/2008	
Scale: 1:1,500	Projection: UTM Nad 27, Zone 17



Appendix 3

Drill Logs and Magnetic Susceptibility Readings

Hole_ID	TD-06-03	Hole_Type	DDH	<i>Purpose/Comments</i> Hole intersected two kimberlitic intrusions at depth; separated by a Nipissing Diabase sill and Gowganda diamictite. Upper KMB intersection is clast-supported whereas the lower KMB intersection is matrix-supported. Both units are fairly homogeneous with a few possible minor phases present differentiated based on clast-content, magnetism, and matrix-colour. Matrix in both consist of minor biotite phenocrysts, minor subeuhedral magnetite, trace potential ilmenite and possibly some apatite set in a fine-grained, carbonate-rich matrix. No KIM's noted, but one potential <1cm lherzolitic nodule noted at 150.10m.
x	593278	Survey_Type	Acid	
y	5238498	Drill_Type	17A	
z	0	Hole_Diameter	NQ	
Azimuth	134	Drill_Operator	Bradley Bros.	
Dip	-45			
Total Length	353.0			
Location	Temagami	StartDate	27-Jul-06	
Grid		EndDate	01-Aug-06	
Project	KRVY	Loggedby	VLV	
Claim	3007432	Sampledby	VLV & GC	
MapSheet	031 M 05	Reloggedby	E.Potter	

Survey Data

Depth	Azimuth	Dip
4.0	134	-45.0
80.0	134	-45.0
122.0	134	-44.0
230.0	134	-44.0
305.0	134	-42.0
350.0	134	-42.0



From (m)	To (m)	Geological Description	Lab #	FROM	TO	INT.
		Formation Name / Unit Name				

0.0	3.0	OVB Overburden Unrecovered				
-----	-----	---	--	--	--	--

3.0	81.0	Arg Argillite Green siltstone and red arkose. Competent core. Minor iron-staining on fractures and seams. No sulphides visible. Bedding planes inclined 50 deg. TCA. Trace calcite-quartz-chlorite veinlets. 47.8 74.0 More fractured and broken into 20 cm intervals (at best) with light-med green clay seams and partings.				
-----	------	---	--	--	--	--

81.0 88.5 **Slst Siltstone**
Red arkose and green siltstone (argillaceous) badly broken.
80.0 88.5
Rubble, material loss, upper contact with kimberlite breccia

88.5 164.1 **KMB Kimberlite**
Heterolithic, clast-supported (60-80% clasts) volcanoclastic breccia with subangular to rounded clasts set in a light green to green, carbonate-bearing matrix. Clasts are typically <5cm and minor lapilli (<5%) were noted. Porphyritic matrix contains 10-15% rounded black biotite phenocrysts and rare macrocrysts up to 12mm in diameter, trace subeuhedral magnetite, trace potential ilmenite, and trace euhedral apatite. Juvenile lapilli and matrix contain minor, small serpentized grains. Unit is weakly magnetic. One possible <1cm mantle nodule (Iherzolitic) noted at 150.10m.

TS-01	88.50	106.70	18.20
TS-02	106.70	131.00	25.70
TS-03	131.00	155.00	24.00
TS-04	155.00	164.10	9.10

100.9 102.1 Kimberlite

Matrix-supported (60% clasts) mottled red and dark green carbonate volcanoclastic breccia (increased iron-oxidation/alteration). Clasts are smaller than main KMB and less lapilli are visible. Very fine-grained matrix contains decreased biotite grains (5%) which are smaller in size. Possible euhedral apatite noted within carbonate-bearing matrix. Unit is strongly magnetic.

161.1 161.9 Kimberlite

Light brown-yellow alteration of matrix and increased abundance of fine-grained biotite. Textures and mineralogy otherwise unchanged.

163.8 164.1 Kimberlite

Matrix-supported (<5% clasts) beige-coloured carbonate volcanoclastic breccia. Increased iron-alteration and corrosion of rounded clasts which are <1cm. Porphyritic groundmass is rich in carbonate (reacts well to HCl) with iron-oxidized biotite grains (~10%, <2mm in diameter) trace magnetite, trace calcite, and trace potential apatite set in a very fine-grained matrix.

164.1 183.7 **Arg Argillite**
Green/Black fine grained to medium grained argillite.

183.7 215.3 **NipD Nipissing Diabase / Meta Gabbro**
 Fine-grained, Nipissing diabase with aphanitic quartz diabase contacts. Trace calcite-quartz veins and veinlets.
 186.5 186.7 Nipissing Diabase / Meta calcite
 Gabbro
 Quartz-calcite-chlorite vein breccia
 215.3 215.6 Nipissing Diabase / Meta
 Gabbro
 Green carbonate-clay alteration reducing core to rubble.

215.3 269.0 **BaCl Basal Conglomerate**
 Matrix-supported <10% clasts set in a green siltstone matrix.
 262.0 269.0 Basal Conglomerate
 Dark red, hematite-altered/oxidized diamictite with increased fracturing

269.0 320.5 **KMB Kimberlite**
 Matrix-supported (5-15% clasts) carbonate volcanoclastic breccia. Predominantly rounded, iron-altered and corroded clasts (<4cm in diameter) set in a light green-grey carbonate-bearing matrix. Matrix is rich in biotite (10-15%, <5mm), contains trace magnetite (subeuhedral) and potential ilmenite. Unit is cross-cut by trace calcite stringers cross-cutting the core at 45 deg. TCA. Unit is magnetic.
 276.7 276.9 Kimberlite
 Very fine-grained, porphyritic carbonate volcanoclastic dike cross-cuts main KMB unit. Contact is sharp and is defined by calcite stringers inclined 25 deg. TCA. Matrix is medium-grey in colour and contains minor <2% biotite phenocrysts (<2mm) and trace (<1%) subeuhedral magnetite in a carbonate-rich groundmass. Contains no clasts and is strongly magnetic.
 284.0 287.0 Kimberlite
 Light yellow-brown alteration of KMB unit with increased iron-staining and corrosion of clasts and matrix. Biotite contents increase (20%) with additional fine-grained honey-brown phlogopite in the groundmass. The clasts are predominantly rounded and <4cm in diameter. Diffuse contacts with unaltered KMB unit. Carbonate-bearing matrix (reacts with HCl). Weakly magnetic.

TS-06	269.00	284.00	0.00
TS-05	284.00	303.30	19.30
TS-07	303.00	320.00	0.00

289.8 292.5 Kimberlite

Light yellow-brown alteration of KMB unit with increased iron-staining and corrosion of clasts and matrix -to a rubble in places. Biotite contents increase (20%) with additional fine-grained honey-brown phlogopite in the groundmass. The clasts are predominantly rounded and <4cm in diameter. Diffuse contacts with unaltered KMB unit. Carbonate-bearing matrix (reacts with HCl). Weakly magnetic.

296.7 299.0 Kimberlite

Matrix-supported (5-10% clasts), porphyritic carbonate volcanoclastic breccia with small (<0.5cm), rounded, iron-altered and corroded clasts set in a light grey, carbonate-rich matrix. Matrix contains fine-grained biotite (10-20%), trace ilmenite, trace magnetite and minor serpentinized grains. Unit is magnetic. Lowermost ~1.5m are overprinted by light yellow-brown alteration with increased biotite concentration.

298.9 299.0

Rep Sample

302.4 303.4 Kimberlite

Light yellow-brown alteration of KMB unit with increased iron-staining and corrosion of clasts and matrix -to a rubble in places. Biotite contents increase (20%) with additional fine-grained, honey-brown phlogopite in the groundmass. The clasts are predominantly rounded and <4cm in diameter. Diffuse contacts with unaltered KMB unit. Carbonate-bearing matrix (reacts with HCl). Weakly magnetic.

307.9 308.3 Kimberlite

Light yellow-brown alteration of KMB unit with increased iron-staining and corrosion of clasts and matrix -to a rubble in places. Biotite contents increase (20%) with additional fine-grained honey-brown phlogopite in the groundmass. The clasts are predominantly rounded and <4cm in diameter. Diffuse contacts with unaltered KMB unit. Carbonate-bearing matrix (reacts with HCl). Weakly magnetic.

310.9 318.1 Kimberlite

Clast-supported (40-60%) essentially monolithic carbonate volcanoclastic breccia. Clasts are all angular, parallel laminated silt- and mudstones with few exceptions and display virtually no iron-alteration and/or corrosion. Otherwise, unit resembles the rest of the KMB intersection: light- to dark green matrix containing 10-15% black biotite (<5mm), trace magnetite (with a few macrocrysts up to 10mm), and trace potential ilmenite. Carbonate-rich matrix is magnetic. Unit is cross-cut by rose calcite veinlets at 311.50-311.85 & 317.30-317.75

316.9 317.0

Rep Sample

318.1 320.5 Kimberlite

Increased iron alteration and corrosion of clasts down to a rubble. Clast content increases approaching contact -contact is calcite-rich with angular clasts cemented by white, interstitial calcite. Iron-staining propagates ~0.5m into the underlying diamictite unit.

320.5 353.0 BaCl **Basal Conglomerate**
Matrix-supported diamictite with <10% clasts in a green siltstone matrix.

353.0 0.0 EOH **End of Hole**

Hole	Depth (m)	Magnetic Susceptibility	Hole	Depth (m)	Magnetic Susceptibility	Hole	Depth (m)	Magnetic Susceptibility
TD-06-03	0.5	Overburden	TD-06-03	30.0	0.07	TD-06-03	59.5	0.14
TD-06-03	1.0	Overburden	TD-06-03	30.5	0.01	TD-06-03	60.0	0.21
TD-06-03	1.5	Overburden	TD-06-03	31.0	0.10	TD-06-03	60.5	0.16
TD-06-03	2.0	Overburden	TD-06-03	31.5	0.09	TD-06-03	61.0	0.16
TD-06-03	2.5	Overburden	TD-06-03	32.0	0.03	TD-06-03	61.5	0.21
TD-06-03	3.0	0.00	TD-06-03	32.5	0.03	TD-06-03	62.0	0.16
TD-06-03	3.5	0.00	TD-06-03	33.0	0.09	TD-06-03	62.5	0.20
TD-06-03	4.0	-0.01	TD-06-03	33.5	0.09	TD-06-03	63.0	0.25
TD-06-03	4.5	0.00	TD-06-03	34.0	0.12	TD-06-03	63.5	0.21
TD-06-03	5.0	-0.01	TD-06-03	34.5	0.12	TD-06-03	64.0	0.21
TD-06-03	5.5	0.14	TD-06-03	35.0	0.03	TD-06-03	64.5	0.34
TD-06-03	6.0	9.00	TD-06-03	35.5	0.07	TD-06-03	65.0	0.16
TD-06-03	6.5	0.01	TD-06-03	36.0	0.03	TD-06-03	65.5	0.20
TD-06-03	7.0	-0.01	TD-06-03	36.5	0.03	TD-06-03	66.0	0.20
TD-06-03	7.5	0.00	TD-06-03	37.0	0.12	TD-06-03	66.5	0.16
TD-06-03	8.0	0.00	TD-06-03	37.5	0.12	TD-06-03	67.0	0.21
TD-06-03	8.5	0.00	TD-06-03	38.0	0.09	TD-06-03	67.5	0.23
TD-06-03	9.0	-0.01	TD-06-03	38.5	0.07	TD-06-03	68.0	0.21
TD-06-03	9.5	0.03	TD-06-03	39.0	0.16	TD-06-03	68.5	0.20
TD-06-03	10.0	0.14	TD-06-03	39.5	0.07	TD-06-03	69.0	0.25
TD-06-03	10.5	0.03	TD-06-03	40.0	0.07	TD-06-03	69.5	0.21
TD-06-03	11.0	0.00	TD-06-03	40.5	0.05	TD-06-03	70.0	0.21
TD-06-03	11.5	0.00	TD-06-03	41.0	0.12	TD-06-03	70.5	0.21
TD-06-03	12.0	0.03	TD-06-03	41.5	0.05	TD-06-03	71.0	0.21
TD-06-03	12.5	0.07	TD-06-03	42.0	0.09	TD-06-03	71.5	0.21
TD-06-03	13.0	0.05	TD-06-03	42.5	0.10	TD-06-03	72.0	0.23
TD-06-03	13.5	0.09	TD-06-03	43.0	0.07	TD-06-03	72.5	0.27
TD-06-03	14.0	0.07	TD-06-03	43.5	0.12	TD-06-03	73.0	0.31
TD-06-03	14.5	0.05	TD-06-03	44.0	0.10	TD-06-03	73.5	0.25
TD-06-03	15.0	0.10	TD-06-03	44.5	0.18	TD-06-03	74.0	0.25
TD-06-03	15.5	0.03	TD-06-03	45.0	0.14	TD-06-03	74.5	0.21
TD-06-03	16.0	0.10	TD-06-03	45.5	0.16	TD-06-03	75.0	0.34
TD-06-03	16.5	0.10	TD-06-03	46.0	0.20	TD-06-03	75.5	0.31
TD-06-03	17.0	0.07	TD-06-03	46.5	0.09	TD-06-03	76.0	0.27
TD-06-03	17.5	0.07	TD-06-03	47.0	0.16	TD-06-03	76.5	0.31
TD-06-03	18.0	0.09	TD-06-03	47.5	0.21	TD-06-03	77.0	0.23
TD-06-03	18.5	0.01	TD-06-03	48.0	0.10	TD-06-03	77.5	0.21
TD-06-03	19.0	0.07	TD-06-03	48.5	0.07	TD-06-03	78.0	0.47
TD-06-03	19.5	0.16	TD-06-03	49.0	0.10	TD-06-03	78.5	0.31
TD-06-03	20.0	0.03	TD-06-03	49.5	0.10	TD-06-03	79.0	0.25
TD-06-03	20.5	0.16	TD-06-03	50.0	0.14	TD-06-03	79.5	0.49
TD-06-03	21.0	0.07	TD-06-03	50.5	0.21	TD-06-03	80.0	0.36
TD-06-03	21.5	0.16	TD-06-03	51.0	0.25	TD-06-03	80.5	0.27
TD-06-03	22.0	0.14	TD-06-03	51.5	0.27	TD-06-03	81.0	0.20
TD-06-03	22.5	0.05	TD-06-03	52.0	0.21	TD-06-03	81.5	0.29
TD-06-03	23.0	0.07	TD-06-03	52.5	0.25	TD-06-03	82.0	0.25
TD-06-03	23.5	0.01	TD-06-03	53.0	0.23	TD-06-03	82.5	0.25
TD-06-03	24.0	0.05	TD-06-03	53.5	0.25	TD-06-03	83.0	0.27
TD-06-03	24.5	0.21	TD-06-03	54.0	0.23	TD-06-03	83.5	0.23
TD-06-03	25.0	0.20	TD-06-03	54.5	0.23	TD-06-03	84.0	2.56
TD-06-03	25.5	0.12	TD-06-03	55.0	0.27	TD-06-03	84.5	2.01
TD-06-03	26.0	0.12	TD-06-03	55.5	0.73	TD-06-03	85.0	0.38
TD-06-03	26.5	0.01	TD-06-03	56.0	0.18	TD-06-03	85.5	0.29
TD-06-03	27.0	0.00	TD-06-03	56.5	0.20	TD-06-03	86.0	4.39
TD-06-03	27.5	0.01	TD-06-03	57.0	0.27	TD-06-03	86.5	8.67
TD-06-03	28.0	0.05	TD-06-03	57.5	0.23	TD-06-03	87.0	0.23
TD-06-03	28.5	0.07	TD-06-03	58.0	0.21	TD-06-03	87.5	3.55
TD-06-03	29.0	0.12	TD-06-03	58.5	0.36	TD-06-03	88.0	0.62
TD-06-03	29.5	0.12	TD-06-03	59.0	0.31	TD-06-03	88.5	3.49

Hole	Depth (m)	Magnetic Susceptibility	Hole	Depth (m)	Magnetic Susceptibility	Hole	Depth (m)	Magnetic Susceptibility
TD-06-03	89.0	3.55	TD-06-03	118.5	5.47	TD-06-03	148.0	2.79
TD-06-03	89.5	6.71	TD-06-03	119.0	11.30	TD-06-03	148.5	1.31
TD-06-03	90.0	7.55	TD-06-03	119.5	6.99	TD-06-03	149.0	3.23
TD-06-03	90.5	3.12	TD-06-03	120.0	2.92	TD-06-03	149.5	2.32
TD-06-03	91.0	2.48	TD-06-03	120.5	63.70	TD-06-03	150.0	0.49
TD-06-03	91.5	1.28	TD-06-03	121.0	3.98	TD-06-03	150.5	4.53
TD-06-03	92.0	0.51	TD-06-03	121.5	1.44	TD-06-03	151.0	3.80
TD-06-03	92.5	4.09	TD-06-03	122.0	1.86	TD-06-03	151.5	2.48
TD-06-03	93.0	3.75	TD-06-03	122.5	3.60	TD-06-03	152.0	1.20
TD-06-03	93.5	4.68	TD-06-03	123.0	2.17	TD-06-03	152.5	1.90
TD-06-03	94.0	2.70	TD-06-03	123.5	3.51	TD-06-03	153.0	2.30
TD-06-03	94.5	0.64	TD-06-03	124.0	2.06	TD-06-03	153.5	0.56
TD-06-03	95.0	0.38	TD-06-03	124.5	5.75	TD-06-03	154.0	1.61
TD-06-03	95.5	0.25	TD-06-03	125.0	2.72	TD-06-03	154.5	4.70
TD-06-03	96.0	0.25	TD-06-03	125.5	4.04	TD-06-03	155.0	0.16
TD-06-03	96.5	4.08	TD-06-03	126.0	9.71	TD-06-03	155.5	1.92
TD-06-03	97.0	3.45	TD-06-03	126.5	2.65	TD-06-03	156.0	2.76
TD-06-03	97.5	3.09	TD-06-03	127.0	2.39	TD-06-03	156.5	2.90
TD-06-03	98.0	2.54	TD-06-03	127.5	1.18	TD-06-03	157.0	1.24
TD-06-03	98.5	1.44	TD-06-03	128.0	3.05	TD-06-03	157.5	8.78
TD-06-03	99.0	0.76	TD-06-03	128.5	2.79	TD-06-03	158.0	1.44
TD-06-03	99.5	1.20	TD-06-03	129.0	3.95	TD-06-03	158.5	1.40
TD-06-03	100.0	4.70	TD-06-03	129.5	1.97	TD-06-03	159.0	1.07
TD-06-03	100.5	3.14	TD-06-03	130.0	1.26	TD-06-03	159.5	0.71
TD-06-03	101.0	2.70	TD-06-03	130.5	2.85	TD-06-03	160.0	0.31
TD-06-03	101.5	3.09	TD-06-03	131.0	2.96	TD-06-03	160.5	0.29
TD-06-03	102.0	2.70	TD-06-03	131.5	4.17	TD-06-03	161.0	0.49
TD-06-03	102.5	7.57	TD-06-03	132.0	4.84	TD-06-03	161.5	0.21
TD-06-03	103.0	1.93	TD-06-03	132.5	3.89	TD-06-03	162.0	0.09
TD-06-03	103.5	3.78	TD-06-03	133.0	0.95	TD-06-03	162.5	0.29
TD-06-03	104.0	7.21	TD-06-03	133.5	0.51	TD-06-03	163.0	0.14
TD-06-03	104.5	4.99	TD-06-03	134.0	2.08	TD-06-03	163.5	0.29
TD-06-03	105.0	8.78	TD-06-03	134.5	missing	TD-06-03	164.0	5.05
TD-06-03	105.5	4.42	TD-06-03	135.0	missing	TD-06-03	164.5	0.27
TD-06-03	106.0	3.60	TD-06-03	135.5	missing	TD-06-03	165.0	0.36
TD-06-03	106.5	3.87	TD-06-03	136.0	0.98	TD-06-03	165.5	0.25
TD-06-03	107.0	2.87	TD-06-03	136.5	2.30	TD-06-03	166.0	0.16
TD-06-03	107.5	3.20	TD-06-03	137.0	3.25	TD-06-03	166.5	0.29
TD-06-03	108.0	7.59	TD-06-03	137.5	2.39	TD-06-03	167.0	0.23
TD-06-03	108.5	4.13	TD-06-03	138.0	1.73	TD-06-03	167.5	0.27
TD-06-03	109.0	4.86	TD-06-03	138.5	4.81	TD-06-03	168.0	0.25
TD-06-03	109.5	9.42	TD-06-03	139.0	1.79	TD-06-03	168.5	0.21
TD-06-03	110.0	2.26	TD-06-03	139.5	0.82	TD-06-03	169.0	0.31
TD-06-03	110.5	6.78	TD-06-03	140.0	0.34	TD-06-03	169.5	0.27
TD-06-03	111.0	3.97	TD-06-03	140.5	1.02	TD-06-03	170.0	0.23
TD-06-03	111.5	0.82	TD-06-03	141.0	2.06	TD-06-03	170.5	0.27
TD-06-03	112.0	4.32	TD-06-03	141.5	2.06	TD-06-03	171.0	0.25
TD-06-03	112.5	1.73	TD-06-03	142.0	22.30	TD-06-03	171.5	0.23
TD-06-03	113.0	14.20	TD-06-03	142.5	2.59	TD-06-03	172.0	0.21
TD-06-03	113.5	5.43	TD-06-03	143.0	3.78	TD-06-03	172.5	0.23
TD-06-03	114.0	4.37	TD-06-03	143.5	1.51	TD-06-03	173.0	0.20
TD-06-03	114.5	6.05	TD-06-03	144.0	2.36	TD-06-03	173.5	0.23
TD-06-03	115.0	6.69	TD-06-03	144.5	1.44	TD-06-03	174.0	0.25
TD-06-03	115.5	5.28	TD-06-03	145.0	2.15	TD-06-03	174.5	0.25
TD-06-03	116.0	1.84	TD-06-03	145.5	0.96	TD-06-03	175.0	0.27
TD-06-03	116.5	9.36	TD-06-03	146.0	2.01	TD-06-03	175.5	0.27
TD-06-03	117.0	8.54	TD-06-03	146.5	0.80	TD-06-03	176.0	0.21
TD-06-03	117.5	9.24	TD-06-03	147.0	3.27	TD-06-03	176.5	0.23
TD-06-03	118.0	5.67	TD-06-03	147.5	1.72	TD-06-03	177.0	0.27

Hole	Depth (m)	Magnetic Susceptibility	Hole	Depth (m)	Magnetic Susceptibility	Hole	Depth (m)	Magnetic Susceptibility
TD-06-03	177.5	0.18	TD-06-03	207.0	0.36	TD-06-03	236.5	0.20
TD-06-03	178.0	0.21	TD-06-03	207.5	0.40	TD-06-03	237.0	0.18
TD-06-03	178.5	0.23	TD-06-03	208.0	0.42	TD-06-03	237.5	0.20
TD-06-03	179.0	0.42	TD-06-03	208.5	0.38	TD-06-03	238.0	0.23
TD-06-03	179.5	0.29	TD-06-03	209.0	0.40	TD-06-03	238.5	0.20
TD-06-03	180.0	0.25	TD-06-03	209.5	0.40	TD-06-03	239.0	0.20
TD-06-03	180.5	0.34	TD-06-03	210.0	0.29	TD-06-03	239.5	0.18
TD-06-03	181.0	0.29	TD-06-03	210.5	0.42	TD-06-03	240.0	0.20
TD-06-03	181.5	0.20	TD-06-03	211.0	0.43	TD-06-03	240.5	0.21
TD-06-03	182.0	0.20	TD-06-03	211.5	0.64	TD-06-03	241.0	0.20
TD-06-03	182.5	0.36	TD-06-03	212.0	1.13	TD-06-03	241.5	0.20
TD-06-03	183.0	0.27	TD-06-03	212.5	0.43	TD-06-03	242.0	0.18
TD-06-03	183.5	0.25	TD-06-03	213.0	0.34	TD-06-03	242.5	0.20
TD-06-03	184.0	0.27	TD-06-03	213.5	0.40	TD-06-03	243.0	0.20
TD-06-03	184.5	0.34	TD-06-03	214.0	0.34	TD-06-03	243.5	0.18
TD-06-03	185.0	0.21	TD-06-03	214.5	0.40	TD-06-03	244.0	0.21
TD-06-03	185.5	0.31	TD-06-03	215.0	0.31	TD-06-03	244.5	0.21
TD-06-03	186.0	0.34	TD-06-03	215.5	0.05	TD-06-03	245.0	0.45
TD-06-03	186.5	0.31	TD-06-03	216.0	0.14	TD-06-03	245.5	0.34
TD-06-03	187.0	0.32	TD-06-03	216.5	0.12	TD-06-03	246.0	0.31
TD-06-03	187.5	0.36	TD-06-03	217.0	0.09	TD-06-03	246.5	1.00
TD-06-03	188.0	0.32	TD-06-03	217.5	0.12	TD-06-03	247.0	0.87
TD-06-03	188.5	0.32	TD-06-03	218.0	0.12	TD-06-03	247.5	0.75
TD-06-03	189.0	0.36	TD-06-03	218.5	0.10	TD-06-03	248.0	0.43
TD-06-03	189.5	0.34	TD-06-03	219.0	0.10	TD-06-03	248.5	0.32
TD-06-03	190.0	0.42	TD-06-03	219.5	0.12	TD-06-03	249.0	0.23
TD-06-03	190.5	0.32	TD-06-03	220.0	0.14	TD-06-03	249.5	0.32
TD-06-03	191.0	0.42	TD-06-03	220.5	0.12	TD-06-03	250.0	0.96
TD-06-03	191.5	0.42	TD-06-03	221.0	0.12	TD-06-03	250.5	0.21
TD-06-03	192.0	0.40	TD-06-03	221.5	0.12	TD-06-03	251.0	0.82
TD-06-03	192.5	0.36	TD-06-03	222.0	0.12	TD-06-03	251.5	0.14
TD-06-03	193.0	0.32	TD-06-03	222.5	0.10	TD-06-03	252.0	0.20
TD-06-03	193.5	0.31	TD-06-03	223.0	0.10	TD-06-03	252.5	0.21
TD-06-03	194.0	0.32	TD-06-03	223.5	0.18	TD-06-03	253.0	0.16
TD-06-03	194.5	0.25	TD-06-03	224.0	0.10	TD-06-03	253.5	0.21
TD-06-03	195.0	0.32	TD-06-03	224.5	0.14	TD-06-03	254.0	0.32
TD-06-03	195.5	0.29	TD-06-03	225.0	0.14	TD-06-03	254.5	0.64
TD-06-03	196.0	0.38	TD-06-03	225.5	0.14	TD-06-03	255.0	0.69
TD-06-03	196.5	0.31	TD-06-03	226.0	0.14	TD-06-03	255.5	0.60
TD-06-03	197.0	0.31	TD-06-03	226.5	0.16	TD-06-03	256.0	0.86
TD-06-03	197.5	0.29	TD-06-03	227.0	0.14	TD-06-03	256.5	0.95
TD-06-03	198.0	0.29	TD-06-03	227.5	0.12	TD-06-03	257.0	0.98
TD-06-03	198.5	0.29	TD-06-03	228.0	0.18	TD-06-03	257.5	0.49
TD-06-03	199.0	0.29	TD-06-03	228.5	0.18	TD-06-03	258.0	1.13
TD-06-03	199.5	0.42	TD-06-03	229.0	0.20	TD-06-03	258.5	1.04
TD-06-03	200.0	0.36	TD-06-03	229.5	0.18	TD-06-03	259.0	0.58
TD-06-03	200.5	0.38	TD-06-03	230.0	0.14	TD-06-03	259.5	1.13
TD-06-03	201.0	0.38	TD-06-03	230.5	0.18	TD-06-03	260.0	0.12
TD-06-03	201.5	0.36	TD-06-03	231.0	12.00	TD-06-03	260.5	0.95
TD-06-03	202.0	0.34	TD-06-03	231.5	0.12	TD-06-03	261.0	1.70
TD-06-03	202.5	0.34	TD-06-03	232.0	0.14	TD-06-03	261.5	0.42
TD-06-03	203.0	0.40	TD-06-03	232.5	0.10	TD-06-03	262.0	0.27
TD-06-03	203.5	0.43	TD-06-03	233.0	0.14	TD-06-03	262.5	0.20
TD-06-03	204.0	0.43	TD-06-03	233.5	0.16	TD-06-03	263.0	0.21
TD-06-03	204.5	0.38	TD-06-03	234.0	0.16	TD-06-03	263.5	0.21
TD-06-03	205.0	0.45	TD-06-03	234.5	0.16	TD-06-03	264.0	0.29
TD-06-03	205.5	0.36	TD-06-03	235.0	0.16	TD-06-03	264.5	0.31
TD-06-03	206.0	0.38	TD-06-03	235.5	0.16	TD-06-03	265.0	0.25
TD-06-03	206.5	0.31	TD-06-03	236.0	0.18	TD-06-03	265.5	0.14

Hole	Depth (m)	Magnetic Susceptibility	Hole	Depth (m)	Magnetic Susceptibility	Hole	Depth (m)	Magnetic Susceptibility
TD-06-03	266.0	0.32	TD-06-03	295.5	14.60	TD-06-03	325.0	0.20
TD-06-03	266.5	0.34	TD-06-03	296.0	20.80	TD-06-03	325.5	0.16
TD-06-03	267.0	0.38	TD-06-03	296.5	20.50	TD-06-03	326.0	0.32
TD-06-03	267.5	0.60	TD-06-03	297.0	23.70	TD-06-03	326.5	0.23
TD-06-03	268.0	1.51	TD-06-03	297.5	26.80	TD-06-03	327.0	0.23
TD-06-03	268.5	1.53	TD-06-03	298.0	9.57	TD-06-03	327.5	0.54
TD-06-03	269.0	1.99	TD-06-03	298.5	12.00	TD-06-03	328.0	0.12
TD-06-03	269.5	38.70	TD-06-03	299.0	11.40	TD-06-03	328.5	0.14
TD-06-03	270.0	43.30	TD-06-03	299.5	19.60	TD-06-03	329.0	0.18
TD-06-03	270.5	35.00	TD-06-03	300.0	25.30	TD-06-03	329.5	0.14
TD-06-03	271.0	53.50	TD-06-03	300.5	10.00	TD-06-03	330.0	0.18
TD-06-03	271.5	23.10	TD-06-03	301.0	19.50	TD-06-03	330.5	0.09
TD-06-03	272.0	27.70	TD-06-03	301.5	11.40	TD-06-03	331.0	0.14
TD-06-03	272.5	7.02	TD-06-03	302.0	18.20	TD-06-03	331.5	1.07
TD-06-03	273.0	50.70	TD-06-03	302.5	16.00	TD-06-03	332.0	0.12
TD-06-03	273.5	42.80	TD-06-03	303.0	22.30	TD-06-03	332.5	5.25
TD-06-03	274.0	5.09	TD-06-03	303.5	26.60	TD-06-03	333.0	0.16
TD-06-03	274.5	49.20	TD-06-03	304.0	27.70	TD-06-03	333.5	0.12
TD-06-03	275.0	34.00	TD-06-03	304.5	34.30	TD-06-03	334.0	0.21
TD-06-03	275.5	50.90	TD-06-03	305.0	18.50	TD-06-03	334.5	0.12
TD-06-03	276.0	9.49	TD-06-03	305.5	6.49	TD-06-03	335.0	0.16
TD-06-03	276.5	55.10	TD-06-03	306.0	16.40	TD-06-03	335.5	0.09
TD-06-03	277.0	3.55	TD-06-03	306.5	3.48	TD-06-03	336.0	0.18
TD-06-03	277.5	22.40	TD-06-03	307.0	30.70	TD-06-03	336.5	0.20
TD-06-03	278.0	48.10	TD-06-03	307.5	22.80	TD-06-03	337.0	0.71
TD-06-03	278.5	40.70	TD-06-03	308.0	6.07	TD-06-03	337.5	0.21
TD-06-03	279.0	52.50	TD-06-03	308.5	43.10	TD-06-03	338.0	0.05
TD-06-03	279.5	30.80	TD-06-03	309.0	39.00	TD-06-03	338.5	0.54
TD-06-03	280.0	47.20	TD-06-03	309.5	43.10	TD-06-03	339.0	0.29
TD-06-03	280.5	58.10	TD-06-03	310.0	51.00	TD-06-03	339.5	4.28
TD-06-03	281.0	48.60	TD-06-03	310.5	44.70	TD-06-03	340.0	0.36
TD-06-03	281.5	67.70	TD-06-03	311.0	31.60	TD-06-03	340.5	0.25
TD-06-03	282.0	66.80	TD-06-03	311.5	28.70	TD-06-03	341.0	0.60
TD-06-03	282.5	27.90	TD-06-03	312.0	19.20	TD-06-03	341.5	1.61
TD-06-03	283.0	34.90	TD-06-03	312.5	53.30	TD-06-03	342.0	2.83
TD-06-03	283.5	2.58	TD-06-03	313.0	39.80	TD-06-03	342.5	0.32
TD-06-03	284.0	37.90	TD-06-03	313.5	39.70	TD-06-03	343.0	3.62
TD-06-03	284.5	30.60	TD-06-03	314.0	45.20	TD-06-03	343.5	1.29
TD-06-03	285.0	28.30	TD-06-03	314.5	19.00	TD-06-03	344.0	1.51
TD-06-03	285.5	22.50	TD-06-03	315.0	46.20	TD-06-03	344.5	1.51
TD-06-03	286.0	16.80	TD-06-03	315.5	52.00	TD-06-03	345.0	3.09
TD-06-03	286.5	18.40	TD-06-03	316.0	49.30	TD-06-03	345.5	0.36
TD-06-03	287.0	14.90	TD-06-03	316.5	36.70	TD-06-03	346.0	0.49
TD-06-03	287.5	6.11	TD-06-03	317.0	45.90	TD-06-03	346.5	0.38
TD-06-03	288.0	1.27	TD-06-03	317.5	42.50	TD-06-03	347.0	0.38
TD-06-03	288.5	14.90	TD-06-03	318.0	33.80	TD-06-03	347.5	1.90
TD-06-03	289.0	37.00	TD-06-03	318.5	28.70	TD-06-03	348.0	3.89
TD-06-03	289.5	7.94	TD-06-03	319.0	0.49	TD-06-03	348.5	2.34
TD-06-03	290.0	20.30	TD-06-03	319.5	5.36	TD-06-03	349.0	1.33
TD-06-03	290.5	19.50	TD-06-03	320.0	1.20	TD-06-03	349.5	3.09
TD-06-03	291.0	30.00	TD-06-03	320.5	0.12	TD-06-03	350.0	1.75
TD-06-03	291.5	10.60	TD-06-03	321.0	0.20	TD-06-03	350.5	2.28
TD-06-03	292.0	16.90	TD-06-03	321.5	0.31	TD-06-03	351.0	1.26
TD-06-03	292.5	12.90	TD-06-03	322.0	0.69	TD-06-03	351.5	2.89
TD-06-03	293.0	15.40	TD-06-03	322.5	0.43	TD-06-03	352.0	2.74
TD-06-03	293.5	20.00	TD-06-03	323.0	0.65	TD-06-03	352.5	3.18
TD-06-03	294.0	19.60	TD-06-03	323.5	0.91	TD-06-03	353.0	3.27
TD-06-03	294.5	24.20	TD-06-03	324.0	0.78			
TD-06-03	295.0	22.70	TD-06-03	324.5	0.98			

Hole_ID	TD-08-07	Hole_Type	surface	<i>Purpose/Comments</i> Large intersection with kimberlitic volcaniclastic breccia from 82-203m depth.. At least three phases were noted within the volcaniclastic breccia. The phases were distinguished based on clast content, presence of interstitial calcite, matrix colour, and grain size. In all phases matrix is porphyritic with minor rounded biotite grains, trace subeuhedral magnetite, possible ilmenite and trace euhedral apatite. No KIM's were noted in the sections, but at least one peridotitic nodule was noted (106.69m).
x	593442	Survey_Type	reflex	
y	5238577	Drill_Type	diamond	
z	0	Hole_Diameter	NQ	
Azimuth	180	Drill_Operator	Lafreniere	
Dip	-45			
Total Length	282.0			
Location	Temagami	StartDate	21-May-08	
Grid		EndDate	23-May-08	
Project	KRVY	Loggedby	E.Potter	
Claim		Sampledby		
MapSheet		Reloggedby		

Survey Data

Depth	Azimuth	Dip
82.0	181.8	-45.6
182.0	183.4	-45.5
282.0	188.4	-44.6



From (m)	To (m)	Geological Description	
		Formation Name / Unit Name	

Lab #	FROM	TO	INT.
(m)			

0.0	4.2	OVB	Overburden
		Casing.	

4.2	8.5	Slst	Siltstone
		Parallel laminated silt- and mudstones with beds inclined 45 deg. TCA.	

8.5	48.0	Sst	Sandstone
		Fine- to medium-grained arkose dark-grey to red in colour. Beds inclined 45 deg TCA.	
8.5	11.1	Fault	
		Broken core with lineations developed on fragments ~30 deg. TCA.	

- 13.4 14.5 Fault
Broken core-rubble.
- 15.1 17.0 Fault
Broken core with minor chlorite-epidote and calcite lined fractures.
- 18.7 19.0 Fault
Broken core with trace calcite on sheared surfaces.
- 25.8 26.9 Sandstone calcite
Minor (1%) light green carbonate (epidote+calcite?) stringers intersecting core at 50 deg.
TCA.

48.0 68.3 **Sst Sandstone**
Fine to medium-grained arkose interbedded with minor mudstone units. Minor calcite-lined fractures cross-cut unit at 40-70 deg. TCA. In arkosic unit, fractures have sub-centimeter, carbonate-bleached halos. Bedding inclined 45 deg TCA.

- 68.3 82.2 **Slst Siltstone**
Parallel laminated silt- and mudstones with bedding contacts inclined 45 deg. TCA. Increasing light-green carbonate veinlets approaching contact with VBX. Veinlets have decomposed to almost a clay-carbonate mud in most occurrences.
- 71.3 72.0 Siltstone
Broken core with light-green carbonate veinlets and iron-staining. Carbonate veinlet has broken down to almost a clay-rich mud.
- 72.9 73.0 Siltstone
Light-green carbonate veinlet (<3cm) intersects core at 10 deg. TCA. Sharp contacts with host rock and rock fragments within veinlet.
- 73.7 73.8 Siltstone
Light-green carbonate veinlet and veinlet-breccia (broken core) with minor iron-staining.
- 74.5 75.3 Siltstone
Light-green carbonate veinlets/stringers in broken core. Stringers cross-cut core at 30 deg.
TCA.

77.5 78.1 Fault
Broken core with light-green carbonate, white calcite and epidote lined fragments.

78.6 78.7 Fault
Broken core with iron-staining and minor calcite stringers.

80.0 80.3 Siltstone
Light-green carbonate stringers and iron-staining within section of broken core. Mudstone fragments within veinlet.

81.3 81.4 Vein carbonate
Light green, carbonate-rich veinlet (almost mud) containing angular siltstone fragments, cross-cuts core at 30 deg. TCA. Non-magnetic, contains minor muscovite flakes (clear-white mica) and is iron-stained along the contacts.

82.2 98.4 **VBX Volcanic Breccia**

Matrix-supported (30-50% clasts), heterolithic volcanoclastic breccia with subangular-to-rounded clasts set in a fine-grained, light to dark green, carbonate-rich matrix. Upper contact is intensely iron-altered; iron-alteration gradually decreases with depth. Clasts are both sedimentary and igneous in origin, although most are too altered to decipher original textures/mineralogy. Rounded phlogopite & biotite phenocrysts are present in 5-10 modal %, with trace (0.1%) elongated, non-magnetic black grains (pos. ilmenite), euhedral apatite, calcite and trace pyrite. Unit is cross-cut by later, white calcite veinlets intersecting core at 20-75 deg. TCA; some of which contain vugs lined with euhedral calcite crystals. Matrix is non-magnetic except for a few magnetite grains.

82.2 84.5 Volcanic Breccia
Intensely iron-altered/oxidized heterolithic volcanoclastic breccia-rubble. All clasts and matrix are intensely altered; unit is almost a gravel rubble.

84.5 91.0 Volcanic Breccia
Decreased iron-alteration and more competent core. Clasts retain some origin textures yet are still dark red in colour due to iron alteration. Matrix is a mottled reddish-green colour. Matrix-supported heterolithic volcanoclastic breccia with 40-50% clasts set in a fine-grained, dark green matrix. Matrix contains minor (1%) rounded biotite phenocrysts and possible elongated ilmenite macrocrysts.

91.0 98.4 Volcanic Breccia
Heterolithic, matrix-supported volcanoclastic breccia with minor iron-alteration of clasts. 30-40% subangular to rounded clasts set in a dark green matrix containing rounded biotite, euhedral apatite and possible elongated ilmenite grains.

98.4 113.6 **VBX Volcanic Breccia**
Clast-supported (80-90% clasts) volcanoclastic breccia consisting of rounded to subangular clasts set in a light grey, calcite-rich matrix. Heterolithic breccia with at least one peridotite nodule noted at 106.69m; possibly more but too altered to decipher original mineralogy. Matrix contains rounded biotite macrocrysts and phenocrysts (5-10%) and possible ilmenite macrocrysts set in a fine-grained, carbonate-rich matrix. Rose-coloured calcite occurs interstitial to clasts. Trace pyrite (<0.01%). In addition to clasts, <5% juvenile lapilli present. Consist of fine-grained matrix material (biotite-rich) cored on an ilmenite or pyroxene crystal. Unit is non-magnetic.

113.6 114.8 **KMB Kimberlite**
Matrix-supported (5-10% clasts), carbonate volcanoclastic dike cross-cuts volcanoclastic breccia at 25 deg. TCA. Fine-grained, inequigranular, porphyritic texture with rounded biotite and ilmenite macrocrysts, set in a light-grey matrix. Matrix also contains a light green hexagonal phase -likely apatite- in addition to serpentinized pyroxene or olivine phenocrysts. Clasts are typically rounded, <1cm and have an reaction rim rich in iron-oxides. Strongly magnetic.

114.8 116.0 **VBX Volcanic Breccia**
Clast-supported (70-80% clasts), volcanoclastic breccia consisting of rounded to subangular clasts set in a light grey, calcite-rich matrix. Matrix contains rounded biotite macrocrysts and phenocrysts (5-10%) and possible ilmenite macrocrysts set in a fine-grained, carbonate-rich matrix. Rose-coloured calcite occurs interstitial to clasts. Trace pyrite (<0.01%). In addition to clasts, several juvenile lapilli were noted. Consist of fine-grained matrix material (biotite-rich) cored on an ilmenite or pyroxene crystal. Unit is non-magnetic.

116.0 116.4 **KMB Kimberlite**
Matrix-supported (10-20% clasts), carbonate volcanoclastic dike cross-cuts volcanoclastic breccia at 35 deg. TCA. Fine-grained, inequigranular, porphyritic texture with rounded biotite and ilmenite macrocrysts, set in a light-grey matrix. Matrix also contains a light green hexagonal phase -likely apatite- in addition to serpentinized pyroxene or olivine phenocrysts. Clasts are typically rounded, <1cm and have an reaction rim rich in iron-oxides. Strongly magnetic.

116.4 120.6 **VBX** **Volcanic Breccia**

Clast-supported (70-80% clasts), volcanoclastic breccia consisting of rounded to subangular clasts set in a light grey, calcite-rich matrix. Matrix contains rounded biotite macrocrysts and phenocrysts (5-10%) and possible ilmenite macrocrysts set in a fine-grained, carbonate-rich matrix. Rose-coloured calcite occurs interstitial to clasts. Trace pyrite (<0.01%). Peridotite nodule noted at 120.12m. In addition to clasts, several juvenile lapilli were noted. Consist of fine-grained matrix material (biotite-rich) cored on an ilmenite or pyroxene crystal. Unit is non-magnetic.

120.6 121.0 **KMB** **Kimberlite**

Matrix-supported (15-20% clasts) carbonate volcanoclastic dike. Unit is cross-cut by calcite stringers intersecting core at 40 deg. TCA accompanied by a 5cm wide, light-green alteration halo rich in phlogopite. Rest of unit is fine-grained, inequigranular, porphyritic with rounded biotite and ilmenite macrocrysts, set in a light-grey matrix. Matrix also contains a light green hexagonal phase -likely apatite in addition to serpentinized pyroxene or olivine phenocrysts. Clasts are typically rounded, <1cm and have an reaction rim rich in iron-oxides. Strongly magnetic.

121.0 121.7 **VBX** **Volcanic Breccia**

Clast-supported (70-80% clasts) volcanoclastic breccia consisting of rounded to subangular clasts set in a light grey, calcite-rich matrix. Matrix contains rounded biotite macrocrysts and phenocrysts (5-10%) and possible ilmenite macrocrysts set in a fine-grained, carbonate-rich matrix. Rose-coloured calcite occurs interstitial to clasts. Trace pyrite (<0.01%). In addition to clasts, several juvenile lapilli were noted. Consist of fine-grained matrix material (biotite-rich) cored on an ilmenite or pyroxene crystal. Unit is non-magnetic.

121.7 122.0 **KMB Kimberlite**
Matrix-supported (15-20% clasts), carbonate volcanoclastic dike cross-cuts volcanoclastic breccia at 35 deg. TCA. Fine-grained, inequigranular, porphyritic texture with rounded biotite and ilmenite macrocrysts, set in a light-grey matrix. Matrix also contains a light green hexagonal phase -likely apatite in addition to serpentinized pyroxene or olivine phenocrysts. Clasts are typically rounded, <1cm and have an reaction rim rich in iron-oxides. Strongly magnetic.

122.0 154.6 **VBX Volcanic Breccia**
Clast-supported (70-80% clasts), volcanoclastic breccia consisting of rounded to subangular clasts set in a light grey, calcite-rich matrix. Matrix contains rounded biotite macrocrysts and phenocrysts (5-10%) and possible ilmenite macrocrysts set in a fine-grained, carbonate-rich matrix. Rose-coloured calcite occurs interstitial to clasts and increases with depth until 154.40m. Trace pyrite (<0.01%). In addition to clasts, several juvenile lapilli were noted. Consist of fine-grained matrix material (biotite-rich) cored on an ilmenite or pyroxene crystal. Unit is non-magnetic.

154.6 197.3 **VBX Volcanic Breccia**
Matrix-supported (30% clasts), volcanoclastic breccia consisting of predominantly rounded clasts set in a medium-grey, calcite-rich matrix. In addition to being more rounded, clasts display more iron-alteration, with well-developed patinas. Matrix contains rounded biotite macrocrysts and phenocrysts (5-10%) and possible ilmenite macrocrysts set in a fine-grained, carbonate-rich matrix. Does not contain interstitial calcite like similar units noted above and is magnetic, containing trace magnetite phenocrysts (<0.5mm). Trace pyrite (<0.01%). In addition to clasts, several juvenile lapilli were noted. Consist of fine-grained matrix material (biotite-rich) cored on an ilmenite or pyroxene crystal. Trace calcite stringers cross-cut core at 50 deg. TCA.

171.4 171.6 Volcanic Breccia

Olive-green alteration of volcanoclastic dike associated with sheared calcite stringers cross-cutting core at 40 deg. TCA. Abundant iron-staining yet unaltered magnetite phenocrysts (~0.5mm) are visible.

192.7 193.5 Volcanic Breccia

Olive-green alteration of volcanoclastic dike with sharp contacts. Center of alteration is focused on rubbly/broken core with trace calcite stringers cross-cutting core at 55 deg. TCA. Weakly magnetic (less than unaltered KMB).

197.3 199.4 **KMB Kimberlite**

Very fine-grained, matrix-supported (10%clasts) carbonate volcanoclastic dike with iron-altered/oxidized, rounded clasts set in a light grey matrix. Clasts are all <5cm, typically ~1cm in diameter. Sharp contact with units above and below at 25 deg. TCA. Fine-grained matrix contains 5-10% small (<3mm) dark brown-black, rounded biotite and 2-5% large phenocrysts of magnetite (<8mm). Small crystals of calcite and potential elongated ilmenite grains are set in a carbonate-rich matrix. Iron alteration/oxidation of matrix increases towards base of unit. Unit is strongly magnetic.

199.4 200.0 **KMB Kimberlite**

Intensely iron-altered, aphanitic unit free of clasts. No visible crystals in the carbonate-rich matrix. Dark red-brown colour with a few greenish-grey spots in the center of the core. Sharp upper contact; lower contact too corroded to accurately locate -just a dramatic increase in clast content. Late calcite stringers sealing fractures. Non magnetic unit.

200.0 203.4 **VBX Volcanic Breccia**

Heterolithic, clast-supported (80% clasts) volcanoclastic breccia with intense iron-alteration/oxidation. Core is altered to the point that it is almost a gravel-sized rubble. Clasts are typically dark red in colour due to alteration. Very fine-grained matrix contains 5% rounded biotite grains (<2mm). Breccia matrix contains interstitial, white calcite. Non-magnetic.

203.3 203.5 Fault

Broken core along contact between units with angular clasts.

203.4 218.2 **Slst Siltstone**

Parallel laminated silt-s and mudstones with bedding contacts at 50 deg. TCA.

207.1 210.2 Siltstone

Broken core with chlorite (and trace calcite) lined fractures and core fragments.

218.2 224.3 **BaCl Basal Conglomerate**
 Matrix-supported, Gowganda diamictite. 1-10cm rounded clasts set in a dark grey, siltstone matrix. Trace calcite-sealed fractures cross-cuts the core at 30-40 deg. TCA.

224.3 252.9 **NipD Nippising Diabase / Meta Gabbro**
 Fine-grained, Nippising Diabase with both quartz and hypersthene varieties present. Sharp contacts with some brecciation along contact.

224.5 224.8 Nippising Diabase / Meta calcite
 Gabbro

Calcite-chlorite-quartz veinlets & breccia cross-cutting core at 35 deg. TCA.

230.6 230.9 Fault

Broken core with chlorite-lineations on fragments. Intersects core at 15 deg. TCA.

236.4 236.5 Nippising Diabase / Meta calcite
 Gabbro

Calcite-chlorite-quartz veins (~5cm) intersect core at 50 deg. TCA.

237.2 238.0 Nippising Diabase / Meta calcite
 Gabbro

Increased epidote-alteration of diabase centered on calcite-chlorite-green serpentine veinlets cross-cutting core at 50 deg. TCA.

245.8 245.9 Nippising Diabase / Meta calcite
 Gabbro

Calcite-quartz-chlorite veinlet (1cm) intersects core at 25 deg. TCA.

246.3 246.4 Nippising Diabase / Meta calcite
 Gabbro

Calcite-quartz-chlorite veinlet (1cm) intersects core at 25 deg. TCA.

247.3 247.4 Nippising Diabase / Meta calcite
 Gabbro

Sheared calcite-chlorite-quartz veinlet (<2cm) intersects core at 45 deg. TCA.

251.9 252.0 Nippising Diabase / Meta
Gabbro

Sheared calcite-chlorite-quartz vein breccia (5cm wide) in quartz diabase Cross-cuts core at
45 deg. TCA.

252.9 282.0 **BaCl Basal Conglomerate**

Matrix-supported Gowganda diamictite with rounded clasts set in a siltstone matrix. Calcite-chlorite-talc? Lined fractures
occur throughout the unit, intersecting the core at 20-50 deg. TCA.

254.2 254.6 Basal Conglomerate calcite

Calcite-talc-quartz vein breccia (rubble) with angular core fragments in a white calcite vein.

256.0 266.2 Basal Conglomerate calcite

Calcite-talc-chlorite fractures cross-cut core at 20 deg. TCA.

265.1 265.4 Basal Conglomerate calcite

Calcite-talc-chlorite fractures cross-cut core at 20 deg. TCA.

266.7 266.7 Basal Conglomerate calcite

Sheared calcite-chlorite veinlet cross-cuts core at 20 deg. TCA.

279.9 280.0 Basal Conglomerate calcite

Calcite-talc-chlorite stringers and sealed fractures cross-cut core at 20 deg. TCA.

282.0 0.0 **EOH End of Hole**

Hole	Depth (m)	Magnetic Susceptibility	Hole	Depth (m)	Magnetic Susceptibility	Hole	Depth (m)	Magnetic Susceptibility
TD-08-07	1.0	Overburden	TD-08-07	60.0	0.12	TD-08-07	119.0	29.60
TD-08-07	2.0	Overburden	TD-08-07	61.0	0.20	TD-08-07	120.0	0.31
TD-08-07	3.0	Overburden	TD-08-07	62.0	0.10	TD-08-07	121.0	0.51
TD-08-07	4.0	0.53	TD-08-07	63.0	0.10	TD-08-07	122.0	0.43
TD-08-07	5.0	1.46	TD-08-07	64.0	0.18	TD-08-07	123.0	0.23
TD-08-07	6.0	1.73	TD-08-07	65.0	0.09	TD-08-07	124.0	0.25
TD-08-07	7.0	1.75	TD-08-07	66.0	0.09	TD-08-07	125.0	0.56
TD-08-07	8.0	0.21	TD-08-07	67.0	0.14	TD-08-07	126.0	0.43
TD-08-07	9.0	0.03	TD-08-07	68.0	0.16	TD-08-07	127.0	0.42
TD-08-07	10.0	0.10	TD-08-07	69.0	0.31	TD-08-07	128.0	0.49
TD-08-07	11.0	0.14	TD-08-07	70.0	0.36	TD-08-07	129.0	0.23
TD-08-07	12.0	0.09	TD-08-07	71.0	0.32	TD-08-07	130.0	0.36
TD-08-07	13.0	0.14	TD-08-07	72.0	0.27	TD-08-07	131.0	0.47
TD-08-07	14.0	0.05	TD-08-07	73.0	0.23	TD-08-07	132.0	0.34
TD-08-07	15.0	0.01	TD-08-07	74.0	0.31	TD-08-07	133.0	0.36
TD-08-07	16.0	0.05	TD-08-07	75.0	0.21	TD-08-07	134.0	0.56
TD-08-07	17.0	0.16	TD-08-07	76.0	0.29	TD-08-07	135.0	0.27
TD-08-07	18.0	0.12	TD-08-07	77.0	0.42	TD-08-07	136.0	0.34
TD-08-07	19.0	0.16	TD-08-07	78.0	0.23	TD-08-07	137.0	0.45
TD-08-07	20.0	0.10	TD-08-07	79.0	0.25	TD-08-07	138.0	0.64
TD-08-07	21.0	0.12	TD-08-07	80.0	0.29	TD-08-07	139.0	1.02
TD-08-07	22.0	0.18	TD-08-07	81.0	0.23	TD-08-07	140.0	1.90
TD-08-07	23.0	0.10	TD-08-07	82.0	0.18	TD-08-07	141.0	0.64
TD-08-07	24.0	0.14	TD-08-07	83.0	0.21	TD-08-07	142.0	1.44
TD-08-07	25.0	0.12	TD-08-07	84.0	0.25	TD-08-07	143.0	0.62
TD-08-07	26.0	0.05	TD-08-07	85.0	0.31	TD-08-07	144.0	0.76
TD-08-07	27.0	0.16	TD-08-07	86.0	0.29	TD-08-07	145.0	1.00
TD-08-07	28.0	0.05	TD-08-07	87.0	0.23	TD-08-07	146.0	0.95
TD-08-07	29.0	0.05	TD-08-07	88.0	0.23	TD-08-07	147.0	0.69
TD-08-07	30.0	0.07	TD-08-07	89.0	0.29	TD-08-07	148.0	0.80
TD-08-07	31.0	0.03	TD-08-07	90.0	0.47	TD-08-07	149.0	0.91
TD-08-07	32.0	0.14	TD-08-07	91.0	0.23	TD-08-07	150.0	2.50
TD-08-07	33.0	0.07	TD-08-07	92.0	0.27	TD-08-07	151.0	0.09
TD-08-07	34.0	0.01	TD-08-07	93.0	0.18	TD-08-07	152.0	0.51
TD-08-07	35.0	0.07	TD-08-07	94.0	0.23	TD-08-07	153.0	1.04
TD-08-07	36.0	0.03	TD-08-07	95.0	0.23	TD-08-07	154.0	3.29
TD-08-07	37.0	0.00	TD-08-07	96.0	0.43	TD-08-07	155.0	34.50
TD-08-07	38.0	0.00	TD-08-07	97.0	0.38	TD-08-07	156.0	34.20
TD-08-07	39.0	0.16	TD-08-07	98.0	0.20	TD-08-07	157.0	34.50
TD-08-07	40.0	0.05	TD-08-07	99.0	0.25	TD-08-07	158.0	39.50
TD-08-07	41.0	0.12	TD-08-07	100.0	0.18	TD-08-07	159.0	29.00
TD-08-07	42.0	0.01	TD-08-07	101.0	0.71	TD-08-07	160.0	30.00
TD-08-07	43.0	0.01	TD-08-07	102.0	0.14	TD-08-07	161.0	35.10
TD-08-07	44.0	0.12	TD-08-07	103.0	0.42	TD-08-07	162.0	33.80
TD-08-07	45.0	0.14	TD-08-07	104.0	0.54	TD-08-07	163.0	36.40
TD-08-07	46.0	0.03	TD-08-07	105.0	0.51	TD-08-07	164.0	31.10
TD-08-07	47.0	0.10	TD-08-07	106.0	0.60	TD-08-07	165.0	31.70
TD-08-07	48.0	0.12	TD-08-07	107.0	0.73	TD-08-07	166.0	32.90
TD-08-07	49.0	0.10	TD-08-07	108.0	2.37	TD-08-07	167.0	35.20
TD-08-07	50.0	0.07	TD-08-07	109.0	1.62	TD-08-07	168.0	31.20
TD-08-07	51.0	0.01	TD-08-07	110.0	0.51	TD-08-07	169.0	25.70
TD-08-07	52.0	-0.01	TD-08-07	111.0	0.47	TD-08-07	170.0	38.50
TD-08-07	53.0	0.03	TD-08-07	112.0	0.45	TD-08-07	171.0	38.10
TD-08-07	54.0	0.12	TD-08-07	113.0	0.51	TD-08-07	172.0	30.40
TD-08-07	55.0	0.21	TD-08-07	114.0	0.47	TD-08-07	173.0	33.80
TD-08-07	56.0	0.09	TD-08-07	115.0	0.45	TD-08-07	174.0	27.00
TD-08-07	57.0	0.09	TD-08-07	116.0	0.51	TD-08-07	175.0	39.20
TD-08-07	58.0	0.12	TD-08-07	117.0	46.90	TD-08-07	176.0	32.90
TD-08-07	59.0	0.16	TD-08-07	118.0	0.34	TD-08-07	177.0	28.90



Hole	Depth (m)	Magnetic Susceptibility	Hole	Depth (m)	Magnetic Susceptibility	Hole	Depth (m)	Magnetic Susceptibility
TD-08-07	178.0	27.20	TD-08-07	237.0	0.36			
TD-08-07	179.0	46.50	TD-08-07	238.0	0.34			
TD-08-07	180.0	29.80	TD-08-07	239.0	0.36			
TD-08-07	181.0	29.60	TD-08-07	240.0	0.36			
TD-08-07	182.0	24.10	TD-08-07	241.0	0.23			
TD-08-07	183.0	14.30	TD-08-07	242.0	0.36			
TD-08-07	184.0	21.60	TD-08-07	243.0	0.29			
TD-08-07	185.0	28.30	TD-08-07	244.0	0.36			
TD-08-07	186.0	21.10	TD-08-07	245.0	0.32			
TD-08-07	187.0	35.70	TD-08-07	246.0	0.23			
TD-08-07	188.0	34.70	TD-08-07	247.0	0.43			
TD-08-07	189.0	29.60	TD-08-07	248.0	0.43			
TD-08-07	190.0	30.20	TD-08-07	249.0	0.38			
TD-08-07	191.0	28.40	TD-08-07	250.0	0.36			
TD-08-07	192.0	17.70	TD-08-07	251.0	0.36			
TD-08-07	193.0	18.60	TD-08-07	252.0	0.34			
TD-08-07	194.0	26.00	TD-08-07	253.0	0.25			
TD-08-07	195.0	8.50	TD-08-07	254.0	0.20			
TD-08-07	196.0	13.90	TD-08-07	255.0	0.20			
TD-08-07	197.0	7.64	TD-08-07	256.0	0.14			
TD-08-07	198.0	35.40	TD-08-07	257.0	0.07			
TD-08-07	199.0	13.60	TD-08-07	258.0	0.14			
TD-08-07	200.0	1.46	TD-08-07	259.0	0.12			
TD-08-07	201.0	0.20	TD-08-07	260.0	0.16			
TD-08-07	202.0	0.38	TD-08-07	261.0	0.18			
TD-08-07	203.0	0.05	TD-08-07	262.0	0.18			
TD-08-07	204.0	0.14	TD-08-07	263.0	0.20			
TD-08-07	205.0	0.27	TD-08-07	264.0	0.21			
TD-08-07	206.0	0.21	TD-08-07	265.0	0.23			
TD-08-07	207.0	0.27	TD-08-07	266.0	0.23			
TD-08-07	208.0	0.21	TD-08-07	267.0	0.23			
TD-08-07	209.0	0.23	TD-08-07	268.0	0.16			
TD-08-07	210.0	0.23	TD-08-07	269.0	0.14			
TD-08-07	211.0	0.25	TD-08-07	270.0	0.18			
TD-08-07	212.0	0.23	TD-08-07	271.0	0.18			
TD-08-07	213.0	0.25	TD-08-07	272.0	0.18			
TD-08-07	214.0	0.25	TD-08-07	273.0	0.47			
TD-08-07	215.0	0.27	TD-08-07	274.0	0.01			
TD-08-07	216.0	0.29	TD-08-07	275.0	0.16			
TD-08-07	217.0	0.34	TD-08-07	276.0	0.23			
TD-08-07	218.0	0.23	TD-08-07	277.0	0.14			
TD-08-07	219.0	0.05	TD-08-07	278.0	0.23			
TD-08-07	220.0	0.12	TD-08-07	279.0	0.42			
TD-08-07	221.0	0.14	TD-08-07	280.0	0.23			
TD-08-07	222.0	0.12	TD-08-07	281.0	0.16			
TD-08-07	223.0	0.16	TD-08-07	282.0	0.23			
TD-08-07	224.0	0.20						
TD-08-07	225.0	0.34						
TD-08-07	226.0	0.27						
TD-08-07	227.0	0.45						
TD-08-07	228.0	0.47						
TD-08-07	229.0	0.45						
TD-08-07	230.0	0.40						
TD-08-07	231.0	0.34						
TD-08-07	232.0	0.43						
TD-08-07	233.0	0.47						
TD-08-07	234.0	0.32						
TD-08-07	235.0	0.40						
TD-08-07	236.0	0.34						

Hole_ID	TD-08-08	Hole_Type	surface	<i>Purpose/Comments</i> Two intersections with kimberlitic volcaniclastic breccia: 150 - 269m and 347 - 472m. Intersections are separated by a Nipissing Diabase sill and Gowganda diamictite. At least four phases of kimberlitic volcaniclastic breccia were noted. Distinguished based on clast content, lapilli abundance, textures (i.e. segregation textures), matrix colour, grain size and magnetism. Latest phases are typically very fine-grained and contain the least amount of clasts. Earliest phases are clast-rich and contain abundant interstitial calcite cementing the clasts.
x	593365	Survey_Type	reflex	
y	5238528	Drill_Type	diamond	
z	0	Hole_Diameter	NQ	
Azimuth	180	Drill_Operator	Lafreniere	
Dip	-60			
Total Length	504.0			
Location	Temagami	StartDate	23-May-08	
Grid		EndDate	28-May-08	
Project	KRVY	Loggedby	E.Potter	
Claim		Sampledby		
MapSheet		Reloggedby		

Survey Data

Depth	Azimuth	Dip
24.0	179.1	-61.0
123.0	179	-60.9
225.0	184.4	-59.8
324.0	187	-59.2
423.0	189.4	-58.4
504.0	191.3	-58.5



<i>From (m)</i>	<i>To (m)</i>	<i>Geological Description</i>	<i>Lab #</i>	<i>FROM</i>	<i>TO</i>	<i>INT.</i>
		<i>Formation Name / Unit Name</i>				<i>(m)</i>

0.0	1.7	OVB	Overburden			
			Casing			

1.7	49.0	Sst	Sandstone			
			Medium to fine-grained arkose units that are dark red to grey in colour. Interbedded with minor parallel laminated silt- and mudstone units. Bedding contacts are inclined 50-60 deg. TCA. Trace carbonate-talc? Lined fractures throughout (preferentially in coarser-grained arkose beds) intersect core at 15 deg.TCA.			

49.0	150.5	Slst	Siltstone			
			Parallel laminated silt- and mudstone units with bedding contacts inclined 60 deg. TCA. Very competent core and no macroscopic signs of alteration aside from fracturing. Minor, <1m thick, red-brown arkose beds throughout. Sharp upper contact but intensely iron-altered and fractured lower contact with VBX.			
			79.0 80.6 Sandstone			

- Broken arkosic core with white carbonate lined fragments.
- 83.4 83.7 Fault carbonate
Broken core/gravel-sized rubble with fragments covered by a light green carbonate "mud".
- 85.3 86.3 Sandstone
Stockwork calcite-talc? stringers in fractured arkose.
- 90.9 91.2 Vein
Fractured core with infilled with a light green carbonate "mud" containing 5-10% tiny muscovite (<1mm white-clear mica) grains.
- 98.3 98.6 Fault
Fractured/ gravel-sized rubble with light green carbonate 'mud' covering fragments and filling stringers.
- 109.9 110.8 Fault
Fractured/ gravel-sized rubble with light green carbonate 'mud' covering fragments and filling stringers cross-cutting core at 15 deg. TCA.
- 114.5 114.6 Fault
Fractured/ gravel-sized rubble with light green carbonate 'mud' covering fragments and filling stringers cross-cutting core at 15 deg. TCA.
- 116.2 117.0 Fault
Fractured/ gravel-sized rubble with light green carbonate 'mud' covering fragments and filling stringers.
- 117.6 119.0 Fault
Fractured/ gravel-sized rubble with light green carbonate 'mud' covering fragments and filling stringers.
- 130.6 130.7 Vein
White calcite-chlorite-quartz stringer cross-cuts core at 20 deg. TCA.
- 136.7 137.3 Vein
White calcite-chlorite-quartz vein breccia with vuggy textures and minor iron staining cross-cuts core at 20 deg. TCA.
- 145.3 145.8 Fault
Broken angular core fragments with chlorite-epidote lined fragments.
- 148.1 149.4 Siltstone
Intense iron-alteration associated with a series of parallel, light-green carbonate stringers cross-cutting core at 20 deg. TCA.

150.5 232.8 **VBX Volcanic Breccia**

Clast-supported (30-70% clasts) carbonate-bearing volcanoclastic breccia with distinct zones based on carbonate content, clast proportions, alteration and juvenile lapilli content.

150.5 164.0 Volcanic Breccia

Clast-supported (40-70% clasts), dark green-grey coloured volcanoclastic breccia. White interstitial calcite is present in first 50cm of unit. Heterolithic with clasts subangular to rounded in shape and abundant (~5%) juvenile lapilli (2-40mm dia) and jacketed clasts. One possible Ilherolitic nodule noted at 162.50m. Matrix consists of 5-10% rounded biotite grains (<2mm), rounded magnetite (5%) and trace elongated black mineral (pos. ilmenite) set in a very fine-grained, carbonate-bearing matrix.

164.0 171.0 Volcanic Breccia

Highly corroded and iron-stained unit with increased iron alteration of clasts. Almost a rubble in places. Clast-supported (80% clasts) with rounded to subangular clasts and minor juvenile lapilli (~5%). Mottle dark green and dark red matrix with iron-oxidized biotite grains, potential ilmenite and possibly apatite grains set in a calcite-poor matrix (very little reaction with HCl). Biotite forms <5% of matrix and is <2mm. Non to weakly magnetic.

171.0 176.6 Volcanic Breccia

Clast-supported volcanoclastic breccia with interstitial white calcite. Clasts are rounded to subangular in shape and the zone contains minor juvenile lapilli (<5%). Matrix is light green in colour, fine-grained and contains trace, rounded biotite grains (<2mm), calcite and possibly trace apatite. Non-magnetic.

176.6 200.0 Volcanic Breccia

Clast-supported (70% clasts), dark green-grey coloured volcanoclastic breccia. Heterolithic with subangular to rounded clasts and minor (~5%) juvenile lapilli. Matrix consists of 5-10% rounded biotite grains (<2mm), 5% rounded magnetite (~5mm) and trace elongated black mineral (pos. ilmenite) set in a very fine-grained, carbonate-bearing (weak reaction with HCl) matrix.

200.0 203.9 Volcanic Breccia

Clast-supported zone (90%) with large angular quartz arenite-arkosic fragments set in a iron-altered, dark red-brown to dark green matrix. Matrix is very fine-grained, and contains 5% rounded biotite crystals in an otherwise aphanitic matrix. Matrix is not reactive with HCl, but there are discrete crystals of white calcite interstitial to the angular quartz arenite clasts. Non-magnetic.

203.9 232.8 Volcanic Breccia

Clast-supported (50-70% clasts), dark green-grey coloured volcanoclastic breccia. Heterolithic with subangular to rounded clasts and trace (<5%) juvenile lapilli. Matrix consists of 5-10% rounded biotite grains (<2mm), <2% rounded magnetite (2-5mm), trace elongated black mineral (pos. ilmenite) and possible euhedral apatite crystals set in a very fine-grained, carbonate-bearing (weak reaction with HCl) matrix. Magnetic matrix and a few grains of pyrite noted. Increased iron-alteration and corrosion of unit 214.25-216.25 but no changes in textures/mineralogy.

232.8 234.9 **KMB Kimberlite**
Light grey, matrix-supported (10-15% clasts) volcanoclastic dike with diffuse intrusive contacts 30 deg. TCA. Clasts are well-rounded, typically <1cm and are highly corroded with iron and carbonate alteration. Small (<2mm) rounded biotite grains and trace rounded magnetite (<4mm) grains are set in a carbonate-rich (reacts well with HCl), fine-grained matrix. Subeuhedral, serpentinized phenocrysts occur in minor amounts (<5%). Aphanitic banding runs roughly parallel with contacts and is associated with rose calcite stringers. Unit is strongly magnetic

234.9 250.5 **VBX Volcanic Breccia**
Clast-supported (40-70% clasts), dark green-grey coloured volcanoclastic breccia. Heterolithic with subangular to rounded clasts and minor (~5%) juvenile lapilli. Matrix consists of 5-10% rounded biotite grains (<2mm), rounded magnetite (5%) and trace elongated black mineral (pos. ilmenite) set in a very fine-grained, carbonate-bearing (weak reaction with HCl) matrix. Continuation of VBX from 150.3-232.8

245.5 249.8 Volcanic Breccia

Clast-supported (~80% clasts), heterolithic, calcite-bearing volcanoclastic breccia with rounded clasts and juvenile lapilli set in a white calcite or medium grey-green, carbonate-poor matrix. Calcite is interstitial to clasts and lapilli cementing the clasts.

250.5 251.6 **KMB Kimberlite**
Matrix-supported (10-20% clasts) dark grey volcanoclastic breccia with intensely iron-altered clasts set in a carbonate-rich matrix (reacts well to HCl). Small biotite (<1mm) grains display iron oxidation/alteration and are set in a fine-grained matrix. No other crystals noted in matrix. Late white calcite stringers cross-cut the unit at 35 deg. TCA.

251.6 269.2 **VBX Volcanic Breccia**
Clast-supported (40-70% clasts), dark green-grey coloured volcanoclastic breccia. Heterolithic with subangular to rounded clasts and minor (~5%) juvenile lapilli. Matrix consists of 5-10% rounded biotite grains (<2mm), rounded magnetite (5%) and trace elongated black mineral (pos. ilmenite) set in a very fine-grained, carbonate-bearing (weak reaction with HCl) matrix. Continuation of VBX from 234.9-250.55. Basal contact (last 1m) of unit displays intense iron-alteration and corrosion to almost a gravel-sized rubble.

252.0 257.5 Volcanic Breccia

Clast-supported (~80% clasts), heterolithic, calcite-bearing volcanoclastic breccia with rounded clasts and juvenile lapilli set in a white calcite or medium grey-green, carbonate-poor matrix. Calcite is interstitial to clasts and lapilli cementing the clasts.

269.2 306.4 **BaCl Basal Conglomerate**

Matrix-supported Gowganda diamictite with rounded clasts set in a siltstone matrix; decreasing clasts concentration with depth.

269.2 270.8 Basal Conglomerate

Iron-stained and fractured core with sharp, angular fragments at contact with VBX above.

273.0 273.3 Basal Conglomerate

Iron stained with trace carbonate and epidote lined fractures cross-cut core at 30 deg. TCA.

274.4 274.8 Basal Conglomerate

Iron stained (with minor green carbonate 'mud') stringers cross-cut core at 30 deg. TCA.

281.7 284.8 Basal Conglomerate calcite

Trace, rose calcite stringers cross-cut core at 30 deg. TCA. Almost stockwork in places.

287.9 289.3 Basal Conglomerate

Broken core with iron-stained, carbonate and epidote-lined fragments. Breaking along fractures inclined 15 deg. TCA.

290.5 291.0 Basal Conglomerate

Broken core with iron-stained, carbonate and epidote-lined fragments. Breaking along fractures inclined 15 deg. TCA.

306.4 347.0 **NipD Nippising Diabase / Meta Gabbro**

Fine to medium grained Nippising Diabase sill with aphanitic, quartz diabase chill margins. Trace quartz-calcite-chlorite+/- antigorite (green serpentine) veinlets throughout at ~45 deg. TCA. Chlorite-spotted contacts inclined 25 deg. TCA.

308.2 208.4 Nippising Diabase / Meta calcite
Gabbro

Sheared quartz-calcite-chlorite-antigorite vein (~5cm) inclined 50 deg. TCA.

312.4	312.6	Nippising Diabase / Meta Gabbro		Trace epidote stringers cross-cut core at 20 deg. TCA.
315.9	316.0	Nippising Diabase / Meta Gabbro	calcite	Sheared, calcite-quartz-chlorite-antigorite veinlet inclined 45 deg. TCA.
326.8	327.0	Nippising Diabase / Meta Gabbro	calcite	Sheared, calcite-quartz-chlorite-antigorite vein (5cm) inclined 50 deg. TCA.
332.7	332.8	Nippising Diabase / Meta Gabbro	calcite	Sheared, calcite-quartz-chlorite-antigorite vein (5cm) inclined 45 deg. TCA.
337.9	338.0	Nippising Diabase / Meta Gabbro	calcite	Calcite-quartz-chlorite-antigorite veinlet (1cm) inclined 50 deg. TCA.
338.3	338.4	Nippising Diabase / Meta Gabbro	chalcopyrite	Calcite-red hematite-quartz-chlorite-antigorite stringers inclined 50 deg. TCA. Trace (0.1%) chalcopyrite in stringer.
339.2	339.6	Nippising Diabase / Meta Gabbro	calcite	Vuggy, calcite veinlets with euhedral calcite crystals lining both veinlet contacts. Inclined 20 deg. TCA.
344.1	344.2	Nippising Diabase / Meta Gabbro	calcite	Calcite-quartz-red hematite veinlet (<2cm) inclined 50 deg. TCA.

347.0 399.1 **BaCl Basal Conglomerate**

Matrix-supported, Gowganda diamictite with <5% rounded clasts set in a siltstone matrix. Carbonate veining and brecciation along upper and lower contacts. Lowermost 12m are intensely veined by carbonate volcanoclastic breccias and iron-altered.

347.0 348.7 Basal Conglomerate

Broken core and rubble with fragments covered by lime-green carbonate 'mud'. Trace stringers inclined 20 deg. TCA.

349.2 351.7 Basal Conglomerate

Minor (~5%) green carbonate 'mud' stringers fracturing core 15-50 deg. TCA. Carbonate stringers are cross-cut by a later, rose calcite stringers that is inclined 50 deg. TCA.

- 367.0 377.1 Basal Conglomerate
Increasing concentration of calcite stringers that have (<0.5cm) iron-alteration halos (become stockwork from 372-377.10m upto 5 modal%). Dominant angle is 30 deg. TCA.
- 377.1 377.3 Kimberlite
Dark grey, matrix-supported carbonate volcanoclastic dike cross-cuts BaCl at 50 deg. TCA. Unit has sharp contacts and reacts well with HCl. 20-30% rounded clasts displaying intense iron-alteration and corrosion. Porphyritic matrix contains 10-15% black biotite, trace subeuhedral magnetite, and trace pyrite. Strongly magnetic.
- 377.3 380.2 Basal Conglomerate
Brecciated, iron-altered diamictite with mottled green and rusty red coloured matrix. Cross-cut by calcite-chlorite stringers.
- 380.2 381.8 Kimberlite
Matrix-supported (~30% clasts) volcanoclastic dike with predominantly rounded, diamictite clasts set in a light-grey, carbonate-rich matrix. Clasts are intensely iron altered/oxidized. Very fine-grained matrix contains trace biotite, and possible euhedral apatite crystals. Magnetic.
- 381.8 383.4 Basal Conglomerate
Brecciated, iron-altered diamictite with mottled green and rusty red coloured matrix. Cross-cut by calcite-chlorite stringers.
- 383.4 383.7 Kimberlite
Matrix-supported (~30% clasts) dark grey volcanoclastic dike rich in juvenile lapilli (40%) with interstitial white calcite (segregation texture). Unit displays flow alignment of clasts and has sharp contacts with breccias above and below. Host to lapilli consists of white calcite and some fine-grained, dark-green carbonate-bearing matrix with 5-10% rounded biotite grains (<3mm). Unit is weakly magnetic.
- 383.7 391.3 Basal Conglomerate
Brecciated, iron-altered diamictite with mottled green and rusty red coloured matrix. Cross-cut by calcite-chlorite stringers. Core reduced to rubble in places and when in this state is covered with light green carbonate 'mud'.
- 391.3 392.2 Kimberlite
Dark grey, matrix-supported carbonate volcanoclastic dike with 20-30% rounded clasts displaying intense iron-alteration and corrosion. Porphyritic matrix contains 20% black biotite, trace subeuhedral magnetite, and trace pyrite. Possible ilmenite phenocrysts (3-4mm) and potential trace pink-red garnets noted at 391.48m on broken (fresh) surface. Brecciated contacts with iron-altered diamictite fragments. Strongly magnetic and reacts well with HCl. Possible VBX#3.
- 392.2 393.7 Basal Conglomerate
Brecciated, iron-altered diamictite with mottled green and rusty red coloured matrix. Cross-cut by calcite-chlorite stringers. Core reduced to rubble in places and when in this state is covered with light green carbonate 'mud'.
- 393.6 398.0 Basal Conglomerate
Brecciated diamictite with angular, iron-altered clasts cemented by white calcite (10%). Non-magnetic.

393.7 394.0 Kimberlite

Matrix-supported (~30% clasts) dark grey volcanoclastic dike rich in juvenile lapilli (50%) with interstitial white calcite (segregation texture). Unit has sharp contacts with breccias above and below ~75 deg. TCA). Host to lapilli consists of white calcite and trace, fine-grained, dark-green carbonate-bearing matrix with 5-10% rounded biotite grains (<3mm). Unit is weakly magnetic.

394.0 394.5 Basal Conglomerate

Brecciated, iron-altered diamictite with mottled green and rusty red coloured matrix. Cross-cut by calcite-chlorite stringers.

394.5 394.8 Kimberlite

Matrix-supported (10% clasts), dark grey carbonate volcanoclastic breccia. Brecciated and iron altered contacts with diamictite. Dark matrix contains 15% biotite, discrete calcite crystals and trace potential apatite crystals set in a carbonate-rich groundmass (reacts well to HCl). Strongly magnetic.

394.8 397.1 Basal Conglomerate

Brecciated, iron-altered diamictite with mottled green and rusty red coloured matrix. Cross-cut by calcite-chlorite stringers. Core reduced to rubble in places and when in this state is covered with light green carbonate 'mud'.

397.1 397.6 Kimberlite

Matrix-supported (~30% clasts) dark grey volcanoclastic dike rich in juvenile lapilli (60%) with interstitial white calcite (segregation texture). Lapilli are rimmed by what appears to be amphibole (hornblende) then cemented in place by the interstitial calcite. Unit is magnetic.

397.6 398.0 Basal Conglomerate

Brecciated diamictite with rounded, iron-altered clasts cemented by white calcite (10%). Non-magnetic.

398.0 398.1 Kimberlite

Matrix-supported (~30% clasts) dark grey volcanoclastic dike rich in juvenile lapilli (60%) with interstitial white calcite (segregation texture). Lapilli are rimmed by what appears to be amphibole (hornblende) then cemented in place by the interstitial calcite. Unit is magnetic.

398.1 398.2 Basal Conglomerate

Brecciated diamictite with rounded, iron-altered clasts cemented by white calcite (10%). Non-magnetic.

398.2 402.5 Sandstone

Matrix-supported diamictite grades into lithic arkose then clast-supported, heterolithic conglomerate. Veined by lapilli-rich VBX.

399.1 402.5 Sst Sandstone

Lithic arenite to conglomeratic unit intensely veined by carbonate volcanoclastic breccias.

399.1 399.5 Kimberlite

Lapilli-rich (60-70%), carbonate volcanoclastic breccia containing minor lithic clasts (<10%) cemented by white calcite (segregation texture) and lesser amounts of a spotted green-red matrix. Juvenile lapilli and trace dark green-dark red matrix are strongly magnetic. Red-spots within green matrix appear to be related to iron-oxidation. Green matrix contains trace (<5%) black biotite and trace rounded magnetite in a very fine-grained groundmass.

399.7 400.7 Kimberlite

Lapilli-rich (60-70%), carbonate volcanoclastic breccia containing minor lithic clasts (<10%) cemented by white calcite (segregation texture) and lesser amounts of a spotted green-red matrix. Juvenile lapilli and trace dark green-dark red matrix are strongly magnetic. Red-spots within green matrix appear to be related to iron-oxidation. Green matrix contains trace (<5%) black biotite and trace rounded magnetite in a very fine-grained groundmass.

400.8 401.0 Kimberlite

Lapilli-rich (60-70%), carbonate volcanoclastic breccia containing minor lithic clasts (<10%) cemented by white calcite (segregation texture) and lesser amounts of a spotted green-red matrix. Juvenile lapilli and trace dark green-dark red matrix are strongly magnetic. Red-spots within green matrix appear to be related to iron-oxidation. Green matrix contains trace (<5%) black biotite and trace rounded magnetite in a very fine-grained groundmass.

401.2 401.5 Kimberlite

Lapilli-rich (60-70%), carbonate volcanoclastic breccia containing minor lithic clasts (<10%) cemented by white calcite (segregation texture) and lesser amounts of a spotted green-red matrix. Juvenile lapilli and trace dark green-dark red matrix are strongly magnetic. Red-spots within green matrix appear to be related to iron-oxidation. Green matrix contains trace (<5%) black biotite and trace rounded magnetite in a very fine-grained groundmass.

402.5 444.5 **KMB Kimberlite**

Lapilli-rich (40-90%) carbonate volcanoclastic breccia. Varying clast proportion (5-40%), but all intensely iron-altered and corroded. Juvenile lapilli are dark green in colour and are surrounded by white calcite and trace dark green carbonate-rich material (segregation texture). When present, the green carbonate groundmass contains minor (5%) biotite, trace (~1%) magnetite (<4mm) and trace ilmenite (<4mm, non-magnetic grains). Lapilli are not typically cored, but do contain trace serpentine pseudomorphs. A few potential Cr-diopside grains were noted coring lapilli at 429.61m and 430.81m. Trace calcite stringers cross-cut the unit at 10-30 deg. TCA.

444.5 472.6 **VBX Volcanic Breccia**

Clast-supported (90%) carbonate volcanoclastic breccia. Clasts are subangular, predominantly diamictite and sandstone in composition and have been fractured in situ. Clasts display minor carbonate alteration (no iron-alteration/corrosion). Minor (<5%) dark green lapilli. Breccia cement is predominantly white calcite with lesser dark red-to green matrix material near the

upper contact. Non-magnetic unit.

450.5 454.6 Volcanic Breccia

Dark red coloured matrix related to iron-alteration/oxidation of clast-supported breccia.

455.3 455.8 Kimberlite

Dark grey, matrix-supported carbonate volcanoclastic dike cross-cuts clast-supported VBX at 50 deg. TCA. Unit has sharp contacts and reacts well with HCl. 20-30% rounded clasts displaying intense iron-alteration and corrosion. Porphyritic matrix contains 10-15% black biotite, trace subeuhedral magnetite, and trace pyrite. Strongly magnetic. Possible VBX#3.

472.6 504.0 BaCl Basal Conglomerate

Matrix-supported, Gowganda diamictite with rounded clasts set in a siltstone matrix.

472.6 475.2 Basal Conglomerate calcite

Minor to trace abundance of rose calcite-chlorite veinlets and light green carbonate stringers. Rose calcite stringers contain trace chalcopyrite (0.1%) while the carbonate stringers have a bleached (carbonate) alteration halo (<0.5cm).

475.6 475.7 Basal Conglomerate calcite

Rose calcite-chlorite veinlet (~1cm) inclined 20 deg. TCA.

478.0 478.5 Basal Conglomerate calcite

Rose calcite-chlorite stringer inclined 5 deg. TCA.

479.7 480.1 Basal Conglomerate calcite

Rose calcite-chlorite veinlet with trace chalcopyrite infilling randomly orientated fractures.

492.0 492.4 Fault chlorite

Broken and fractured core with angular fragments displaying chlorite lineations.

504.0 504.0 EOH End of Hole

From (m)

T

Geological Description

Formation Name / Unit Name

Lab # FROM

INT.

(m)

Hole	Depth (m)	Magnetic Susceptibility	Hole	Depth (m)	Magnetic Susceptibility	Hole	Depth (m)	Magnetic Susceptibility
TD-08-08	2.0	0.07	TD-08-08	61.0	1.51	TD-08-08	120.0	0.89
TD-08-08	3.0	0.03	TD-08-08	62.0	1.37	TD-08-08	121.0	0.43
TD-08-08	4.0	0.10	TD-08-08	63.0	1.68	TD-08-08	122.0	0.69
TD-08-08	5.0	0.14	TD-08-08	64.0	1.22	TD-08-08	123.0	1.48
TD-08-08	6.0	0.09	TD-08-08	65.0	0.32	TD-08-08	124.0	0.31
TD-08-08	7.0	0.09	TD-08-08	66.0	0.31	TD-08-08	125.0	0.34
TD-08-08	8.0	0.09	TD-08-08	67.0	1.18	TD-08-08	126.0	0.32
TD-08-08	9.0	0.09	TD-08-08	68.0	0.43	TD-08-08	127.0	0.31
TD-08-08	10.0	0.09	TD-08-08	69.0	1.35	TD-08-08	128.0	0.36
TD-08-08	11.0	0.09	TD-08-08	70.0	1.70	TD-08-08	129.0	0.34
TD-08-08	12.0	0.12	TD-08-08	71.0	1.86	TD-08-08	130.0	0.29
TD-08-08	13.0	0.07	TD-08-08	72.0	1.24	TD-08-08	131.0	0.10
TD-08-08	14.0	0.03	TD-08-08	73.0	0.98	TD-08-08	132.0	0.27
TD-08-08	15.0	0.14	TD-08-08	74.0	1.09	TD-08-08	133.0	0.25
TD-08-08	16.0	0.14	TD-08-08	75.0	0.62	TD-08-08	134.0	0.27
TD-08-08	17.0	0.03	TD-08-08	76.0	0.43	TD-08-08	135.0	0.29
TD-08-08	18.0	0.10	TD-08-08	77.0	0.25	TD-08-08	136.0	0.36
TD-08-08	19.0	0.12	TD-08-08	78.0	0.29	TD-08-08	137.0	0.31
TD-08-08	20.0	0.03	TD-08-08	79.0	0.21	TD-08-08	138.0	0.29
TD-08-08	21.0	0.10	TD-08-08	80.0	0.20	TD-08-08	139.0	0.31
TD-08-08	22.0	0.05	TD-08-08	81.0	0.21	TD-08-08	140.0	0.36
TD-08-08	23.0	0.05	TD-08-08	82.0	0.27	TD-08-08	141.0	0.31
TD-08-08	24.0	0.03	TD-08-08	83.0	0.16	TD-08-08	142.0	0.32
TD-08-08	25.0	0.18	TD-08-08	84.0	0.14	TD-08-08	143.0	0.32
TD-08-08	26.0	0.07	TD-08-08	85.0	0.20	TD-08-08	144.0	0.34
TD-08-08	27.0	0.01	TD-08-08	86.0	0.09	TD-08-08	145.0	0.31
TD-08-08	28.0	0.12	TD-08-08	87.0	0.21	TD-08-08	146.0	0.40
TD-08-08	29.0	0.07	TD-08-08	88.0	0.20	TD-08-08	147.0	0.29
TD-08-08	30.0	0.03	TD-08-08	89.0	0.14	TD-08-08	148.0	0.31
TD-08-08	31.0	0.14	TD-08-08	90.0	0.23	TD-08-08	149.0	0.14
TD-08-08	32.0	0.09	TD-08-08	91.0	0.20	TD-08-08	150.0	0.34
TD-08-08	33.0	0.12	TD-08-08	92.0	0.27	TD-08-08	151.0	9.58
TD-08-08	34.0	0.07	TD-08-08	93.0	0.31	TD-08-08	152.0	61.50
TD-08-08	35.0	0.01	TD-08-08	94.0	0.20	TD-08-08	153.0	17.60
TD-08-08	36.0	-0.09	TD-08-08	95.0	0.21	TD-08-08	154.0	38.70
TD-08-08	37.0	0.20	TD-08-08	96.0	0.25	TD-08-08	155.0	66.40
TD-08-08	38.0	0.09	TD-08-08	97.0	0.23	TD-08-08	156.0	59.80
TD-08-08	39.0	0.20	TD-08-08	98.0	0.27	TD-08-08	157.0	65.10
TD-08-08	40.0	0.05	TD-08-08	99.0	0.18	TD-08-08	158.0	50.20
TD-08-08	41.0	0.10	TD-08-08	100.0	0.07	TD-08-08	159.0	34.20
TD-08-08	42.0	0.18	TD-08-08	101.0	0.18	TD-08-08	160.0	33.70
TD-08-08	43.0	0.14	TD-08-08	102.0	0.25	TD-08-08	161.0	39.40
TD-08-08	44.0	0.21	TD-08-08	103.0	0.21	TD-08-08	162.0	38.80
TD-08-08	45.0	0.21	TD-08-08	104.0	0.16	TD-08-08	163.0	43.90
TD-08-08	46.0	0.20	TD-08-08	105.0	0.21	TD-08-08	164.0	26.00
TD-08-08	47.0	0.09	TD-08-08	106.0	0.29	TD-08-08	165.0	31.70
TD-08-08	48.0	0.16	TD-08-08	107.0	0.43	TD-08-08	166.0	9.74
TD-08-08	49.0	0.21	TD-08-08	108.0	0.36	TD-08-08	167.0	9.33
TD-08-08	50.0	0.38	TD-08-08	109.0	0.62	TD-08-08	168.0	5.91
TD-08-08	51.0	0.78	TD-08-08	110.0	0.29	TD-08-08	169.0	4.50
TD-08-08	52.0	0.89	TD-08-08	111.0	0.78	TD-08-08	170.0	1.95
TD-08-08	53.0	0.60	TD-08-08	112.0	0.87	TD-08-08	171.0	2.01
TD-08-08	54.0	0.32	TD-08-08	113.0	0.76	TD-08-08	172.0	2.15
TD-08-08	55.0	1.28	TD-08-08	114.0	0.43	TD-08-08	173.0	0.23
TD-08-08	56.0	1.18	TD-08-08	115.0	0.56	TD-08-08	174.0	9.02
TD-08-08	57.0	1.15	TD-08-08	116.0	0.29	TD-08-08	175.0	1.72
TD-08-08	58.0	1.51	TD-08-08	117.0	0.32	TD-08-08	176.0	1.79
TD-08-08	59.0	1.22	TD-08-08	118.0	0.16	TD-08-08	177.0	6.86
TD-08-08	60.0	1.37	TD-08-08	119.0	0.38	TD-08-08	178.0	5.98

Hole	Depth (m)	Magnetic Susceptibility	Hole	Depth (m)	Magnetic Susceptibility	Hole	Depth (m)	Magnetic Susceptibility
TD-08-08	179.0	6.64	TD-08-08	238.0	1.46	TD-08-08	295.0	0.16
TD-08-08	180.0	6.42	TD-08-08	239.0	1.15	TD-08-08	296.0	0.16
TD-08-08	181.0	5.87	TD-08-08	240.0	1.13	TD-08-08	297.0	0.18
TD-08-08	182.0	4.86	TD-08-08	241.0	1.81	TD-08-08	298.0	0.16
TD-08-08	183.0	4.79	TD-08-08	242.0	2.01	TD-08-08	299.0	0.14
TD-08-08	184.0	12.80	TD-08-08	243.0	3.34	TD-08-08	300.0	0.18
TD-08-08	185.0	8.30	TD-08-08	244.0	2.70	TD-08-08	301.0	0.18
TD-08-08	186.0	6.11	TD-08-08	245.0	0.65	TD-08-08	302.0	0.18
TD-08-08	187.0	4.35	TD-08-08	246.0	1.46	TD-08-08	303.0	0.14
TD-08-08	188.0	11.70	TD-08-08	247.0	2.36	TD-08-08	304.0	0.14
TD-08-08	189.0	4.19	TD-08-08	248.0	6.44	TD-08-08	305.0	0.27
TD-08-08	190.0	6.25	TD-08-08	249.0	0.54	TD-08-08	306.0	0.27
TD-08-08	191.0	7.68	TD-08-08	250.0	7.86	TD-08-08	307.0	0.32
TD-08-08	192.0	1.62	TD-08-08	250.6	63.50	TD-08-08	308.0	0.38
TD-08-08	193.0	9.57	TD-08-08	251.0	41.10	TD-08-08	309.0	0.40
TD-08-08	194.0	10.10	TD-08-08	251.5	25.00	TD-08-08	310.0	0.23
TD-08-08	195.0	9.60	TD-08-08	252.0	2.43	TD-08-08	311.0	0.29
TD-08-08	196.0	5.50	TD-08-08	253.0	1.92	TD-08-08	312.0	0.38
TD-08-08	197.0	8.19	TD-08-08	254.0	4.17	TD-08-08	313.0	0.36
TD-08-08	198.0	10.20	TD-08-08	255.0	2.15	TD-08-08	314.0	0.43
TD-08-08	199.0	5.47	TD-08-08	256.0	0.82	TD-08-08	315.0	0.40
TD-08-08	200.0	2.90	TD-08-08	257.0	2.85	TD-08-08	316.0	0.32
TD-08-08	201.0	1.99	TD-08-08	258.0	21.60	TD-08-08	317.0	0.38
TD-08-08	202.0	0.62	TD-08-08	259.0	12.80	TD-08-08	318.0	0.38
TD-08-08	203.0	1.29	TD-08-08	260.0	6.53	TD-08-08	319.0	0.42
TD-08-08	204.0	3.27	TD-08-08	261.0	7.57	TD-08-08	320.0	0.36
TD-08-08	205.0	4.77	TD-08-08	262.0	21.30	TD-08-08	321.0	0.40
TD-08-08	206.0	8.05	TD-08-08	263.0	9.62	TD-08-08	322.0	0.38
TD-08-08	207.0	6.13	TD-08-08	264.0	8.38	TD-08-08	323.0	0.38
TD-08-08	208.0	8.72	TD-08-08	265.0	9.13	TD-08-08	324.0	0.34
TD-08-08	209.0	10.40	TD-08-08	266.0	1.83	TD-08-08	325.0	0.34
TD-08-08	210.0	4.15	TD-08-08	267.0	0.86	TD-08-08	326.0	0.36
TD-08-08	211.0	3.40	TD-08-08	268.0	2.83	TD-08-08	327.0	0.42
TD-08-08	212.0	6.78	TD-08-08	269.0	3.45	TD-08-08	328.0	0.53
TD-08-08	213.0	9.15	TD-08-08	270.0	0.16	TD-08-08	329.0	0.36
TD-08-08	214.0	6.35	TD-08-08	271.0	0.21	TD-08-08	330.0	0.40
TD-08-08	215.0	6.99	TD-08-08	272.0	0.16	TD-08-08	331.0	0.40
TD-08-08	216.0	7.46	TD-08-08	273.0	0.16	TD-08-08	332.0	0.38
TD-08-08	217.0	10.10	TD-08-08	274.0	0.18	TD-08-08	333.0	0.38
TD-08-08	218.0	4.37	TD-08-08	275.0	0.20	TD-08-08	334.0	0.38
TD-08-08	219.0	9.57	TD-08-08	276.0	0.20	TD-08-08	335.0	0.47
TD-08-08	220.0	10.90	TD-08-08	277.0	0.18	TD-08-08	336.0	0.38
TD-08-08	221.0	11.80	TD-08-08	278.0	0.21	TD-08-08	337.0	0.40
TD-08-08	222.0	11.90	TD-08-08	279.0	0.14	TD-08-08	338.0	0.32
TD-08-08	223.0	7.64	TD-08-08	280.0	0.40	TD-08-08	339.0	0.40
TD-08-08	224.0	9.36	TD-08-08	281.0	0.16	TD-08-08	340.0	0.38
TD-08-08	225.0	11.20	TD-08-08	282.0	0.16	TD-08-08	341.0	0.38
TD-08-08	226.0	8.80	TD-08-08	283.0	0.16	TD-08-08	342.0	0.40
TD-08-08	227.0	6.71	TD-08-08	284.0	0.16	TD-08-08	343.0	0.47
TD-08-08	228.0	7.55	TD-08-08	285.0	0.16	TD-08-08	344.0	0.31
TD-08-08	229.0	5.80	TD-08-08	286.0	0.16	TD-08-08	345.0	0.42
TD-08-08	230.0	4.35	TD-08-08	287.0	0.14	TD-08-08	346.0	0.36
TD-08-08	231.0	6.22	TD-08-08	288.0	0.12	TD-08-08	347.0	0.20
TD-08-08	232.0	12.20	TD-08-08	289.0	0.18	TD-08-08	348.0	0.18
TD-08-08	233.0	68.50	TD-08-08	290.0	0.18	TD-08-08	349.0	0.18
TD-08-08	234.0	71.17	TD-08-08	291.0	0.14	TD-08-08	350.0	0.14
TD-08-08	235.0	73.50	TD-08-08	292.0	0.20	TD-08-08	351.0	0.20
TD-08-08	236.0	4.26	TD-08-08	293.0	0.16	TD-08-08	352.0	0.27
TD-08-08	237.0	3.47	TD-08-08	294.0	0.12	TD-08-08	353.0	0.12

Hole	Depth (m)	Magnetic Susceptibility	Hole	Depth (m)	Magnetic Susceptibility	Hole	Depth (m)	Magnetic Susceptibility
TD-08-08	354.0	0.21	TD-08-08	400.0	65.20	TD-08-08	448.0	0.18
TD-08-08	355.0	0.20	TD-08-08	401.0	22.50	TD-08-08	449.0	0.18
TD-08-08	356.0	0.18	TD-08-08	401.5	6.62	TD-08-08	450.0	0.12
TD-08-08	357.0	0.18	TD-08-08	402.0	4.26	TD-08-08	451.0	0.07
TD-08-08	358.0	0.10	TD-08-08	402.0	55.40	TD-08-08	452.0	0.12
TD-08-08	359.0	0.20	TD-08-08	403.0	73.90	TD-08-08	453.0	0.16
TD-08-08	360.0	0.20	TD-08-08	403.5	55.40	TD-08-08	454.0	0.16
TD-08-08	361.0	0.21	TD-08-08	404.0	25.00	TD-08-08	455.0	0.14
TD-08-08	362.0	0.18	TD-08-08	405.0	51.80	TD-08-08	456.0	0.10
TD-08-08	363.0	0.14	TD-08-08	406.0	47.20	TD-08-08	457.0	0.62
TD-08-08	364.0	0.23	TD-08-08	407.0	77.30	TD-08-08	458.0	0.16
TD-08-08	365.0	0.21	TD-08-08	408.0	51.80	TD-08-08	459.0	0.12
TD-08-08	366.0	0.16	TD-08-08	409.0	77.20	TD-08-08	460.0	0.14
TD-08-08	367.0	0.18	TD-08-08	410.0	63.90	TD-08-08	461.0	0.16
TD-08-08	368.0	0.20	TD-08-08	411.0	54.30	TD-08-08	462.0	0.14
TD-08-08	369.0	0.20	TD-08-08	412.0	25.50	TD-08-08	463.0	0.16
TD-08-08	370.0	0.20	TD-08-08	413.0	66.60	TD-08-08	464.0	0.12
TD-08-08	371.0	0.20	TD-08-08	414.0	74.90	TD-08-08	465.0	0.10
TD-08-08	372.0	0.34	TD-08-08	415.0	72.80	TD-08-08	466.0	0.14
TD-08-08	373.0	0.31	TD-08-08	416.0	28.50	TD-08-08	467.0	0.14
TD-08-08	374.0	0.56	TD-08-08	417.0	43.10	TD-08-08	468.0	0.12
TD-08-08	375.0	0.27	TD-08-08	418.0	57.80	TD-08-08	469.0	0.32
TD-08-08	376.0	0.27	TD-08-08	419.0	55.50	TD-08-08	470.0	0.16
TD-08-08	377.0	0.98	TD-08-08	420.0	69.10	TD-08-08	471.0	0.14
TD-08-08	378.0	0.47	TD-08-08	421.0	81.20	TD-08-08	472.0	0.12
TD-08-08	379.0	0.40	TD-08-08	422.0	44.80	TD-08-08	473.0	0.14
TD-08-08	379.5	19.80	TD-08-08	423.0	72.10	TD-08-08	474.0	0.18
TD-08-08	380.0	1.57	TD-08-08	424.0	67.10	TD-08-08	475.0	0.32
TD-08-08	381.0	28.20	TD-08-08	425.0	65.80	TD-08-08	476.0	0.16
TD-08-08	381.5	31.20	TD-08-08	426.0	79.20	TD-08-08	477.0	0.14
TD-08-08	382.0	7.33	TD-08-08	427.0	70.10	TD-08-08	478.0	0.14
TD-08-08	382.5	1.35	TD-08-08	428.0	47.60	TD-08-08	479.0	0.14
TD-08-08	383.0	3.58	TD-08-08	429.0	64.10	TD-08-08	480.0	0.16
TD-08-08	384.0	0.27	TD-08-08	430.0	66.40	TD-08-08	481.0	0.14
TD-08-08	385.0	0.75	TD-08-08	431.0	76.70	TD-08-08	482.0	0.14
TD-08-08	386.0	0.86	TD-08-08	432.0	77.30	TD-08-08	483.0	0.18
TD-08-08	387.0	0.34	TD-08-08	433.0	81.10	TD-08-08	484.0	0.23
TD-08-08	388.0	0.29	TD-08-08	434.0	69.80	TD-08-08	485.0	0.20
TD-08-08	389.0	0.45	TD-08-08	435.0	63.00	TD-08-08	486.0	0.21
TD-08-08	390.0	1.70	TD-08-08	436.0	26.20	TD-08-08	487.0	0.21
TD-08-08	390.5	1.86	TD-08-08	436.5	58.00	TD-08-08	488.0	0.25
TD-08-08	391.0	6.20	TD-08-08	437.0	11.40	TD-08-08	489.0	0.12
TD-08-08	391.5	65.60	TD-08-08	437.5	27.50	TD-08-08	490.0	0.14
TD-08-08	392.0	34.10	TD-08-08	438.0	2.79	TD-08-08	491.0	0.29
TD-08-08	392.5	1.26	TD-08-08	438.5	32.60	TD-08-08	492.0	0.20
TD-08-08	393.0	3.31	TD-08-08	439.0	25.90	TD-08-08	493.0	0.32
TD-08-08	393.5	1.40	TD-08-08	439.5	1.68	TD-08-08	494.0	0.25
TD-08-08	394.0	0.40	TD-08-08	440.0	3.82	TD-08-08	495.0	0.25
TD-08-08	394.5	46.30	TD-08-08	440.5	66.10	TD-08-08	496.0	0.21
TD-08-08	395.0	0.67	TD-08-08	441.0	61.50	TD-08-08	497.0	0.27
TD-08-08	395.5	3.25	TD-08-08	441.5	59.50	TD-08-08	498.0	0.21
TD-08-08	396.0	2.36	TD-08-08	442.0	52.40	TD-08-08	499.0	0.31
TD-08-08	396.5	2.52	TD-08-08	442.5	33.30	TD-08-08	500.0	0.16
TD-08-08	397.0	0.87	TD-08-08	443.0	20.40	TD-08-08	501.0	0.16
TD-08-08	397.5	17.70	TD-08-08	443.5	7.92	TD-08-08	502.0	0.12
TD-08-08	398.0	36.30	TD-08-08	444.0	1.22	TD-08-08	503.0	0.14
TD-08-08	398.5	55.20	TD-08-08	445.0	0.21	TD-08-08	504.0	0.18
TD-08-08	399.0	2.72	TD-08-08	446.0	0.20			
TD-08-08	399.5	7.17	TD-08-08	447.0	0.16			

Hole_ID	TD-08-09	Hole_Type	surface	<i>Purpose/Comments</i> Hole consists of Huronian sediments underlain by a large Nipissing Diabase sill (EOH in diabase). Trace calcite-quartz-chlorite veinlets throughout the hole. Contact between the Gowganda diamictite and Nipissing Diabase sill is brecciated and several meters of drill core were not recovered - possible carbonate alteration along contact.
x	593275	Survey_Type	reflex	
y	5238300	Drill_Type	diamond	
z	0	Hole_Diameter	NQ	
Azimuth	42	Drill_Operator	Lafreniere	
Dip	-60			
Total Length	224.0			
Location	Temagami	StartDate	28-May-08	
Grid		EndDate	30-May-08	
Project	KRVY	Loggedby	E.Potter	
Claim		Sampledby		
MapSheet		Reloggedby		

Depth	Azimuth	Dip
30.0	46.5	-60.3
112.0	50.7	-62.0
224.0	53.8	-62.3



From (m)	To (m)	Geological Description	Lab #	FROM	TO	INT.
		Formation Name / Unit Name				(m)

0.0	1.9	OVB Casing	Overburden			
-----	-----	----------------------	-------------------	--	--	--

1.9	26.8	Sst	Sandstone	Dark grey to dark red, fine-grained arkose. Massive, competent core with very little fracturing.		
-----	------	------------	------------------	--	--	--

26.8	159.9	Slst	Siltstone	Parallel laminated silt- and mudstone with bedding inclined 60 deg. TCA. Mostly siltstone with <1cm mudstone beds. More fractured than overlying arkose; fractures are predominantly chlorite-lined and cross-cut the core at 30-40 deg. TCA. Trace interbedded dark red, fine-grained arkosic units <1m thick.		
	33.4	33.6	Fault	Possible fault with broken core with angular fragments		
	65.6	66.1	Fault	Possible fault with broken core and trace calcite-epidote mixture covering the fragments.		

95.6	95.7	Fault	Possible fault with broken core with angular fragments
97.4	97.9	Fault	Possible fault with broken core with angular fragments
108.4	108.5	Siltstone	calcite Calcite-chlorite veinlet breccia with minor (~5%) pyrite within veinlet breccia.
113.1	114.9	Fault	Possible fault with broken core with angular fragments
119.8	120.1	Siltstone	chlorite Broken core with chlorite-lined fractures running parallel TCA
133.0	133.5	Siltstone	calcite Broken core with sheared, quartz-chlorite-calcite veinlets.
133.5	133.9	Fault	Broken core with angular fragments and carbonate sealed fractures.
134.2	136.0	Siltstone	calcite Broken core with calcite-chlorite stringers fracturing the core at 10 deg. TCA.
137.0	140.7	Rubble	calcite Rubble with calcite stringers and trace light green carbonate 'mud'. Stringers cross-cut core at shallow angles.
141.4	141.8	Fault	Broken, angular core fragments and trace calcite stringers in fragments.
142.2	143.0	Siltstone	calcite Calcite-chlorite-quartz-epidote stringer fracturing core at 10 deg. TCA. Minor iron-staining along vein contacts
144.6	145.8		calcite Calcite-chlorite-quartz-epidote stringer running parallel TCA and fracturing. Minor iron-staining along vein contacts
146.3	147.7	Rubble	calcite Rubble with mior calcite and green carbonate 'mud' lining fragments.
150.3	152.7	Siltstone	calcite Fractured and broken core with calcite-quartz-epidote lined angular fragments. Fractures are inclined 10-20 deg. TCA.

152.7 153.5 Rubble
 Calcite-quartz-chlorite veinlet breccia and rubble. Some vuggy textures preserved on fragments.

153.5 154.5 Siltstone calcite
 Calcite-quartz stringers (5%) fracturing siltstone. Stringers cross-cut core at 30 deg. TCA.

154.5 156.0 Rubble calcite
 Calcite-quartz-chlorite vein rubble with trace vuggy calcite veinlet breccias. Poor recovery of core.

156.0 156.7 Siltstone calcite
 Calcite-quartz-chlorite veinlet running parallel TCA with minor fracturing.

157.5 158.2 Siltstone calcite
 Trace (<1%) calcite-quartz-chlorite stringers fracturing core at 10-20 deg. TCA.

159.9 176.5 **BaCl Basal Conglomerate**
 Matrix-supported (<10%), Gowganda diamictite with rounded clasts set in a siltstone matrix.

160.5 160.7 Basal Conglomerate calcite
 Broken core centered on calcite-quartz-chlorite veinlet cross-cutting at 25 deg. TCA.

161.6 161.7 Basal Conglomerate calcite
 Broken core centered on calcite-quartz-chlorite veinlet cross-cutting at 25 deg. TCA.

162.8 163.0 Basal Conglomerate calcite
 Calcite-quartz-chlorite veinlet running parallel TCA.

163.0 163.1 Rubble calcite
 Rubble with calcite-chlorite-quartz veinlet fragments.

163.1 164.0 Basal Conglomerate calcite
 Trace (<0.01%) calcite-quartz-chlorite stringers cross-cutting core at 25 deg. TCA.

169.5 170.5 Basal Conglomerate calcite
 Calcite-chlorite-quartz veinlets running parallel TCA with euhedral calcite crystals lining fractures.

173.3	173.6	Basal Conglomerate	calcite	Quartz-calcite vein (5cm) with iron-staining cross-cutting core at 40 deg. TCA.
173.9	175.3	Basal Conglomerate	carbonate	Light green carbonate 'mud' fracturing core. Orientated parallel to 15 deg. TCA.
176.2	180.1	Basal Conglomerate	calcite	Calcite-chlorite-quartz-epidote vein and vein breccia with poor recovery (177-180m missing) and minor vuggy, euhedral calcite crystals on lining fragments.

176.5 180.0 **Rub Rubble**
 Unrecovered contact with abundant carbonate veinlet breccia fragments bordering this section.

180.0 224.0 **NipD Nippising Diabase / Meta Gabbro**
 Fine-grained Nippising diabase with trace calcite-quartz-chlorite veinlets and stringers. Upper contact is brecciated with abundant carbonate stringers and fracturing of the aphanitic quartz diabase. EOH is within medium-grained, hypersthene diabase. Stringer concentration decreases with depth.

180.3	181.0	Nippising Diabase / Meta Gabbro		Iron-altered diabase with calcite-chlorite-quartz veinlets and veinlet breccia with vuggy textures (with euhedral calcite). Diabase fragments within veinlet breccia are extremely carbonate and epidote altered -decomposed to almost a green 'sand'.
181.4	181.5	Rubble	calcite	Calcite veinlet rubble.
181.6	181.8	Nippising Diabase / Meta Gabbro	calcite	Parallel, white and rose calcite-quartz-chlorite veinlets (<3cm) cross-cut core at 25 deg. TCA.
182.0	182.8	Nippising Diabase / Meta Gabbro	calcite	Calcite-quartz-epidote-chlorite veinlets and veinlet breccia (rubble). Vuggy with euhedral white calcite crystals. Intensely carbonate and epidote altered diabase fragments partially decomposed to green sand.

183.4	183.8	Nippising Diabase / Meta Gabbro	calcite	Calcite-quartz-chlorite veinlets and veinlet breccia with large vugs lined with euhedral calcite crystals cross-cutting core at 10 deg. TCA.
184.7	184.8	Nippising Diabase / Meta Gabbro	calcite	Sheared calcite-quartz chlorite veinlet with euhedral calcite in veinlet center. Veinlet cross-cut core at 15 deg. TCA.
185.1	185.3	Nippising Diabase / Meta Gabbro	calcite	Sheared calcite-quartz chlorite veinlet with euhedral calcite in veinlet center. Veinlet cross-cut core at 15 deg. TCA.
185.6	185.9	Nippising Diabase / Meta Gabbro	calcite	Calcite-quartz-chlorite veinlets cross-cutting core at 15 and 30 deg. TCA.
190.8	191.0	Nippising Diabase / Meta Gabbro	calcite	Rose calcite-chlorite-quartz veinlet cross-cutting core at 20 deg. TCA. Veinlet contains hornblende crystals and trace pyrite <0.01% on fracture surfaces.
195.5	195.7	Nippising Diabase / Meta Gabbro	calcite	Sheared calcite-quartz chlorite veinlet (3cm) cross-cuts core at 55 deg. TCA.
197.9	198.0	Nippising Diabase / Meta Gabbro	calcite	Sheared calcite-quartz chlorite veinlet (3cm) cross-cuts core at 55 deg. TCA with iron-alteration of diabase fragments.
203.0	203.0	Nippising Diabase / Meta Gabbro	calcite	Sheared calcite-quartz chlorite veinlet (<1cm) cross-cuts core at 40 deg. TCA.
210.8	210.9	Nippising Diabase / Meta Gabbro	calcite	Sheared calcite-quartz chlorite veinlet (<1cm) cross-cuts core at 40 deg. TCA.
212.0	212.1	Nippising Diabase / Meta Gabbro		Asbestiform antigorite-calcite-chlorite veinlet ~3cm cross-cutting core at 30 deg. TCA.
212.1	213.5	Nippising Diabase / Meta Gabbro	calcite	Sheared calcite-chlorite-quartz stringers running parallel TCA.
213.8	214.8	Nippising Diabase / Meta Gabbro	calcite	Trace (<0.01%) calcite-quartz-chlorite veinlets cross-cutting 30-50 deg. TCA.
218.4	218.4	Nippising Diabase / Meta Gabbro		Antigorite-calcite-chlorite veinlet cross-cutting core at 60 deg. TCA.

From (m)

7

Geological Description
Formation Name / Unit Name

Lab # FROM

INT.
(m)

224.0 224.0 EOH End of Hole

Hole	Depth (m)	Magnetic Susceptibility	Hole	Depth (m)	Magnetic Susceptibility	Hole	Depth (m)	Magnetic Susceptibility
TD-08-09	2.0	-0.67	TD-08-09	61.0	0.64	TD-08-09	120.0	0.23
TD-08-09	3.0	0.05	TD-08-09	62.0	0.16	TD-08-09	121.0	0.25
TD-08-09	4.0	0.00	TD-08-09	63.0	0.21	TD-08-09	122.0	0.27
TD-08-09	5.0	-0.07	TD-08-09	64.0	0.18	TD-08-09	123.0	0.25
TD-08-09	6.0	0.00	TD-08-09	65.0	0.20	TD-08-09	124.0	0.27
TD-08-09	7.0	0.09	TD-08-09	66.0	0.21	TD-08-09	125.0	0.29
TD-08-09	8.0	0.07	TD-08-09	67.0	0.31	TD-08-09	126.0	0.25
TD-08-09	9.0	0.00	TD-08-09	68.0	0.54	TD-08-09	127.0	0.29
TD-08-09	10.0	0.00	TD-08-09	69.0	1.81	TD-08-09	128.0	0.29
TD-08-09	11.0	0.05	TD-08-09	70.0	0.27	TD-08-09	129.0	0.29
TD-08-09	12.0	0.00	TD-08-09	71.0	0.05	TD-08-09	130.0	0.25
TD-08-09	13.0	-0.03	TD-08-09	72.0	1.13	TD-08-09	131.0	0.27
TD-08-09	14.0	0.07	TD-08-09	73.0	0.12	TD-08-09	132.0	0.29
TD-08-09	15.0	0.03	TD-08-09	74.0	0.09	TD-08-09	133.0	0.32
TD-08-09	16.0	0.12	TD-08-09	75.0	0.18	TD-08-09	134.0	0.27
TD-08-09	17.0	0.01	TD-08-09	76.0	0.51	TD-08-09	135.0	0.20
TD-08-09	18.0	0.07	TD-08-09	77.0	1.26	TD-08-09	136.0	0.27
TD-08-09	19.0	0.00	TD-08-09	78.0	0.56	TD-08-09	137.0	0.18
TD-08-09	20.0	0.00	TD-08-09	79.0	0.21	TD-08-09	138.0	0.25
TD-08-09	21.0	0.09	TD-08-09	80.0	0.25	TD-08-09	139.0	0.27
TD-08-09	22.0	0.00	TD-08-09	81.0	0.67	TD-08-09	140.0	0.16
TD-08-09	23.0	0.03	TD-08-09	82.0	0.32	TD-08-09	141.0	0.18
TD-08-09	24.0	0.16	TD-08-09	83.0	0.65	TD-08-09	142.0	0.27
TD-08-09	25.0	0.07	TD-08-09	84.0	0.47	TD-08-09	143.0	0.29
TD-08-09	26.0	0.05	TD-08-09	85.0	0.49	TD-08-09	144.0	0.20
TD-08-09	27.0	0.09	TD-08-09	86.0	0.21	TD-08-09	145.0	0.29
TD-08-09	28.0	0.18	TD-08-09	87.0	0.51	TD-08-09	146.0	0.23
TD-08-09	29.0	0.21	TD-08-09	88.0	0.21	TD-08-09	147.0	0.23
TD-08-09	30.0	0.16	TD-08-09	89.0	0.36	TD-08-09	148.0	0.31
TD-08-09	31.0	0.20	TD-08-09	90.0	0.38	TD-08-09	149.0	0.27
TD-08-09	32.0	1.37	TD-08-09	91.0	0.16	TD-08-09	150.0	0.03
TD-08-09	33.0	1.18	TD-08-09	92.0	0.21	TD-08-09	151.0	0.18
TD-08-09	34.0	1.31	TD-08-09	93.0	0.38	TD-08-09	152.0	0.20
TD-08-09	35.0	2.59	TD-08-09	94.0	3.55	TD-08-09	153.0	0.18
TD-08-09	36.0	2.58	TD-08-09	95.0	2.70	TD-08-09	154.0	0.21
TD-08-09	37.0	2.03	TD-08-09	96.0	0.32	TD-08-09	155.0	0.25
TD-08-09	38.0	2.14	TD-08-09	97.0	0.54	TD-08-09	156.0	0.23
TD-08-09	39.0	3.29	TD-08-09	98.0	0.58	TD-08-09	157.0	0.25
TD-08-09	40.0	3.01	TD-08-09	99.0	0.27	TD-08-09	158.0	0.23
TD-08-09	41.0	3.16	TD-08-09	100.0	0.31	TD-08-09	159.0	0.27
TD-08-09	42.0	3.31	TD-08-09	101.0	0.29	TD-08-09	160.0	0.20
TD-08-09	43.0	2.81	TD-08-09	102.0	0.29	TD-08-09	161.0	0.14
TD-08-09	44.0	3.09	TD-08-09	103.0	0.36	TD-08-09	162.0	0.14
TD-08-09	45.0	3.95	TD-08-09	104.0	0.00	TD-08-09	163.0	0.14
TD-08-09	46.0	3.86	TD-08-09	105.0	0.25	TD-08-09	164.0	0.18
TD-08-09	47.0	3.95	TD-08-09	106.0	0.18	TD-08-09	165.0	0.18
TD-08-09	48.0	3.91	TD-08-09	107.0	0.20	TD-08-09	166.0	0.09
TD-08-09	49.0	3.33	TD-08-09	108.0	0.25	TD-08-09	167.0	0.18
TD-08-09	50.0	3.42	TD-08-09	109.0	0.25	TD-08-09	168.0	0.12
TD-08-09	51.0	2.96	TD-08-09	110.0	0.27	TD-08-09	169.0	0.10
TD-08-09	52.0	2.79	TD-08-09	111.0	0.21	TD-08-09	170.0	0.09
TD-08-09	53.0	2.94	TD-08-09	112.0	0.29	TD-08-09	171.0	0.23
TD-08-09	54.0	2.98	TD-08-09	113.0	0.32	TD-08-09	172.0	0.21
TD-08-09	55.0	3.91	TD-08-09	114.0	0.29	TD-08-09	173.0	0.21
TD-08-09	56.0	2.19	TD-08-09	115.0	0.29	TD-08-09	174.0	0.20
TD-08-09	57.0	2.90	TD-08-09	116.0	0.29	TD-08-09	175.0	0.25
TD-08-09	58.0	1.72	TD-08-09	117.0	0.21	TD-08-09	176.0	0.23
TD-08-09	59.0	1.90	TD-08-09	118.0	0.31	TD-08-09	177.0	0.25
TD-08-09	60.0	1.31	TD-08-09	119.0	0.25	TD-08-09	178.0	0.31

Hole	Depth (m)	Magnetic Susceptibility	Hole	Depth (m)	Magnetic Susceptibility	Hole	Depth (m)	Magnetic Susceptibility
TD-08-09	179.0	0.36						
TD-08-09	180.0	0.31						
TD-08-09	181.0	0.42						
TD-08-09	182.0	0.38						
TD-08-09	183.0	0.36						
TD-08-09	184.0	0.43						
TD-08-09	185.0	0.31						
TD-08-09	186.0	0.38						
TD-08-09	187.0	0.32						
TD-08-09	188.0	0.42						
TD-08-09	189.0	0.45						
TD-08-09	190.0	0.40						
TD-08-09	191.0	0.38						
TD-08-09	192.0	0.42						
TD-08-09	193.0	0.40						
TD-08-09	194.0	0.43						
TD-08-09	195.0	0.38						
TD-08-09	196.0	0.40						
TD-08-09	197.0	0.40						
TD-08-09	198.0	0.38						
TD-08-09	199.0	0.36						
TD-08-09	200.0	0.36						
TD-08-09	201.0	0.42						
TD-08-09	202.0	0.38						
TD-08-09	203.0	0.36						
TD-08-09	204.0	0.42						
TD-08-09	205.0	0.40						
TD-08-09	206.0	0.42						
TD-08-09	207.0	0.38						
TD-08-09	208.0	0.34						
TD-08-09	209.0	0.42						
TD-08-09	210.0	0.38						
TD-08-09	211.0	0.38						
TD-08-09	212.0	0.32						
TD-08-09	213.0	0.36						
TD-08-09	214.0	0.38						
TD-08-09	215.0	0.34						
TD-08-09	216.0	0.38						
TD-08-09	217.0	0.36						
TD-08-09	218.0	0.36						
TD-08-09	219.0	0.42						
TD-08-09	220.0	0.38						
TD-08-09	221.0	0.36						
TD-08-09	222.0	0.45						
TD-08-09	223.0	0.45						
TD-08-09	224.0	0.43						

Hole_ID	TD-08-10	Hole_Type	surface	Purpose/Comments Main kimberlitic volcanoclastic intersection from 301-411m intruding diamictite. Minor kimberlitic veining in Gowganda diamictite from 420-433m. At least three kimberlitic phases identified and distinguished based on clast content, matrix colour, magnetism and abundance of lapilli. EOH was within fine-grained Nipissing Diabase.
x	593209	Survey_Type	reflex	
y	5238353	Drill_Type	diamond	
z	0	Hole_Diameter	NQ & BQ	
Azimuth	60	Drill_Operator	Lafreniere	
Dip	-55			
Total Length	636.0			
Location	Temagami	StartDate	30-May-08	
Grid		EndDate	10-Jun-08	
Project	KRVY	Loggedby	E.Potter	
Claim		Sampledby		
MapSheet		Reloggedby		

Depth	Azimuth	Dip
24.0	58.6	-54.4
126.0	63.2	-56.7
225.0	65.3	-57.4
402.0	236.3	-58.2
423.0	57.5	-57.9
534.0	58.4	-59.5
636.0	65.6	-57.5



From (m)	To (m)	Geological Description	Lab #	FROM	TO	INT.
		Formation Name / Unit Name				
0.0	3.0	OVB Overburden				

3.0	31.8	Sst Sandstone				
Fine-grained, dark red and grey arkose units with minor interbedded (<30cm) parallel laminated silt and mudstones. Bedding planes are inclined 45 deg. TCA.						
	7.9	7.9 Sandstone	calcite			
Rose calcite-quartz veinlet (<1cm) cross-cuts core at 50 deg. TCA.						
	9.2	9.3 Sandstone	calcite			
Calcite sealed fractures running parallel TCA.						
	14.3	14.7 Sandstone	calcite			
Broken core with angular fragments and trace calcite stringers.						
	16.3	16.5 Sandstone	calcite			
Calcite stringers fracturing core and a granular calcite veinlet cross-cut the core at 50 deg. TCA.						
	18.8	19.0 Sandstone	calcite			
Calcite stringers fracturing core and a granular calcite veinlet cross-cut the core at 50 deg. TCA.						

19.6 19.9 Sandstone calcite

Calcite stringers fracturing the core.

31.8 173.8 **Slst Siltstone**

Parallel laminated silt- and mudstones. Predominantly green siltstone interbedded by <1cm black mudstone beds. Trace arkosic units <1m. Bedding planes are inclined 50 deg. TCA.

141.2 141.4 Siltstone calcite

10cm quartz-chlorite-calcite vein and vein breccia with angular siltstone fragments within vein. Minor iron-staining associated with the vein breccia and angular clasts. Cross-cuts core at 30 deg. TCA, perpendicular to bedding.

144.8 144.9 Siltstone calcite

Calcite-quartz stringers fracturing the core at 15 deg. TCA.

173.8 301.2 **BaCl Basal Conglomerate**

Matrix-supported (<10% clasts), Gowganda diamictite. Green siltstone matrix with rounded clasts. Trace lithic arkose (<1m thick) and conglomeratic units (<10cm). Arkosic units display trace carbonate and epidote alteration.

209.7 209.8 Basal Conglomerate calcite

Calcite stringers cross-cutting core at 40 deg. TCA.

224.3 224.3 Basal Conglomerate calcite

Calcite stringers cross-cutting core at 40 deg. TCA.

229.5 229.6 Sandstone

Fine-grained arkose bed with mild carbonate - and epidote alteration.

229.9 230.0 Sandstone

Fine-grained arkose bed with mild carbonate - and epidote alteration.

230.2 230.6 Sandstone

Fine-grained arkose bed with mild carbonate - and epidote alteration interbedded by 10 cm conglomeratic unit with minor (5-10%) clay alteration of potassium feldspars and iron-staining.

246.0	246.4 Basal Conglomerate	calcite	Calcite-chalcopyrite stringers brecciating diamictite. Stringers ~5% modal (overall) and chalcopyrite 1% overall. Minor iron-staining within stringers.
253.8	253.9 Sandstone	calcite	Calcite stringers fracturing fine-grained arkose creating a stockwork textures.
254.1	254.4 Basal Conglomerate	calcite	Calcite stringers fracturing diamictite creating a stockwork texture (0.1% stringers overall)
255.0	255.2 Sandstone	calcite	Calcite stringers fracturing fine-grained arkose creating a stockwork textures.
260.4	261.3 Sandstone	calcite	Calcite stringers/stockwork and iron-staining within a fine-grained arkose.
265.0	266.5 Sandstone	calcite	Calcite stringers/stockwork and iron-staining within a fine-grained arkose.
266.9	267.1 Basal Conglomerate	calcite	Calcite stringers and minor iron-staining cross-cutting diamictite at 20 deg. TCA.
268.6	268.7 Basal Conglomerate	calcite	Parallel calcite stringers cross-cutting core at 40 deg. TCA.
270.5	270.6 Basal Conglomerate	calcite	Calcite stringers running parallel TCA.
271.5	273.9 Basal Conglomerate	calcite	Trace (<0.01%) calcite stringers with minor iron-staining along fractures cross-cut core at 40 deg. TCA.
276.2	276.4 Basal Conglomerate	calcite	Calcite stringers cross-cutting core at a shallow angle (<5 deg).
276.5	276.7 Basal Conglomerate	calcite	Calcite stringers cross-cutting core at a shallow angle (<5 deg).
278.6	278.7 Basal Conglomerate	calcite	Calcite stringers fracturing and brecciating core (40 deg. TCA.)
278.9	279.0 Basal Conglomerate	calcite	Calcite stringers fracturing and brecciating core (40 deg. TCA.)

282.3	286.5	Basal Conglomerate	calcite	Trace (1%) calcite stringers fracturing core at 20-40 deg. TCA. Minor iron-staining and chlorite associated with fractures.
287.4	287.7	Basal Conglomerate	calcite	Calcite-epidote veinlet breccia.
288.5	288.9	Basal Conglomerate	calcite	Broken core with calcite stringers and minor iron-staining of fragments.
289.9	290.0	Basal Conglomerate	calcite	Calcite stringers fracturing diamictite at 20 deg. TCA.
293.2	293.3	Basal Conglomerate	calcite	Rose calcite veinlet breccia cross-cutting core at 30 deg. TCA.
294.3	294.5	Basal Conglomerate	calcite	Rose calcite veinlet breccia cross-cutting core at 30 deg. TCA.
295.5	295.6	Basal Conglomerate	calcite	Calcite stringers fracturing core at 30 deg. TCA.
297.7	297.8	Basal Conglomerate	calcite	Calcite stringers and veinlet breccia cross-cutting core at 20 deg. TCA.

301.2	306.1	VBX	Volcanic Breccia	Matrix-supported (10-15% clasts), carbonate volcanoclastic breccia. Dark grey matrix rich in carbonate (reacts well with HCl) containing juvenile lapilli (30-50%) and trace interstitial white calcite (surrounds lapilli). Very fine grained matrix contains 5-10% black biotite grains (<3mm), trace subeuhedral magnetite, trace potential ilmenite and trace pyrite. Biotite and ilmenite (pos.) core some of the lapilli. Sharp contact with diamictite inclined 30 deg. TCA. Strongly magnetic.
301.2	301.2	Volcanic Breccia	calcite	Calcite veinlet cross-cutting volcanoclastic dike with VBX fragments within veinlet. Inclined 35 deg. TCA -almost parallel to contact.

306.1 312.9 **KMB Kimberlite**
Clast-supported (40-60% clasts) carbonate volcanoclastic breccia. Predominantly subangular clasts are intensely iron-altered and are corroded. Decreasing lapilli concentration (decreases away from contact 20 to <5% in center). Some large, rounded diamictite clasts within breccia. Lapilli-rich boundary contains interstitial white calcite. Lapilli and matrix are dark grey to green in colour. Matrix contains minor biotite (<5%, <2mm), trace subeuhedral magnetite (up to 5%) and possible ilmenite crystals 2-4mm in length. Unit is magnetic.

312.9 330.6 **VBX Volcanic Breccia**
Clast-supported (60-80% clasts) carbonate volcanoclastic breccia consisting of predominantly rounded, iron-altered and corroded clasts set in a light brown-green coloured matrix. Contains minor lapilli (5-10%) which have also be iron-oxidized to a dark red colour. Matrix contains minor biotite 5-10% with a few macrocrystals as large as 1cm in diameter, trace magnetite and trace possible ilmenite. Some lapilli noted to be cored on biotite, ilmenite and rarely magnetite grains. Lapilli tend to host serpentinized crystals <1mm in length. Matrix is non-magnetic except for occassional magnetite grains.

330.6 332.3 **KMB Kimberlite**
Matrix-supported (30% clasts) carbonate volcanoclastic dike with minor flow alignment of iron-altered and corroded, subangular clasts. Sharp contacts inclined 30 deg. TCA. Matrix is dark green-grey in colour and contains 30% small (<2mm) biotite grains, trace magnetite, calcite, pyrite and possible ilmenite. Light green alteration is associated with trace calcite stringers cross-cutting the dike at 40 deg. TCA. Strongly magnetic.

332.3 337.6 **VBX Volcanic Breccia**
Clast-supported (80% clasts) carbonate volcanoclastic breccia consisting of predominantly rounded, iron-altered and corrod clasts set in a light brown-green coloured matrix. Contains minor lapilli (5-10%) which have also be iron-oxidized to a dark red colour. Matrix contains minor biotite 5%, trace magnetite and trace possible ilmenite. Some lapilli noted to be cored on biotite, ilmenite and rarely magnetite grains. Lapilli tend to host serpentinized crystals <1mm in length. Matrix is non-magnetic except for occassional magnetite grains. Interstitial calcite content increases towards sharp contact with quartzite

below.

337.6 350.1 **MetaSED Meta sediments**
Mildly foliated quartzite to arkose (with preserved potassium feldspars). Sharp contacts with VBX.

350.1 362.7 **VBX Volcanic Breccia**
Clast-supported (80% clasts) carbonate volcanoclastic breccia consisting of predominantly rounded, iron-altered and corroded clasts set in a light brown-green coloured matrix. Contains minor lapilli (5-10%) which have also be iron-oxidized to a dark red colour. Matrix contains minor biotite 5%, trace magnetite and trace possible ilmenite. Some lapilli noted to be cored on biotite, ilmenite and rarely magnetite grains. Lapilli tend to host serpentinized crystals <1mm in length. Matrix is non-magnetic except for occassional magnetite grains. Interstitial calcite content increases towards sharp contact with quartzite above.
361.0 361.8 Rubble
Increased iron-alteration and corrosion of core to a rubble.

362.7 411.0 **KMB Kimberlite**
Clast-supported (40-60% clasts) carbonate volcanoclastic breccia. Predominantly subangular clasts are intensely iron-altered and are corroded. Variable lapilli concentration (5-20%). Lapilli-rich zones contain trace interstitial white calcite. Lapilli and matrix are dark grey to green in colour. Matrix contains minor biotite (<5%, <2mm), trace subeuhedral magnetite and possible ilmenite crystals. Unit is magnetic.

- 411.0 606.7 **BaCl Basal Conglomerate**
Matrix-supported (5-10% clasts) Gowganda diamictite with rounded clasts set in a siltstone matrix. Trace kimberlitic veining in upper ~20m and minor carbonate stringers centered around kimberlitic contacts.
- 411.0 411.1 Basal Conglomerate calcite
Calcite veinlet associated iron-staining cross-cutting core at 25 deg. TCA.
- 412.0 412.0 Basal Conglomerate calcite
Rose calcite veinlet and veinlet breccia cross-cutting core at 25 deg. TCA.
- 413.4 413.4 Basal Conglomerate calcite
Rose calcite veinlet and veinlet breccia cross-cutting core at 25 deg. TCA.
- 413.7 413.8 Basal Conglomerate calcite
Rose calcite veinlet and veinlet breccia cross-cutting core at 15 deg. TCA.
- 419.6 419.9 Vein carbonate
Carbonate-rich, fine-grained aplitic-textured vein (~5cm) cross-cuts core at 35 deg. TCA. Vein is pink to light purple in colour and has iron-staining along contacts. No minerals large enough to be identified within groundmass. Magnetic.
- 420.0 421.2 Kimberlite
Matrix-supported, very fine-grained carbonate volcanoclastic breccia. Subangular clasts of diamictite within vein which consists of a dark grey-green, aphanitic groundmass with trace (<5%) mica (too small to tell which mica) and trace euhedral apatite grains. Dike is magnetic and cross-cuts the diamictite at 35 deg. TCA. Dike is cross-cut by later calcite stringers with iron-stained contacts. Contacts of vein/dike are pink to light purple in colour -similar to aplitic textured veins described above and below.
- 421.4 42145. Vein carbonate
0
Carbonate-rich, fine-grained aplitic-textured vein (~5cm) cross-cuts core at 35 deg. TCA. Vein is pink to light purple in colour and has iron-staining along contacts. No minerals large enough to be identified within groundmass. Magnetic.
- 421.6 421.7 Vein carbonate
Carbonate-rich, fine-grained aplitic-textured vein (~5cm) cross-cuts core at 35 deg. TCA. Vein is pink to light purple in colour and has iron-staining along contacts. No minerals large enough to be identified within groundmass. Magnetic.
- 422.3 422.4 Vein carbonate
Carbonate-rich, fine-grained aplitic-textured vein (~5cm) cross-cuts core at 35 deg. TCA. Vein is pink to light purple in colour and has iron-staining along contacts. No minerals large enough to be identified within groundmass. Magnetic.
- 422.9 423.0 Vein carbonate
Carbonate-rich, fine-grained aplitic-textured vein (~5cm) cross-cuts core at 35 deg. TCA. Vein is pink to light purple in colour and has iron-staining along contacts. No minerals large enough to be identified within groundmass. Magnetic.

424.6	424.7 Vein	carbonate	Carbonate-rich, fine-grained aplitic-textured vein (~5cm) cross-cuts core at 35 deg. TCA. Vein is pink to light purple in colour and has increased iron-staining along contacts and within veinlet. No minerals large enough to be identified within groundmass. Magnetic.
424.8	424.9 Vein	carbonate	Carbonate-rich, fine-grained aplitic-textured vein (~5cm) cross-cuts core at 35 deg. TCA. Vein is pink to light purple in colour and has increased iron-staining along contacts and within veinlet. No minerals large enough to be identified within groundmass. Non-magnetic.
425.2	425.4 Vein	calcite	Very fine-grained, parallel calcite-chlorite veinlets cross-cut core at 35 deg. TCA. Calcite is granular and small grains of phlogopite (<5%) were noted within the groundmass. Non-magnetic.
428.6	429.0 Basal Conglomerate	calcite	Calcite stringers fracturing core and increased iron-staining of diamictite.
431.7	433.3 Kimberlite		Matrix-supported (<5% clasts), fine-grained, porphyritic carbonate volcanoclastic dike. Cross-cuts diamictite at 25 deg. TCA. Clasts are small (<1cm) and intensely iron-altered and corroded. Light green-grey matrix contains 5-10% black biotite (<3mm), trace oxidized magnetite, trace possible ilmenite and small serpentinized grains in a non-magnetic (except for occasional magnetite grains) carbonate-rich matrix. Unit is cross-cut by vuggy calcite stringers inclined 15 deg. TCA.
433.3	434.5 Basal Conglomerate	calcite	Calcite stringers fracturing core and rubble in places with increased iron-alteration. Some of the calcite stringers have vugs lined with euhedral calcite crystals.
435.4	436.0 Basal Conglomerate	calcite	Calcite stringers fracturing core (running parallel TCA) with iron-alteration. Some of the calcite stringers have vugs lined with euhedral calcite crystals.
440.3	442.8 Basal Conglomerate	calcite	Calcite stringer fracturing core (broken core) with intense iron-staining of fragments.
443.0	443.9 Basal Conglomerate	calcite	Calcite stringers running parallel TCA fracturing core.
444.3	446.0 Basal Conglomerate	calcite	Calcite stringers (stockwork texture) fracturing core (reduced to rubble in center) with intense iron-alteration.
447.3	447.4 Basal Conglomerate	calcite	Rose calcite-chlorite and iron-stained veinlet cross-cuts core at 30 deg. TCA.
448.0	448.0 Basal Conglomerate	calcite	Parallel rose calcite-chlorite and iron-stained veinlets cross-cuts core at 30 deg. TCA.

470.2	470.3	Basal Conglomerate	calcite	Sheared rose calcite-chlorite veinlet cross-cutting core at 15 deg. TCA.
492.9	493.0	Basal Conglomerate	calcite	Calcite-quartz-chlorite veinlet intersecting core at 10 deg. TCA.
499.7	499.8	Basal Conglomerate	calcite	Parallel rose calcite-quartz stringers cross-cutting core at 20 deg. TCA.
508.0	508.1	Basal Conglomerate	calcite	Calcite-quartz stringers intersect core at 15 deg. TCA.
512.8	513.0	Basal Conglomerate	calcite	Rose calcite-quartz-chlorite veinlet (<2cm) cross-cuts core at 15 deg. TCA.
520.6	521.6	Basal Conglomerate	calcite	Calcite-quartz stringer running parallel TCA.
532.0	533.5	Fault		Fractured and broken core (parallel TCA)
548.6	548.7	Basal Conglomerate	pyrite	Calcite-filled fractures in diamictite (5% modal) with minor pyrite (1% modal)
551.2	551.5	Basal Conglomerate	pyrite	Subeuhedral, disseminated pyrite (1% modal) within a foliated metasediment clast -pyrite post foliation but timing to inclusion within diamictite uncertain.
562.0	562.3	Basal Conglomerate	calcite	Zone of increased, but still trace abundance (0.1%), calcite-sealed fractures cross-cutting core at 30-50 deg. TCA.
569.8	570.0	Basal Conglomerate	calcite	Calcite-chlorite veinlet breccia with angular diamictite clasts cross-cutting core at 40 deg. TCA.
602.3	605.0	Fault		Broken and fractured core with large, chlorite-lined fragments running parallel TCA.

From (m)	To (m)	Geological Description	Formation Name / Unit Name
606.7	636.0	NipD Aphanitic to fine-grained Nipissing Diabase. Brecciated upper contact with diamictite within aphanitic quartz diabase. Grain size increases away from depth and transitions into fine-grained hypersthene diabase at EOH. Trace calcite-quartz-chlorite veinlets.	Nippising Diabase / Meta Gabbro
607.7	607.8	Nippising Diabase / Meta Gabbro Calcite-quartz-chlorite veinlet breccia cross-cuts core at 50 deg. TCA.	calcite
611.5	611.6	Nippising Diabase / Meta Gabbro Calcite-quartz-chlorite veinlet cross-cuts core at 25 deg. TCA.	calcite
616.8	616.9	Nippising Diabase / Meta Gabbro Calcite-quartz veinlet breccia with iron-staining intersects core at 20 deg. TCA.	calcite
618.4	618.8	Nippising Diabase / Meta Gabbro Sheared calcite-quartz stringer intersecting core 5 deg. TCA.	calcite
621.0	621.2	Nippising Diabase / Meta Gabbro Sheared calcite-quartz stringer intersecting core 5 deg. TCA.	calcite
626.3	626.4	Nippising Diabase / Meta Gabbro Quartz-calcite-chlorite-antigorite (asbestiform) veinlet cross-cutting core at 45 deg. TCA.	quartz

636.0 636.0 **EOH** **End of Hole**

Hole	Depth (m)	Magnetic Susceptibility	Hole	Depth (m)	Magnetic Susceptibility	Hole	Depth (m)	Magnetic Susceptibility
TD-08-10	4.0	0.09	TD-08-10	63.0	2.34	TD-08-10	122.0	0.38
TD-08-10	5.0	0.10	TD-08-10	64.0	2.12	TD-08-10	123.0	0.34
TD-08-10	6.0	0.20	TD-08-10	65.0	1.42	TD-08-10	124.0	0.34
TD-08-10	7.0	0.16	TD-08-10	66.0	1.29	TD-08-10	125.0	0.34
TD-08-10	8.0	0.07	TD-08-10	67.0	0.75	TD-08-10	126.0	0.29
TD-08-10	9.0	0.16	TD-08-10	68.0	0.65	TD-08-10	127.0	0.38
TD-08-10	10.0	0.18	TD-08-10	69.0	0.49	TD-08-10	128.0	0.34
TD-08-10	11.0	0.10	TD-08-10	70.0	0.29	TD-08-10	129.0	0.27
TD-08-10	12.0	0.20	TD-08-10	71.0	0.27	TD-08-10	130.0	0.23
TD-08-10	13.0	0.09	TD-08-10	72.0	0.40	TD-08-10	131.0	0.34
TD-08-10	14.0	0.14	TD-08-10	73.0	0.67	TD-08-10	132.0	0.32
TD-08-10	15.0	0.16	TD-08-10	74.0	0.58	TD-08-10	133.0	0.32
TD-08-10	16.0	0.20	TD-08-10	75.0	0.40	TD-08-10	134.0	0.31
TD-08-10	17.0	0.00	TD-08-10	76.0	0.32	TD-08-10	135.0	0.34
TD-08-10	18.0	0.12	TD-08-10	77.0	0.00	TD-08-10	136.0	0.29
TD-08-10	19.0	0.14	TD-08-10	78.0	0.16	TD-08-10	137.0	0.29
TD-08-10	20.0	0.10	TD-08-10	79.0	0.18	TD-08-10	138.0	0.31
TD-08-10	21.0	0.07	TD-08-10	80.0	0.16	TD-08-10	139.0	0.34
TD-08-10	22.0	0.09	TD-08-10	81.0	0.21	TD-08-10	140.0	0.29
TD-08-10	23.0	0.20	TD-08-10	82.0	0.27	TD-08-10	141.0	0.29
TD-08-10	24.0	0.18	TD-08-10	83.0	0.78	TD-08-10	142.0	0.25
TD-08-10	25.0	0.03	TD-08-10	84.0	1.18	TD-08-10	143.0	0.32
TD-08-10	26.0	0.03	TD-08-10	85.0	1.44	TD-08-10	144.0	0.27
TD-08-10	27.0	0.16	TD-08-10	86.0	1.44	TD-08-10	145.0	0.25
TD-08-10	28.0	0.09	TD-08-10	87.0	1.83	TD-08-10	146.0	0.31
TD-08-10	29.0	0.12	TD-08-10	88.0	1.84	TD-08-10	147.0	0.42
TD-08-10	30.0	0.12	TD-08-10	89.0	1.68	TD-08-10	148.0	0.29
TD-08-10	31.0	0.12	TD-08-10	90.0	0.96	TD-08-10	149.0	0.27
TD-08-10	32.0	0.20	TD-08-10	91.0	1.46	TD-08-10	150.0	0.32
TD-08-10	33.0	0.31	TD-08-10	92.0	1.46	TD-08-10	151.0	0.31
TD-08-10	34.0	0.60	TD-08-10	93.0	1.00	TD-08-10	152.0	0.29
TD-08-10	35.0	1.18	TD-08-10	94.0	0.40	TD-08-10	153.0	0.31
TD-08-10	36.0	1.62	TD-08-10	95.0	0.40	TD-08-10	154.0	0.36
TD-08-10	37.0	1.79	TD-08-10	96.0	0.91	TD-08-10	155.0	0.31
TD-08-10	38.0	1.90	TD-08-10	97.0	1.00	TD-08-10	156.0	0.31
TD-08-10	39.0	2.10	TD-08-10	98.0	0.95	TD-08-10	157.0	0.27
TD-08-10	40.0	2.21	TD-08-10	99.0	0.95	TD-08-10	158.0	0.29
TD-08-10	41.0	1.92	TD-08-10	100.0	1.53	TD-08-10	159.0	0.27
TD-08-10	42.0	2.23	TD-08-10	101.0	1.31	TD-08-10	160.0	0.25
TD-08-10	43.0	2.10	TD-08-10	102.0	1.75	TD-08-10	161.0	0.23
TD-08-10	44.0	2.17	TD-08-10	103.0	3.73	TD-08-10	162.0	0.25
TD-08-10	45.0	1.40	TD-08-10	104.0	4.11	TD-08-10	163.0	0.29
TD-08-10	46.0	1.97	TD-08-10	105.0	4.26	TD-08-10	164.0	0.27
TD-08-10	47.0	2.36	TD-08-10	106.0	3.93	TD-08-10	165.0	0.27
TD-08-10	48.0	3.00	TD-08-10	107.0	4.50	TD-08-10	166.0	0.25
TD-08-10	49.0	1.92	TD-08-10	108.0	5.52	TD-08-10	167.0	0.27
TD-08-10	50.0	2.25	TD-08-10	109.0	5.74	TD-08-10	168.0	0.29
TD-08-10	51.0	1.99	TD-08-10	110.0	5.28	TD-08-10	169.0	0.29
TD-08-10	52.0	2.63	TD-08-10	111.0	5.81	TD-08-10	170.0	0.32
TD-08-10	53.0	2.23	TD-08-10	112.0	5.43	TD-08-10	171.0	0.32
TD-08-10	54.0	2.65	TD-08-10	113.0	4.61	TD-08-10	172.0	0.31
TD-08-10	55.0	2.17	TD-08-10	114.0	4.06	TD-08-10	173.0	0.29
TD-08-10	56.0	1.90	TD-08-10	115.0	4.77	TD-08-10	174.0	0.18
TD-08-10	57.0	2.47	TD-08-10	116.0	3.22	TD-08-10	175.0	0.10
TD-08-10	58.0	2.15	TD-08-10	117.0	2.30	TD-08-10	176.0	0.00
TD-08-10	59.0	1.90	TD-08-10	118.0	1.42	TD-08-10	177.0	0.12
TD-08-10	60.0	2.28	TD-08-10	119.0	0.40	TD-08-10	178.0	0.14
TD-08-10	61.0	2.12	TD-08-10	120.0	0.36	TD-08-10	179.0	0.10
TD-08-10	62.0	2.32	TD-08-10	121.0	0.34	TD-08-10	180.0	0.14

Hole	Depth (m)	Magnetic Susceptibility	Hole	Depth (m)	Magnetic Susceptibility	Hole	Depth (m)	Magnetic Susceptibility
TD-08-10	181.0	0.12	TD-08-10	240.0	0.78	TD-08-10	299.0	1.66
TD-08-10	182.0	0.14	TD-08-10	241.0	0.58	TD-08-10	300.0	2.10
TD-08-10	183.0	0.16	TD-08-10	242.0	0.82	TD-08-10	300.5	36.50
TD-08-10	184.0	0.16	TD-08-10	243.0	1.88	TD-08-10	301.0	69.80
TD-08-10	185.0	0.18	TD-08-10	244.0	1.33	TD-08-10	302.0	80.80
TD-08-10	186.0	0.47	TD-08-10	245.0	1.13	TD-08-10	303.0	74.00
TD-08-10	187.0	1.09	TD-08-10	246.0	0.96	TD-08-10	304.0	59.90
TD-08-10	188.0	2.45	TD-08-10	247.0	1.51	TD-08-10	305.0	43.80
TD-08-10	189.0	2.72	TD-08-10	248.0	1.64	TD-08-10	306.0	57.00
TD-08-10	190.0	1.77	TD-08-10	249.0	1.90	TD-08-10	307.0	26.80
TD-08-10	191.0	1.83	TD-08-10	250.0	2.14	TD-08-10	308.0	35.90
TD-08-10	192.0	2.96	TD-08-10	251.0	1.27	TD-08-10	309.0	16.70
TD-08-10	193.0	1.99	TD-08-10	252.0	1.22	TD-08-10	310.0	14.60
TD-08-10	194.0	2.85	TD-08-10	253.0	1.81	TD-08-10	311.0	2.90
TD-08-10	195.0	2.65	TD-08-10	254.0	1.22	TD-08-10	312.0	2.36
TD-08-10	196.0	4.64	TD-08-10	255.0	0.27	TD-08-10	313.0	6.51
TD-08-10	197.0	4.52	TD-08-10	256.0	0.31	TD-08-10	314.0	9.16
TD-08-10	198.0	3.64	TD-08-10	257.0	1.09	TD-08-10	315.0	6.36
TD-08-10	199.0	3.34	TD-08-10	258.0	0.89	TD-08-10	316.0	7.81
TD-08-10	200.0	3.14	TD-08-10	259.0	1.06	TD-08-10	317.0	5.19
TD-08-10	201.0	2.83	TD-08-10	260.0	1.28	TD-08-10	318.0	5.45
TD-08-10	202.0	2.85	TD-08-10	261.0	0.20	TD-08-10	319.0	4.06
TD-08-10	203.0	4.09	TD-08-10	262.0	0.76	TD-08-10	320.0	1.22
TD-08-10	204.0	2.12	TD-08-10	263.0	0.95	TD-08-10	321.0	6.77
TD-08-10	205.0	2.03	TD-08-10	264.0	0.53	TD-08-10	322.0	3.34
TD-08-10	206.0	1.33	TD-08-10	265.0	0.36	TD-08-10	323.0	3.60
TD-08-10	207.0	1.62	TD-08-10	266.0	0.27	TD-08-10	324.0	2.54
TD-08-10	208.0	1.44	TD-08-10	267.0	1.15	TD-08-10	325.0	1.86
TD-08-10	209.0	0.67	TD-08-10	268.0	0.98	TD-08-10	326.0	1.92
TD-08-10	210.0	0.43	TD-08-10	269.0	1.39	TD-08-10	327.0	1.75
TD-08-10	211.0	1.09	TD-08-10	270.0	1.29	TD-08-10	328.0	2.48
TD-08-10	212.0	0.93	TD-08-10	271.0	0.76	TD-08-10	329.0	1.77
TD-08-10	213.0	0.29	TD-08-10	272.0	0.96	TD-08-10	330.0	1.93
TD-08-10	214.0	0.47	TD-08-10	273.0	2.89	TD-08-10	331.0	18.60
TD-08-10	215.0	0.87	TD-08-10	274.0	1.79	TD-08-10	332.0	18.10
TD-08-10	216.0	1.11	TD-08-10	275.0	1.81	TD-08-10	333.0	3.53
TD-08-10	217.0	1.02	TD-08-10	276.0	2.26	TD-08-10	334.0	0.89
TD-08-10	218.0	0.60	TD-08-10	277.0	2.04	TD-08-10	335.0	1.62
TD-08-10	219.0	2.43	TD-08-10	278.0	2.01	TD-08-10	336.0	1.13
TD-08-10	220.0	0.64	TD-08-10	279.0	1.48	TD-08-10	337.0	0.89
TD-08-10	221.0	0.95	TD-08-10	280.0	0.53	TD-08-10	338.0	0.09
TD-08-10	222.0	3.16	TD-08-10	281.0	1.57	TD-08-10	339.0	-0.05
TD-08-10	223.0	1.06	TD-08-10	282.0	2.01	TD-08-10	340.0	-0.03
TD-08-10	224.0	3.07	TD-08-10	283.0	1.90	TD-08-10	341.0	-0.12
TD-08-10	225.0	2.81	TD-08-10	284.0	1.51	TD-08-10	342.0	0.00
TD-08-10	226.0	2.74	TD-08-10	285.0	1.86	TD-08-10	343.0	-0.01
TD-08-10	227.0	1.51	TD-08-10	286.0	1.79	TD-08-10	344.0	-0.03
TD-08-10	228.0	2.54	TD-08-10	287.0	1.55	TD-08-10	345.0	0.00
TD-08-10	229.0	5.25	TD-08-10	288.0	1.33	TD-08-10	346.0	0.00
TD-08-10	230.0	2.52	TD-08-10	289.0	0.95	TD-08-10	347.0	0.00
TD-08-10	231.0	1.55	TD-08-10	290.0	0.47	TD-08-10	348.0	0.00
TD-08-10	232.0	0.98	TD-08-10	291.0	0.96	TD-08-10	349.0	0.00
TD-08-10	233.0	0.95	TD-08-10	292.0	0.25	TD-08-10	350.0	0.00
TD-08-10	234.0	0.98	TD-08-10	293.0	0.62	TD-08-10	350.2	0.35
TD-08-10	235.0	1.00	TD-08-10	294.0	0.67	TD-08-10	351.0	1.57
TD-08-10	236.0	1.66	TD-08-10	295.0	0.71	TD-08-10	352.0	0.62
TD-08-10	237.0	1.53	TD-08-10	296.0	0.67	TD-08-10	353.0	1.42
TD-08-10	238.0	1.33	TD-08-10	297.0	0.71	TD-08-10	354.0	1.35
TD-08-10	239.0	0.64	TD-08-10	298.0	1.35	TD-08-10	355.0	1.20

Hole	Depth (m)	Magnetic Susceptibility	Hole	Depth (m)	Magnetic Susceptibility	Hole	Depth (m)	Magnetic Susceptibility
TD-08-10	356.0	1.39	TD-08-10	415.0	0.20	TD-08-10	474.0	0.16
TD-08-10	357.0	0.99	TD-08-10	416.0	0.24	TD-08-10	475.0	0.16
TD-08-10	358.0	2.28	TD-08-10	417.0	0.22	TD-08-10	476.0	0.18
TD-08-10	359.0	3.44	TD-08-10	418.0	0.22	TD-08-10	477.0	0.18
TD-08-10	360.0	2.76	TD-08-10	419.0	2.15	TD-08-10	478.0	0.16
TD-08-10	361.0	5.58	TD-08-10	420.0	11.50	TD-08-10	479.0	0.16
TD-08-10	362.0	1.28	TD-08-10	421.0	47.00	TD-08-10	480.0	0.18
TD-08-10	363.0	2.59	TD-08-10	422.0	3.05	TD-08-10	481.0	0.18
TD-08-10	364.0	13.70	TD-08-10	423.0	0.18	TD-08-10	482.0	0.16
TD-08-10	365.0	24.90	TD-08-10	424.0	0.10	TD-08-10	483.0	0.20
TD-08-10	366.0	21.90	TD-08-10	425.0	0.24	TD-08-10	484.0	0.14
TD-08-10	367.0	22.50	TD-08-10	426.0	0.08	TD-08-10	485.0	0.16
TD-08-10	368.0	29.50	TD-08-10	427.0	0.12	TD-08-10	486.0	0.16
TD-08-10	369.0	20.10	TD-08-10	428.0	0.10	TD-08-10	487.0	0.16
TD-08-10	370.0	29.90	TD-08-10	429.0	0.12	TD-08-10	488.0	0.16
TD-08-10	371.0	24.20	TD-08-10	430.0	0.12	TD-08-10	489.0	0.14
TD-08-10	372.0	32.70	TD-08-10	431.0	0.69	TD-08-10	490.0	0.12
TD-08-10	373.0	32.80	TD-08-10	432.0	4.01	TD-08-10	491.0	0.06
TD-08-10	374.0	35.60	TD-08-10	433.0	0.30	TD-08-10	492.0	0.24
TD-08-10	375.0	27.90	TD-08-10	434.0	0.16	TD-08-10	493.0	0.16
TD-08-10	376.0	28.20	TD-08-10	435.0	0.16	TD-08-10	494.0	0.12
TD-08-10	377.0	34.80	TD-08-10	436.0	0.14	TD-08-10	495.0	0.14
TD-08-10	378.0	32.40	TD-08-10	437.0	0.18	TD-08-10	496.0	0.16
TD-08-10	379.0	29.80	TD-08-10	438.0	0.14	TD-08-10	497.0	0.16
TD-08-10	380.0	26.40	TD-08-10	439.0	0.14	TD-08-10	498.0	0.16
TD-08-10	381.0	23.30	TD-08-10	440.0	0.14	TD-08-10	499.0	0.18
TD-08-10	382.0	29.40	TD-08-10	441.0	0.14	TD-08-10	500.0	0.14
TD-08-10	383.0	23.50	TD-08-10	442.0	0.10	TD-08-10	501.0	0.16
TD-08-10	384.0	27.90	TD-08-10	443.0	0.14	TD-08-10	502.0	0.18
TD-08-10	385.0	30.20	TD-08-10	444.0	0.12	TD-08-10	503.0	0.14
TD-08-10	386.0	31.00	TD-08-10	445.0	0.12	TD-08-10	504.0	0.16
TD-08-10	387.0	31.80	TD-08-10	446.0	0.12	TD-08-10	505.0	0.16
TD-08-10	388.0	43.60	TD-08-10	447.0	0.12	TD-08-10	506.0	0.18
TD-08-10	389.0	33.50	TD-08-10	448.0	0.16	TD-08-10	507.0	0.16
TD-08-10	390.0	54.80	TD-08-10	449.0	0.14	TD-08-10	508.0	0.18
TD-08-10	391.0	44.80	TD-08-10	450.0	0.14	TD-08-10	509.0	0.22
TD-08-10	392.0	36.70	TD-08-10	451.0	0.12	TD-08-10	510.0	0.22
TD-08-10	393.0	18.70	TD-08-10	452.0	0.12	TD-08-10	511.0	0.16
TD-08-10	394.0	33.00	TD-08-10	453.0	0.18	TD-08-10	512.0	0.20
TD-08-10	395.0	29.20	TD-08-10	454.0	0.14	TD-08-10	513.0	0.12
TD-08-10	396.0	21.90	TD-08-10	455.0	0.18	TD-08-10	514.0	0.18
TD-08-10	397.0	23.20	TD-08-10	456.0	0.14	TD-08-10	515.0	0.18
TD-08-10	398.0	33.80	TD-08-10	457.0	0.14	TD-08-10	516.0	0.24
TD-08-10	399.0	24.10	TD-08-10	458.0	0.10	TD-08-10	517.0	0.20
TD-08-10	400.0	26.50	TD-08-10	459.0	0.12	TD-08-10	518.0	0.22
TD-08-10	401.0	25.80	TD-08-10	460.0	0.10	TD-08-10	519.0	0.22
TD-08-10	402.0	24.90	TD-08-10	461.0	0.14	TD-08-10	520.0	0.22
TD-08-10	403.0	24.50	TD-08-10	462.0	0.14	TD-08-10	521.0	0.20
TD-08-10	404.0	21.60	TD-08-10	463.0	0.14	TD-08-10	522.0	0.18
TD-08-10	405.0	20.60	TD-08-10	464.0	0.22	TD-08-10	523.0	0.20
TD-08-10	406.0	30.00	TD-08-10	465.0	0.16	TD-08-10	524.0	0.18
TD-08-10	407.0	19.90	TD-08-10	466.0	0.14	TD-08-10	525.0	0.18
TD-08-10	408.0	13.50	TD-08-10	467.0	0.10	TD-08-10	526.0	0.18
TD-08-10	409.0	11.10	TD-08-10	468.0	0.12	TD-08-10	527.0	0.24
TD-08-10	410.0	1.20	TD-08-10	469.0	0.14	TD-08-10	528.0	0.18
TD-08-10	411.0	0.61	TD-08-10	470.0	0.16	TD-08-10	529.0	0.18
TD-08-10	412.0	0.30	TD-08-10	471.0	0.16	TD-08-10	530.0	0.20
TD-08-10	413.0	0.26	TD-08-10	472.0	0.16	TD-08-10	531.0	0.18
TD-08-10	414.0	0.24	TD-08-10	473.0	0.14	TD-08-10	532.0	0.20

Hole	Depth (m)	Magnetic Susceptibility	Hole	Depth (m)	Magnetic Susceptibility	Hole	Depth (m)	Magnetic Susceptibility
TD-08-10	533.0	0.16	TD-08-10	590.0	0.16			
TD-08-10	534.0	0.16	TD-08-10	591.0	0.24			
TD-08-10	535.0	0.22	TD-08-10	592.0	0.20			
TD-08-10	536.0	0.16	TD-08-10	593.0	0.24			
TD-08-10	537.0	0.18	TD-08-10	594.0	0.30			
TD-08-10	538.0	0.20	TD-08-10	595.0	0.30			
TD-08-10	539.0	0.16	TD-08-10	596.0	0.26			
TD-08-10	540.0	0.14	TD-08-10	597.0	0.24			
TD-08-10	541.0	0.18	TD-08-10	598.0	0.20			
TD-08-10	542.0	0.20	TD-08-10	599.0	0.30			
TD-08-10	543.0	0.22	TD-08-10	600.0	0.20			
TD-08-10	544.0	0.18	TD-08-10	601.0	0.30			
TD-08-10	545.0	0.18	TD-08-10	602.0	0.36			
TD-08-10	546.0	0.16	TD-08-10	603.0	0.36			
TD-08-10	547.0	0.18	TD-08-10	604.0	0.38			
TD-08-10	548.0	0.20	TD-08-10	605.0	0.16			
TD-08-10	549.0	0.20	TD-08-10	606.0	0.45			
TD-08-10	550.0	0.20	TD-08-10	607.0	0.38			
TD-08-10	551.0	0.18	TD-08-10	608.0	0.49			
TD-08-10	552.0	0.47	TD-08-10	609.0	0.38			
TD-08-10	553.0	0.20	TD-08-10	610.0	0.45			
TD-08-10	554.0	0.16	TD-08-10	611.0	0.41			
TD-08-10	555.0	0.06	TD-08-10	612.0	0.43			
TD-08-10	556.0	0.26	TD-08-10	613.0	0.30			
TD-08-10	557.0	0.06	TD-08-10	614.0	0.45			
TD-08-10	558.0	1.02	TD-08-10	615.0	0.41			
TD-08-10	559.0	0.20	TD-08-10	616.0	0.43			
TD-08-10	560.0	0.22	TD-08-10	617.0	0.38			
TD-08-10	561.0	0.18	TD-08-10	618.0	0.34			
TD-08-10	562.0	0.16	TD-08-10	619.0	0.34			
TD-08-10	563.0	0.28	TD-08-10	620.0	0.53			
TD-08-10	564.0	0.18	TD-08-10	621.0	0.38			
TD-08-10	565.0	0.20	TD-08-10	622.0	0.36			
TD-08-10	566.0	0.20	TD-08-10	623.0	0.41			
TD-08-10	567.0	0.16	TD-08-10	624.0	0.18			
TD-08-10	568.0	0.38	TD-08-10	625.0	0.38			
TD-08-10	568.5	0.32	TD-08-10	626.0	0.43			
TD-08-10	569.0	10.00	TD-08-10	627.0	0.36			
TD-08-10	569.5	11.00	TD-08-10	628.0	0.26			
TD-08-10	570.0	0.16	TD-08-10	629.0	0.45			
TD-08-10	571.0	1.66	TD-08-10	630.0	0.43			
TD-08-10	572.0	0.20	TD-08-10	631.0	0.45			
TD-08-10	573.0	0.16	TD-08-10	632.0	0.36			
TD-08-10	574.0	0.16	TD-08-10	633.0	0.41			
TD-08-10	575.0	0.16	TD-08-10	634.0	0.43			
TD-08-10	576.0	0.18	TD-08-10	635.0	0.30			
TD-08-10	577.0	0.20	TD-08-10	636.0	0.38			
TD-08-10	578.0	0.18						
TD-08-10	579.0	0.14						
TD-08-10	580.0	0.20						
TD-08-10	581.0	0.20						
TD-08-10	582.0	0.18						
TD-08-10	583.0	0.26						
TD-08-10	584.0	0.18						
TD-08-10	585.0	0.18						
TD-08-10	586.0	0.18						
TD-08-10	587.0	0.22						
TD-08-10	588.0	0.22						
TD-08-10	589.0	0.18						